

This item was submitted to Loughborough University as an MPhil thesis by the author and is made available in the Institutional Repository (<https://dspace.lboro.ac.uk/>) under the following Creative Commons Licence conditions.



For the full text of this licence, please go to:
<http://creativecommons.org/licenses/by-nc-nd/2.5/>

Pilkington Library

Author/Filing Title QUANT, S.J.

Accession/Copy No.

Vol. No.

Class Mark T

Open shelf copy
Open shelf copy

0401658767



BADMINTON PRESS
UNIT 4 BROOKS
SYSTEM
LEICESTER LE1 1GD
ENGLAND
TEL 0116 266 2917
FAX 0116 266 6439

**AN EVALUATION OF MASTICATION
AND THE DEVELOPMENT OF A PREDICTIVE MODEL
FOR THE RUBBER MIXING PROCESS.**

by


SARAH JANE QUANT BSc (Hons)

**A Masters Thesis submitted in
partial fulfilment of the requirements
for the award Master of Philosophy
of Loughborough University.**

May 1997

**Director of research Dr M O W Richardson
Supervisor: Dr P K Freakley, Institute of
Polymer Technology & Materials Engineering.**

by S J Quant, 1996

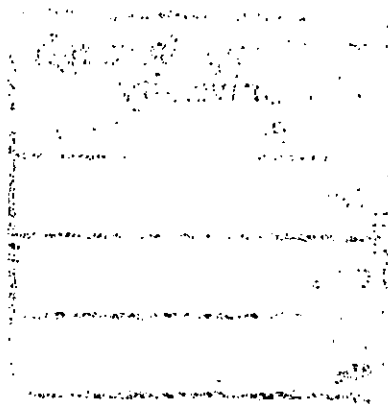
| | |
|--|-----------|
|  Loughborough University | |
| P. | Library |
| Date | July 98 |
| Class | |
| Acc No. | 040165876 |

K0630787

I certify that I am responsible for the work submitted in this thesis. Further I certify that no part of this thesis has been submitted to this or any other University for the award of a higher degree.

References to other people's work have been clearly identified and credit given.

.....
S.J.Quant



To Mum, Dad & Michael
With Love

ACKNOWLEDGEMENTS.

The author wishes to gratefully thank the contribution of a number of individuals whose helpfulness and support have been essential in the execution of this study:

Dr P.K. Freakley, my research supervisor, for his untiring and frequent encouragement during the course of the research, and for his kind advice during the writing of this thesis.

Mr L.J. Millichip, my industrial supervisor, for his valued organisation of the project within Avon Polymers Ltd.

Mr D.M. Turner, Independent Consultant for the project, for his direction and assistance with the development of the predictive model, but mostly for the enormous enthusiasm he showered upon my work.

ABSTRACT.

The research presented initially evaluated the effect mixing conditions have on the efficiency of mastication through a series of central composite experimental designs. The resulting regression analysis showed that mixing time, rotor speed, circulating water temperature and fill factor all have an effect on final batch temperature and viscosity; and that each parameter causes a consistent pattern. This observation lead to the research concentrating on the development of a predictive model for the rubber mixing process.

A predictive model was developed for a laboratory tangential rotor internal mixer, a Farrel BR Banbury, for the mastication of a premasticated SMR L natural rubber and dispersive mixing with 27 phr of N660 carbon black over a wide range of mixing conditions. The model operates by predicting the energy supplied and lost in the mixing process as a function of material and machine behaviour. The model successfully estimated 90% of the mixing cycles within +/- 5°C of the actual final temperature and within 7% of the final power consumption.

Experimental work was then undertaken in an attempt to develop a material database which would enable the mixing cycles of a wide range of carbon blacks at different loadings to be modelled. However the mixing data produced was insufficient to produce the material database, although regression analysis on the data allowed the effect of water temperature, rotor speed, mixing time, loading and type of carbon black on dispersive mixing to be examined. This is illustrated by a series of graphs.

CONTENTS

| | |
|--|----|
| Nomenclature list | i |
| Chapter 1: Introduction and objectives | 1 |
| 1.0 The role of rubber mixing | 1 |
| 1.1 Background to the project | 2 |
| 1.2 Statement of objectives | 3 |
| Chapter 2: Literature survey | 5 |
| 2.0 Development of the internal mixer | 5 |
| 2.1 The design of an internal mixer | 5 |
| 2.1.1 Developments in the design of internal mixers | 7 |
| 2.1.1.1 Rotor design | 7 |
| 2.1.1.2 Chamber design | 9 |
| 2.1.1.3 Rotor speed | 10 |
| 2.2 Methods of internal mixing | 10 |
| 2.2.1 Mixing variables that affect mixing performance | 11 |
| 2.2.1.1 Rotor speed | 11 |
| 2.2.1.2 Circulating water temperature | 12 |
| 2.2.1.3 Ram pressure | 13 |
| 2.2.1.4 Fill factor | 13 |
| 2.2.1.5 Mixing procedures (loading pattern) | 13 |
| 2.3 Control of the mixer and mixing cycles | 14 |
| 2.4 Measurement of batch temperature | 15 |
| 2.5 Materials | 18 |
| 2.5.1 Natural rubber | 18 |

| | | |
|-----------|--|----|
| 2.5.2 | Carbon black | 18 |
| 2.6 | The mixing process | 21 |
| 2.6.1 | Mastication | 22 |
| 2.6.1.1 | Mechanism of mastication | 23 |
| 2.6.2 | Dispersive mixing | 25 |
| 2.6.2.1 | Mechanism of dispersive mixing | 25 |
| 2.7 | Development of properties during dispersive mixing | 28 |
| 2.7.1 | Changes in the viscosity of the rubber compound | 29 |
| 2.7.2 | Development of tensile properties | 31 |
| 2.7.3 | Dynamic mechanical properties | 31 |
| 2.7.4 | Other properties that are significant | 35 |
| 2.8 | Modelling of the process in the internal mixer | 36 |
| 2.8.1 | Modelling the flow | 36 |
| 2.8.2 | Statistical models | 37 |
| 2.8.3 | Energy balance models | 37 |
| Chapter 3 | General experimental details | 42 |
| 3.0 | Banbury Mixer | 42 |
| 3.1 | Testing | 44 |
| 3.1.1 | Negretti TMS biconical rheometer | 44 |
| 3.1.2 | Monstanto moving die rheometer | 47 |
| Chapter 4 | Effect of mixing parameters on mastication | 49 |
| 4.0 | Objectives | 49 |
| 4.1 | General experimental details | 50 |
| 4.2 | Part one - time, water temperature & speed | 51 |
| 4.2.1 | Experimental procedure | 51 |

| | | |
|-----------|--|----|
| 4.2.1.1 | Experiment one | 51 |
| 4.2.1.2 | Experiment two | 53 |
| 4.2.2 | Results for part one | 54 |
| 4.2.2.1 | Results for experiment one | 54 |
| 4.2.2.2 | Results for experiment two | 55 |
| 4.2.3 | Regression analysis of the results | 56 |
| 4.2.4 | Summary of findings in part one | 60 |
| 4.2.4.1 | The effect of mixing time | 61 |
| 4.2.4.2 | The effect of rotor speed | 61 |
| 4.2.4.3 | The effect of water temperature | 61 |
| 4.2.4.4 | Effect of mixing parameters on final temperature | 62 |
| 4.2.4.5 | Rotor revolutions | 62 |
| 4.3 | Part two - fill factor | 63 |
| 4.3.1 | Experimental procedure | 63 |
| 4.3.2 | Results for part two | 64 |
| 4.3.3 | Regression analysis of the results | 64 |
| 4.3.4 | Summary of findings in part two | 66 |
| 4.4 | Part three - variation in initial viscosity | 67 |
| 4.4.1 | Experimental procedure | 68 |
| 4.4.2 | Results for part three | 70 |
| 4.4.3 | Summary of findings in part three | 71 |
| 4.5 | Recommendation for the control of mastication | 71 |
| Chapter 5 | Development of a predictive model | 73 |
| 5.0 | Introduction | 73 |
| 5.1 | Benefits of a predictive model | 74 |

| | | |
|---------|---|-----|
| 5.2 | Overall development of the model | 75 |
| 5.2.1 | Operation of the model | 76 |
| 5.3 | Predicting the energy generated | 78 |
| 5.3.1 | During mastication | 78 |
| 5.3.1.1 | Effect of speed | 79 |
| 5.3.1.2 | Effect of batch temperature | 80 |
| 5.3.1.3 | Effect of mastication | 81 |
| 5.3.1.4 | Effect of fill factor | 82 |
| 5.3.2 | During dispersive mixing | 82 |
| 5.3.2.1 | Determination of the rate of disagglomeration | 83 |
| 5.3.2.2 | Determination of the filler volume | 86 |
| 5.3.2.3 | Changing the K and n constants | 87 |
| 5.4 | Predicting the energy out | 89 |
| 5.4.1 | Statistical analysis | 90 |
| 5.4.1.1 | Summary of findings | 96 |
| 5.4.2 | Validation of the heat transfer model | 98 |
| 5.4.2.1 | Operation of the model | 100 |
| 5.4.2.2 | Development of the model | 103 |
| 5.4.2.3 | Temperature profiles from the heat transfer model | 106 |
| 5.4.2.4 | Accuracy of the heat transfer model | 110 |
| 5.5 | Coefficients for initial predictive model | 112 |
| 5.6 | Accuracy of the model for simulating temperature | 114 |
| 5.7 | Accuracy of the model for simulating power | 115 |
| 5.8 | Profiles produced using the predictive model | 116 |
| 5.9 | The effect of oil additions | 118 |

| | | |
|------------|---|-----|
| 5.9.1 | Experimental details | 119 |
| 5.9.2 | Observations from the experiment | 120 |
| Chapter 6: | Development of a material database | 121 |
| 6.0 | Introduction | 121 |
| 6.1 | Experimental design | 123 |
| 6.1.1 | The defined ranges of the experiment | 123 |
| 6.1.2 | Additional experimental details | 127 |
| 6.1.3 | Statistical analysis | 128 |
| 6.2 | Observations from the experiment | 129 |
| 6.2.1 | The mastication stage | 129 |
| 6.2.2 | After addition of carbon black | 130 |
| 6.3 | Analysis to determine effect of disagglomeration | 132 |
| 6.3.1 | Coefficients required | 132 |
| 6.3.2 | Determining RS for the 45 mixes | 133 |
| 6.3.2.1 | Initial method | 133 |
| 6.3.2.2 | Second method | 135 |
| 6.4 | Determining effect of disagglomeration using torque | 139 |
| 6.5 | Regression eq. to predict temperature and torque | 140 |
| 6.5.1 | Regression eq. for torque profiles | 141 |
| 6.5.1.1 | Torque profiles of rubber in the carbon black mixes | 141 |
| 6.5.1.2 | Generation of separate regression equations | 143 |
| 6.5.2 | Generation of regression eq. for temperature | 144 |
| 6.5.3 | Regression equations generated | 145 |
| 6.5.4 | The effect of parameters on torque and temperature | 146 |
| 6.5.4.1 | The effect of material parameters | 147 |

| | | |
|------------|---|-----|
| 6.5.4.2 | The effect of mixing parameters | 151 |
| 6.6 | Predicting temperature using batch thermocouple | 153 |
| Chapter 7: | Conclusions and possible future work | 155 |
| 7.0 | Chapter 4 | 155 |
| 7.1 | Chapter 5 | 155 |
| 7.2 | Chapter 6 | 157 |
| 7.3 | Future work | 160 |
| Appendix 1 | | 161 |
| Appendix 2 | | 163 |
| Appendix 3 | | 174 |
| References | | 181 |

NOMENCLATURE LIST.

| | |
|---------|---|
| b | = Batch temperature constant (equation 5.9). |
| d | = Mastication constant one (equation 5.10). |
| dT | = Temperature change (°C). |
| dW | = Energy absorbed (J). |
| g | = Rate of disagglomeration. |
| hfmw | = heat flow from the mixer body to the circulating water (W). |
| hfrm | = Heat flow from the mixing batch to the mixer body (W) |
| load | = Loading of carbon black (phr). |
| mv | = Minimum value of torque (dNm). |
| n | = Power index. |
| rindex | = Index for the dependence of transrm on rotor speed. |
| rps | = Rotor speed in (rps). |
| s | = A second interval (secs). |
| t | = Mastication mixing (secs). |
| to | = Constant (equation 6.15). |
| transmw | = Heat transfer coefficient from the mixer body to the circulating water. |
| transpm | = Heat transfer coefficient from batch thermocouple to mixer body. |
| transrm | = Heat transfer coefficient from the mixing batch to the mixer body. |
| transrp | = Heat transfer coefficient from mixing batch to batch thermocouple. |
| wf | = Conversion factor (equation 5.20). |
| x | = fill factor constant (equation 5.11). |
| yo | = Mastication constant two (equation 5.10). |
| F | = Fill factor of the Farrel BR Banbury mixer (%). |

| | |
|----------------|--|
| K | = Consistency constant. |
| M | = Mixing time (secs). |
| M_a | = Machine factor (equation 5.7). |
| M_H | = Maximum torque in moving die rheometer (dNm). |
| M_L | = Minimum torque in moving die rheometer (dNm). |
| P_{cb} | = Density of carbon black (g/cm^3). |
| P_{fac} | = Drive efficiency factor (%). |
| R | = Number of rotor revolutions of mastication. |
| RR | = Number of rotor revolution of dispersive mixing. |
| RR_{RSmin} | = Number of rotor revolutions to get to RS_{min} . |
| RS | = Relative shear stress. |
| RS_{min} | = Minimum RS achievable under mixing conditions. |
| S | = Rotor speed in Farrel BR Banbury mixer (rpm). |
| T_m | = Predicted mixer thermocouple values ($^{\circ}C$). |
| T_{mixer} | = Effective mixer body temperature predicted by heat transfer model ($^{\circ}C$). |
| T_p | = Predicted batch thermocouple values ($^{\circ}C$). |
| T_{pst} | = Initial batch thermocouple values ($^{\circ}C$). |
| T_{rubber} | = Temperature of the batch predicted using the heat transfer model ($^{\circ}C$). |
| $TS1$ | = Time to reach a rise of 1 dNm above the initial minimum torque (secs). |
| T_{water} | = Temperature at which the circulating water temperature is set ($^{\circ}C$). |
| α | = Constant (equation 5.14). |
| β | = Constant (equation 5.15). |
| $\dot{\gamma}$ | = Shear rate (s^{-1}). |
| η_a | = Apparent viscosity (KPa.s). |
| σ | = volume fraction of immobilised rubber in an agglomerate. |

| | |
|----------|---|
| τ | = shear stress (KPa). |
| ϕ_a | = Volume fraction of agglomerates. |
| ϕ_e | = Effective volume fraction of agglomerates. |
| ϕ_t | = Volume fraction of carbon black (calculated from true density). |
| ϕ_r | = Volume of immobilised rubber in an agglomerate. |
| ψ | = Specific surface area of carbon black ($\text{m}^2/100\text{g}$). |

ABBREVIATIONS.

| | |
|------|---|
| ACED | = Algorithm for construction of experimental designs. |
| CTAB | = Cetyltrimethylammonium bromide (m^2/g). |
| DBPA | = Dibutyl phthalate absorption ($\text{ml}/100\text{g}$). |
| MDR | = Moving die rheometer. |
| TMS | = Turner-Moore-Smith (biconical rheometer). |

CHAPTER ONE.

AN INTRODUCTION TO RUBBER MIXING AND THE OBJECTIVES OF THIS RESEARCH.

1.0 The role of rubber mixing.

The objective of the rubber mixing process is to produce a product (mixed batch) that has its "ingredients" sufficiently incorporated and dispersed to ensure that it will process easily in the shaping step, cure efficiently and give the required end-use properties.

The ingredients of a rubber compound are very diverse and are dependent on application. However the main ingredients are the elastomeric polymers, particulate fillers, liquid plasticisers, antidegradants and a number of other ingredients which enable crosslinking to take place and are known collectively as the vulcanisation system [1]. The only elastomeric polymer and particulate filler discussed in this research are natural rubber and carbon black respectively.

Internal mixers are used by the vast majority of the rubber industry to produce mixed batches. In order to be capable and commercially viable, internal mixers need to achieve in-batch and batch-to-batch uniformity of physical properties, from grossly separate feedstock, in the shortest time and using the least amount of energy.

The frequently used expression "that rubber mixing is an art rather than a science" describes an industry which matured with a minimum of test equipment for characterization but an infinite column of experts who were "human computers". Unfortunately this dependence upon the human effort is too inconsistent for today's demands of increased raw material costs, higher energy costs and a need to reduce waste and improve quality in an increasingly competitive industry [2]. Hence there has recently been a surge in scientific investigations undertaken to increase the understanding of the physical processes that take place during mixing and to use this new knowledge to optimise mixing cycles in terms of both quality and productivity. The speed with which "new" knowledge has been collected has been made possible by the development of electronic technology, particularly the production of microcomputers which have enabled more efficient monitoring of mixing responses, closed loop control and data manipulation.

1.1 Background to the project.

This research was carried out as part of a Teaching Company Scheme project between the Institute of Polymer Technology and Materials Engineering (IPTME) at Loughborough University and Specialist Mixing, a division of Avon Automotive Components Ltd (AAC).

1.2 Statement of objectives.

At the onset of the project the main objective was:

To determine operating conditions and procedures for optimising in-batch and batch-to-batch uniformity from laboratory and production mixing systems with reference to the chemistry of mixing and carbon black dispersion and their subsequent influence on the deformation and failure behaviour of the mixed rubber.

An investigation to study the effect mixing parameters have upon the efficiency of mastication, detailed in chapter four, was the first work undertaken by the author to achieve this objective.

However in the course of this investigation the objective of the project changed direction for two reasons:

(1) The installation of a Chronos Richardson control system [3] at Specialist Mixing brought significant improvements in mixed rubber quality in terms of both in-batch and batch-to-batch variation. This can be illustrated by the fact the amount of rejects was reduced from approximately 8.5% to 1.4% after the introduction of the Chronos Richardson system.

(2) The anticipated growth demands of Specialist Mixing customers was such that in order to satisfy predicted demand it was necessary either to invest in a second mixing

line or create increased capacity on the existing mixing line by improving productivity.

As a result the project changed direction with emphasis being placed on projects to increase productivity whilst maintaining the high level of in-batch and batch-to-batch uniformity of mixed rubber compounds that had already been achieved.

Consequently the main project undertaken by the author was to develop an initial computerised model that could predict the temperature rise and the power consumption during mixing in an internal mixer depending on the mixing parameters and the materials introduced into the mixer.

This project was chosen because if the mixing process could be fully quantified and predictions made about performance it would give the facility to quickly determine minimum effective mixing cycles required to achieve a desired state of mix, instead of having to undertake time consuming and expensive experiments and relying upon rubber compounder/technologist experience each time new data is required. The target was that the mixing cycles for new compounds could be developed using the computerised model. Consequently the model would reduce lead times for new compounds and improve productivity.

CHAPTER TWO.

LITERATURE SURVEY.

2.0 Development of the internal mixer.

Internal mixers have a long history of mixing rubber compounds. In the case of the Banbury mixer the first patent was issued in 1916 to F H Banbury [4] and the design of the initial Banbury mixer was completed in the early 1920's. Today there are two main classifications of internal mixers, a tangential (nonintermeshing) and a intermeshing rotor machine. A Banbury mixer is a typical tangential internal mixer. The internal mixer is still the most popular machine to masticate rubber and to incorporate and disperse fillers and other ingredients within the rubber industry [5]. The predictions of the 1960's that internal mixers had no future and would be replaced by continuous mixers has not come to fruition [6]. A continuous mixer is a mixer, a warmer, a blender and an extruder all in one [7]. It is only in the plastics industry that the continuous mixer has partially replaced the internal mixer. There is currently no alternative to the internal mixer for effectively mixing highly filler loaded rubber compounds.

2.1 The design of an internal mixer.

Basically an internal mixer has two rotors, a chamber, a floating weight (ram), a feed hopper, and a drop door for discharging the mix. The rubber is sheared and plasticized between the rotors and also in the space between the rotor and the inner

surface of the chamber (see figure 2.1) [8].

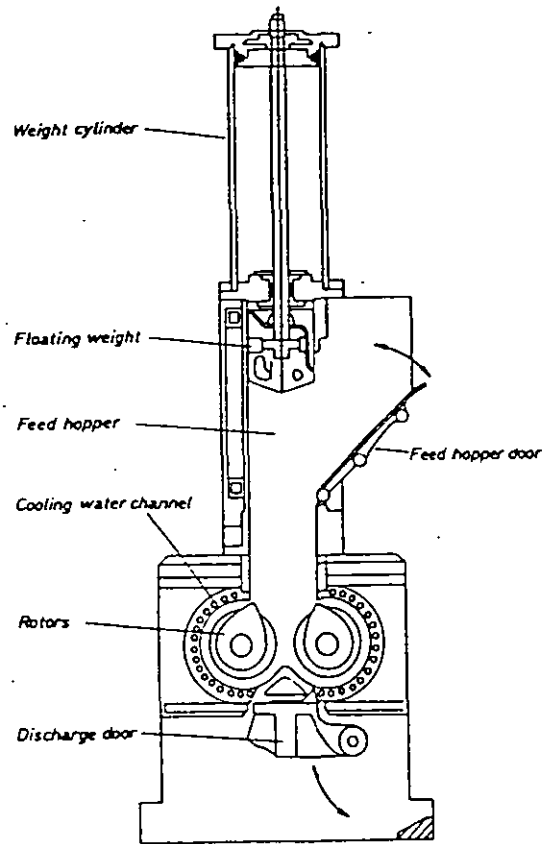


Figure 2.1 - Diagram of a Banbury mixer.

The main advantages of an internal mixer are [9]:

- high dispersive effect,
- high deformation and convective mixing effect,
- relative indifference to varying raw materials,
- ease of raw material feeding compared for instance to screw machines where special technical solutions are required,
- capable of large batches.

The main disadvantages are:

- discontinuous mode of operation,
- high power consumption,
- rapid rise in batch temperature.

2.1.1. Developments in the design of internal mixers.

Since the 1920's the productivity of the internal mixer and its mixing characteristics have been improved by increasing the rotor speed and by making changes in rotor design, cooling capacity, and other more minor modifications. These changes have evolved as a result of the ever changing product and the requirements of industry for improved quality and productivity. However, although modifications have been made, the basic purpose of the various elements of the internal mixer have remained unchanged [10].

2.1.1.1 Rotor design.

In the 1960's people began to study the mixing mechanisms and as a result found that the shape of the rotors significantly affects the dispersion of carbon black and as a result much research has been done on the design of the rotors [11,12,13,14]. Today internal mixers can be classified into two types, tangential (non-intermeshing) and intermeshing.

The Banbury mixer is a typical non-intermeshing mixer with the tangential rotors.

The rotors have an oval shape and they usually run at a friction ratio of 1.15:1. The friction ratio is defined as the ratio of the individual revolving speeds of the two rotors [15,16]. Originally all Banbury mixers had two-wing rotors, however in the 1970s, in order to overcome the inflated energy costs that accompanied the oil crisis, users increasingly demanded that their requirements for saving energy were met. Consequently a four-wing rotor was developed and introduced into a tyre company in Japan to increase the productivity of the Banbury mixer. Although it was claimed that the original four-wing rotor gave more output and less energy consumption per batch, distributive mixing of vulcanization ingredients proved to be poor when compared to the conventional two wing mixer [11]. However since the original four-wing rotor was introduced further work has been undertaken to improve their performance by changing the wing length ratio and orientation. This was achieved by modelling the process with two-dimensional and three-dimensional tests [13].

In the 1930s the Francis Shaw company produced the Intermix with an intermeshing rotor system. In the intermeshing system the two rotors have interlocking projections (nogs), a large helical one and two smaller ones on each rotor. Both rotors run at the same speed and the most intensive mixing region is believed to be between the rotors [12].

Although there have been extensive investigations of the intermeshing and non-intermeshing systems, neither system has emerged as being the overall superior one. Basir and Freakley [17] showed that the mixing action of intermeshing rotors achieves a better overall heat transfer and therefore better temperature control. Griffin [18] and

Min and White [19] argued that in a tangential design there is a greater tendency for stagnation of rubber in the region below the ram, therefore the efficiency of carbon black distribution is not as effective. However the intermeshing rotors have a larger volume than tangential rotors with the same centre distance and in general they operate at lower fill factors. Therefore, to achieve the same batch size, a chamber larger than by a factor of 1.65 is required for intermeshing rotors [20]. The investigations of Wiedman and Schmid [20,21] concluded that tangential mixers give higher machine efficiency, ie fast feeding, fast discharge and fast incorporation and consequently they are deemed to be better for short mixing cycles and multi-stage mixing. Whereas the intermeshing system is deemed to be better for compounds that are difficult to disperse or which give rapid heat generation.

2.1.1.2. Chamber design.

The sides of the mixing chamber and rotors are provided with drilled water passages to facilitate cooling of the mixer to help prevent rapid rise in rubber temperature [22]. Through the use of finite element methods cooling passages have been enlarged and re-positioned strategically to optimize heat transfer without compromising the structural integrity of the machinery [23]. Also the temperature of the heat transfer water is now usually accurately controlled by a heat exchanger system rather than being cooled by simply service water.

2.1.1.3. Rotor speed.

Rotor speed in Banbury mixers has historically been controlled through A.C. motors and compatible gearing to provide from one to four fixed rotor speeds. Today most new Banbury mixers are equipped with D.C. motors giving the facility for variable speed mixing [23].

2.2 Methods of internal mixing and the mixing variables that effect it.

There are two primary approaches to the internal mixing of rubber compounds:

- single stage
- two or more stages

In single stage mixing all the ingredients of a rubber compound are mixed together during one mixing cycle. Traditionally rubber compounds are mixed using a two stage procedure rather than a single stage procedure because of the risk of premature crosslinking of the rubber compound (scorching) due to chemical reactivity of curatives at elevated temperatures. A sharp temperature rise occurs when the carbon black is dispersed within the rubber.

In a two or more stage mixing cycle the carbon blacks are dispersed within the rubber in the first stage and the curatives are not added until the second or later stage to minimize the risk of scorching. With the development of more sophisticated control systems for mixing (see section 2.3) there is currently a move towards single stage

mixing. The advantages of single stage mixing are that it is more efficient as storing and handling of masterbatches is eliminated and also more cost effective in terms of both power consumption and man hours.

2.2.1 Mixing variables that effect mixing performance.

Freakley has stated that the state of mix of a compound after mixing is dominated by the number of rotor revolutions received in the mixer [24,25]. This hypothesis is controversial and is not generally accepted throughout the industry. However it is generally recognised that the following independent variables [26,27] can exert a significant influence on mixing performance and hence final compound properties:

2.2.1.1. Rotor speed.

Rotor speed affects directly total shear strain or deformation and thus the rate of mixing. The rate of mixing is usually limited by the maximum allowable batch temperature ie by the heat balance between heat generation and heat removal [28]. The reduction in viscosity caused by temperature rise results in decreased shear stress and therefore decreased dispersive action. Thus there is a trade-off between increased rate of mixing and a less well dispersed or homogenized product. Consequently in most commercial mixers there is a limit to practicable rotor speeds [20].

The availability of variable speed in modern Banbury mixers provides a wider range of speeds to optimize quality and efficiency. Speed is usually fixed throughout a

mixing cycle. However, by means of automatic control, one may now change speed within a mixing cycle (see section 2.3).

2.2.1.2. Circulating water temperature.

The objective of the cooling system is to transfer heat from the rubber to the cooling water; the greater the thermal gradient the greater the heat flow across the gradient. It is beneficial to reduce batch temperature rise during mixing since any increase results in slower dispersive mixing due to the degeneration of shear stress in the batch. Also at elevated batch temperature the risk of scorching is higher. It is important to control the rate of heat energy transfer by accurately controlling the temperature of the mixer to prevent batch to batch variation [29].

However the cooling system in a Banbury can be too efficient [22]. When the surface temperature of the metal in contact with the rubber is too low (below the dew point) moisture can form on the rotors and chamber wall surfaces causing the rubber to slip on the cold surfaces. For good dispersion of filler and other particulate additives shear stress energy is required. This can only be applied when the rubber is adhered between the rotor tip and the chamber wall and cannot occur if the rubber is slipping. Water temperature in the region of 20 to 40°C has been recommended [30,31].

2.2.1.3. Ram pressure.

A high ram pressure will facilitate the combination of ingredients into the mixing chamber as rapidly and uniformly as possible [28]. Once this has been accomplished high ram pressure can impede material flow within the mixing chamber whilst a lower level of pressure will enhance the mix by permitting the complete utilization of rotor geometry for dispersive mixing [23,32].

2.2.1.4. Fill factor.

It is important to optimize chamber loading [8,33]. Sufficient material is required in the chamber to produce the ram pressure effects described above. Inappropriate batch sizes will create too many voids in the case of the undersized batch and poor circulation or stagnation with the oversized batch [23]. The optimum batch weight for a particular mix depends on the type and level of rubber, filler and plasticiser.

2.2.1.5. Mixing procedures (loading pattern).

In industry each rubber compound has a different mixing procedure. The procedure used has usually evolved through a series of iterations depending on the approach of the compounders or rubber technologist. However the following general techniques are used:

- conventional mixing,

The rubber is loaded first, followed by the addition of the other ingredients after a prescribed period of time.

- dump mixing,

All of the ingredients are dumped into the mixer.

altogether.

- upside-down mixing,

The powders and oil (or plasticisers) are added first, followed by the polymer.

In summary, the following general rules are used [34,35]. It is preferable to add fillers early in the mixing cycle to achieve good dispersion because of the higher viscosity and thus higher shear stress at the lower temperatures. For the same reason oils and plasticiser, which reduce viscosity if present in large quantities, are usually added later as they can slow down dispersive mixing. However, if oils and plasticisers in large quantities are added after the fillers are incorporated, they can coat the metal surface and slow down dispersive mixing by acting as a lubricant. For this reason upside-down mixing procedures and techniques such as adding oil and carbon black together are used in these circumstances.

2.3 Control of the mixer and mixing cycles.

Originally mixer operations were controlled manually. However, with the advent of the microprocessor, the system can now be controlled automatically [30]. All major mixing actions such as feeding of raw materials [36], ram and drop door movements

[3], and rotor speed [30] can now be controlled automatically. Also frequent data scans and recordings through computer control now divulge much more information during the mixing cycle. This has facilitated closed loop control of the mixing cycle, where mixing steps/operations are automatically adjusted/triggered depending on the information from the parameters monitored. The three main parameters used as triggers are mixing time, batch temperature and power consumption (mixing energy) [37,38]. Body temperature and ram pressure can also be monitored to give additional information. Other more sophisticated closed loop techniques have also been investigated, including the possibility of using torque control [39] and heat history control [40] to control mixing cycles.

Automation has not only occurred for direct mixer operations but also for auxiliary operations such as computer controlled weighing systems. Microprocessor control has improved productivity and product quality, both in terms of in-batch and batch to batch uniformity, and consequently has resulted in savings in manpower and energy [3,41].

2.4 Measurement of batch temperature.

As already stated, temperature is an important control parameter [32]. The standard thermocouple used to measure temperature in the internal mixer is the J type (Iron Constantan). These thermocouples have been designed and redesigned so that under test conditions the J type will now indicate an ambient to 100°C step temperature increase in approximately two seconds [23]. Unfortunately the thermocouple in an

internal mixer is not in an ideal environment and is subjected to both steady-state errors and transient errors. These errors are caused by poor thermal contact with the batch, the large heat capacity of rubber compounds and heat conduction from the thermocouple probe through its supporting structure [42].

Moore and Brett [42] undertook trials to look at whether a multi thermocouple probe (MTP) could improve the monitoring of batch temperature. Figure 2.2 shows a section through the multi thermocouple. With the exception of the arrangement at the tip, the overall form was the same as the commercially available J type. In order to improve temperature measurement in the vicinity of the tip of the probe a thermocouple junction was located in a small steel insert that was thermally insulated from the main body of the probe. Unlike the inserts used on J type thermocouples the insert protruded beyond the main body of the probe in order to increase the area of heat path between the mix and thermocouple junction. In addition to this three other thermocouples were installed to provide a measure of thermal gradients. They found [42] that the MTP improved the monitoring of batch temperature with the steady-state error of 8% for the j type thermocouple being reduced to less than 1%. However the specially designed tip thermocouple was found not to be robust enough for the typical rugged operation of an internal mixer.

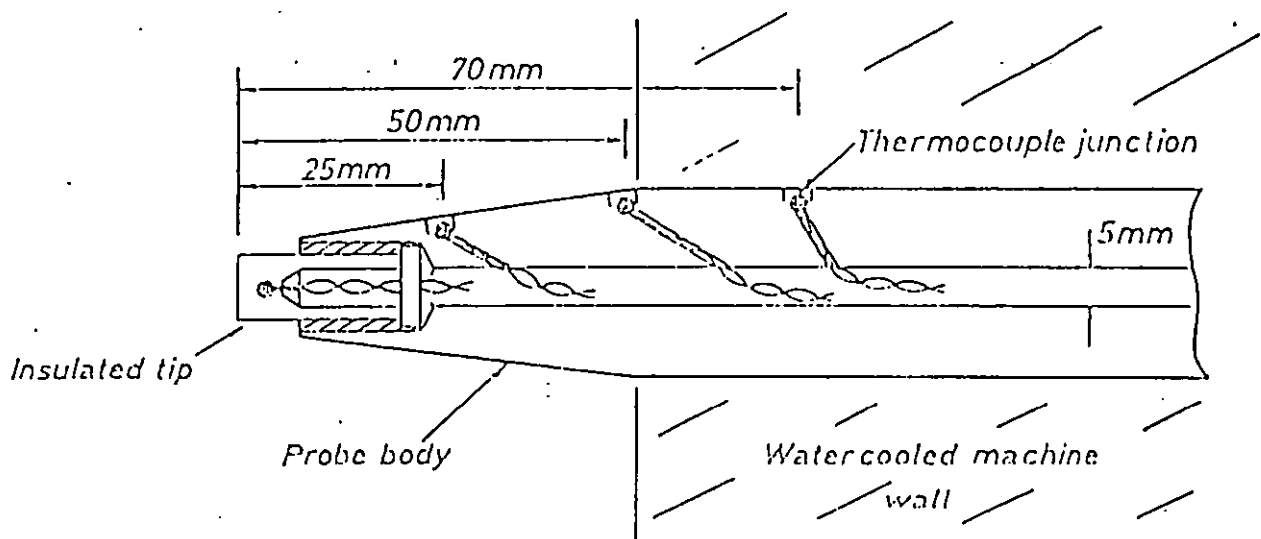


Figure 2.2 - Section through the devised multi thermocouple showing the location of thermocouple junctions.

Infrared thermocouples were also found to be more accurate than the J type thermocouple but they also proved to be too fragile. However several authors [15,32] have found that by shrouding the tip of the of the infrared sensor in a corrosion and abrasion resistant sheath they can be used in practice.

Historically internal batch mixer thermocouples have been located in either the side frame or the drop door and it is now generally excepted that the drop door is the better location [15]. It should be noted that the batch temperature during mixing will depend on the initial temperature of the mixer, which in turn will be influenced by the time interval allowed between successive batches. Failure to control this interval is therefore a potential source of batch to batch non-reproducibility. As this effect normally occurs at the start of a series of runs it is often referred to as the "the first batch effect" [43].

2.5 Materials.

2.5.1 Natural rubber.

Natural rubber is commonly obtained from the latex of a special species of plant called *Hevea Brasiliensis*. Natural rubber contains 93-95 % of cis-polyisoprene. Technically specified rubber (TSR) was introduced by the Malaysians in 1965 under the Standard Malaysian Rubber (SMR) scheme, which was the forerunner of all TSR schemes. Other natural rubber producing countries soon followed with their own versions, Indonesia (SIR), Singapore (SSR) and Thailand (TTR). All versions of TSR are analyzed with the same set of tests to determine quality but small differences exist in the specification limits and the permissible raw materials [29,44]

2.5.2 Carbon black.

Carbon black is the pre-eminent reinforcing filler for rubber and its importance for rubber products is well established. The incorporation of carbon black into rubber vulcanizates generally gives improved tensile strength, extensibility and fatigue and abrasion resistance [45,46]. It is composed of primary particles, carbon atoms arranged in imperfect graphite layers, which are fused together to form an aggregate. In turn aggregates cluster together under the influence of surface forces in collections of aggregates referred to as agglomerates. An aggregate is in the order of 0.1 μm in size whilst an agglomerate is in the order of 10 -100 μm [47].

Carbon blacks can be characterised in terms of their surface area and their structure. The specific surface area is the surface area of a sample of carbon black divided by its weight. Generally in the carbon black industry, liquid phase techniques are used to determine specific surface area. The most common liquid phase technique is the adsorption of iodine under controlled conditions to give the iodine number. However the iodine number is somewhat sensitive to the porosity and surface chemistry of some high surface area blacks. To avoid this cetyltrimethylammonium bromide, a bulky molecule, is used and this gives the "CTAB surface area" [1].

The most common method of determining the structure of carbon black is based on the measurement of the combined intra and inter-aggregate void volume by oil absorption, traditionally using dibutyl phthalate (DBP) [1]. The internal void volume may also be measured by the compressibility of the carbon black at high pressures [48]. Higher structured carbon blacks have higher oil absorption and higher compressibility for a given weight of carbon black. Both of these methods can be run quickly and precisely however they are limited in scope as they are performed on bulk samples of carbon black and provide no information on aggregate shape.

Each aggregate has a unique shape or morphology. Transmission electron microscopy (TEM), in conjunction with image analysis has been used extensively for carbon-black morphological characterisation. Medalia and Heckman [49] first reported the use of image analysis techniques to manually digitise carbon black aggregates from TEM micrographs. Hess et al [50] were the first to combine TEM with automated image analysis for the morphological characterisation of carbon black. As image analysis

instruments became increasingly sophisticated more parameters have become available for size and shape analysis [51,52]. Recently Herd et al [48] have shape classified carbon black into four classes using a specialised image analysis erosion technique termed skeletonization.

Many different grades of carbon black are manufactured. The range covered is approximately 9 to 300 m²/g in CTAB surface area and 30 to 180 ml/100g in absorption of DBP (DBPA) [1,45]. However these grades are not evenly distributed but have been developed to meet specific industrial needs. Historically classification of different carbon blacks was achieved by using a system of type names; however this became too cumbersome with new grades being continually developed and old grades occasionally being dropped. In 1967 the American Society for Testing and Materials (ASTM) published a new system consisting of one letter followed by three numerals [53] to resolve this problem. The letter denotes the curing characteristics in sulphur-accelerator recipes ("N" for "normal curing", "S" for "slow curing"). The first number indicates the range of surface area and the remaining two numerals are selected arbitrarily but one rule applies, in the case of a carbon black with a standard level of structure the second numeral is always a repeat of the first numeral and the last is a zero. Typical grades used in the automotive industry are listed in table 2.0. Although carbon black manufacturers strive to produce carbon blacks that meet both the analytical and performance specifications of each grade, owing to differences in furnace design and feedstock, carbon blacks of the same grade made by different manufacturers are not identical. For this reason most rubber manufacturers have only one regular supplier with a back-up supplier for each grade of carbon black as a

safeguard.

| Grade | CTAB (m ² /g) | DBPA (cm ³ /100g) | Principal properties and applications |
|-------|-----------------------------|---------------------------------|---|
| N110 | 111 | 114 | Reinforcing black - tire treads, high abrasion resistance. |
| N330 | 82 | 102 | Reinforcing black - good abrasion resistance, moderate hysteresis. |
| N550 | 42 | 121 | Semi-reinforcing black - tire carcass and sidewalls, extruded products. |
| N774 | 29 | 72 | Semi-reinforcing black - low hysteresis, high loading capacity, used in industrial rubber compounds |
| N990 | 9 | 43 | Thermal black (non-reinforcing) - very high loading, low hysteresis, smooth extrusion. |

Table 2.1 - A table of some of the carbon blacks used in the automotive industry.

2.6 The mixing process.

The mixing of natural rubber/carbon black compounds can be divided into two stages [54]:

- Mastication of the rubber.
- Dispersion of the particles of carbon black and minor components into the natural rubber matrix to give a uniform and homogeneously mixed compound.

2.6.1 Mastication.

The need for reduction in the molecular weight of natural rubber for further processing was recognised by Hancock [55]. Today the importance of reducing the viscosity of the rubber before incorporating the fillers and chemicals, termed mastication, is still as significant as in the past. Mastication in an internal mixer can be a separate operation prior to mixing or the first stage of an actual mixing process. There are several reasons why mastication is necessary [56]:

- To achieve blending of rubber from various sources.
- When using old slow-speed mixers to ensure that mixing actually ensues rather than crumbling which can occur if bale rubber is used.
- When using modern high-speed high-pressure mixers to ensure that adequate incorporation and dispersion of filler occurs before excessive heat generation requires that the batch is dumped.
- To obtain a compounded material having a viscosity appropriate for further processing such as extrusion and injection moulding or a material of lower viscosity to minimize scorch during further processing.

2.6.1.1. Mechanism of mastication.

The reduction in molecular weight of the natural rubber occurs as a result of two separate reactions, the one which predominates at any one time is dependent on the temperature of the rubber. The dominant reaction at lower temperatures is termed cold mastication and the one that predominates at higher temperatures is termed hot mastication. Cold mastication is most efficient at temperatures below 80°C whilst hot mastication is progressively more efficient at temperature above 115°C [56]. When the efficiency of mastication is plotted against temperature a characteristic U shape curve is produced showing a minimum at approximately 115°C, see figure 2.3 [57,58].

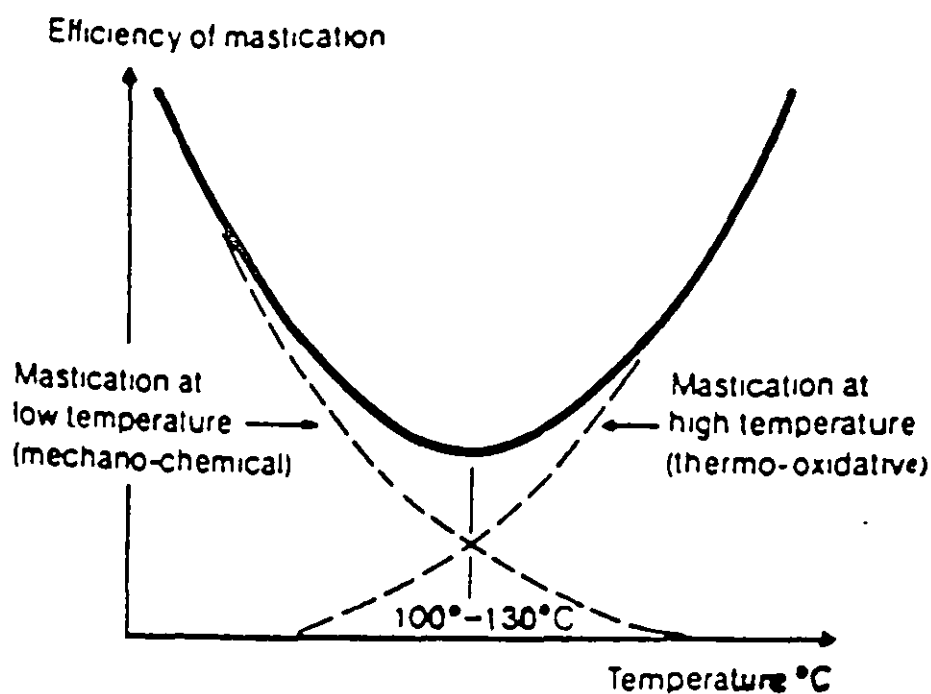


Figure 2.3 - The characteristic U shape curve for mastication.

Cold mastication is a mechano-chemical reaction; the long chain molecules are ruptured by the high shearing forces during bulk deformation of the rubber in the mixer. The ruptured chains have free radicals at their ends and if these are not stabilised they can combine again into long chain molecules, see figure 2.4 [59]. During "normal" mixing the radicals are stabilised by oxygen in the air. However oxygen has no specific function in the breakdown process and another radical acceptor can be equally as effective [59]. By this bond scission process the molecular weight of the rubber becomes progressively lower and consequently the viscosity of the bulk is reduced. However the longer, higher molecular weight molecules are the most easily ruptured and, as mastication progresses, the rate of rupture will decrease due to the diminishing availability of long molecular chains. Cold mastication has a negative rate temperature coefficient since at lower temperatures the rubber is more viscous which increases shearing forces [60].

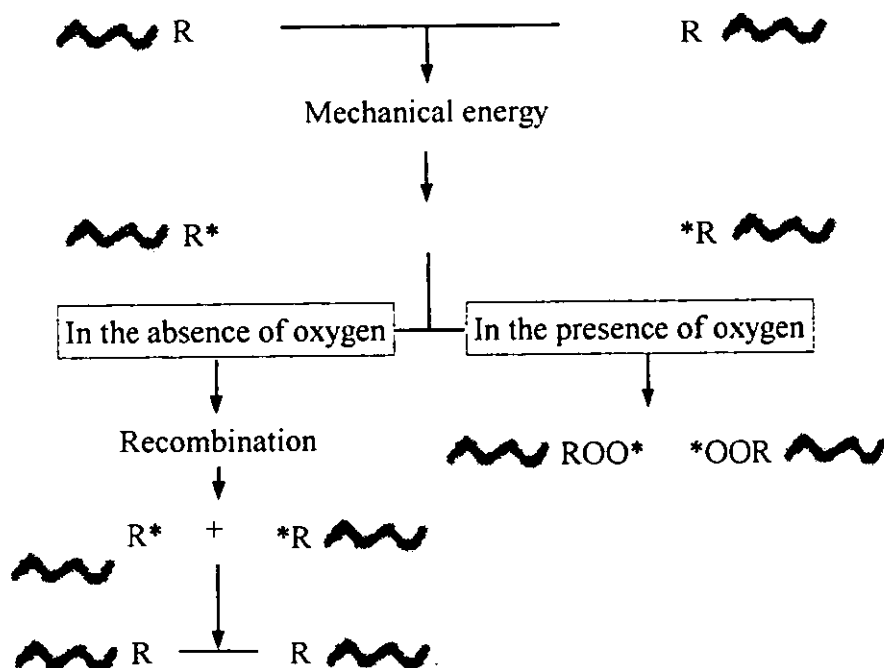


Figure 2.4 - Cold mastication flow chart.

Hot mastication is a thermo-oxidative reaction and therefore has a temperature dependence in line with that expected of a conventional chemical reaction [59]. Hot mastication, unlike mechanical rupture, can be accelerated and largely controlled by catalysts which are termed peptisers. However many commercial peptisers also have the dual function of acting as radical acceptors so can promote both types of mastication. The most common dual action peptisers used are di-o-benzamidophenyl disulphide and mercaptobenzthiazole [53].

2.6.2 Dispersive mixing.

The dispersion of carbon black agglomerates into rubber is a complex process. In an ideal mixing operation the dispersive mixing process would result in all the carbon black agglomerates being broken down into aggregates uniformly dispersed throughout the rubber matrix [47]. In practice imperfect dispersion of carbon black is always observed even after prolonged mixing. The presence of agglomerates larger than a few micrometers reduces the reinforcement properties of the resulting vulcanized compound since they act as failure-initiating flaws [62].

2.6.2.1. Mechanism for dispersive mixing.

Medalia [63] classified the stages of a mixing operation for the dispersion of carbon black agglomerates into rubber as (1) incorporation involving wetting of the agglomerates by the rubber, (2) disagglomeration by the breaking up of the agglomerates, (3) distribution of the agglomerates and aggregates throughout the

polymer by random patterns of flow and (4) flocculation involving diffusion and cohesion of aggregates into a network. Tokita and Pleskin [64,65] took a slightly different point of view and identified only three stages in mixing carbon black and rubber (1) filler wetting or induction, (2) disagglomeration and (3) rubber breakdown and interaction with the filler.

In any classification incorporation is the first step of mixing. At the end of this step the loose filler particles disappear and all the air introduced in the compound by entrapment with the agglomerates has been replaced by rubber. The rubber wets the filler and penetrates into the void spaces of the agglomerates [66]. The rubber filling the void spaces is called immobilised rubber [66].

It is generally recognized that the breakdown of agglomerates into smaller fragments, down to aggregate size, is the most difficult step and it is therefore the rate-determining one in any mixing operation. In general two distinct breakage mechanisms have been observed in disagglomeration, denoted as erosion and rupture [47]. Erosion is the process of continuous detachment of aggregates from the outer surface of the agglomerate, whilst rupture is an abrupt, large-scale fragmentation process. Rupture is initiated at higher applied shear stresses than erosion [47].

Bolen and Colwell [67] were the first to propose that rupture occurs when internal stresses, induced by a viscous drag on the agglomerates, exceed a threshold value. Following this observation several researchers have developed models for the mixing process. However, because of the complexity of the process, none of these models

perfectly depicts all aspects of dispersion but they have resulted in a better understanding of the process.

Manas-Zloczower, Nir, and Tadmor [5] derived a model for agglomerate dispersion in a simple shear flow. This model assumed that disagglomeration was a repetitive process with cleavage of the agglomerate always occurring at the midplane. This model therefore did not take into consideration erosion of the agglomerates. Shiga and Furuta [68] proposed the "onion model" which suggested that disagglomeration was due to aggregates either individually or collectively being eroded from the surface of the agglomerate when being passed through a high shear zone. Later work undertaken by Manas-Zloczower with Rwei and Feke [69] resulted in a model which took into consideration the effects of both rupture and erosion.

The time required for incorporation of carbon black may be obtained by measuring the time to reach the "second power peak" [70]. This is not a new idea, Beach et al [71] introduced this concept in 1959 and named it the BIT index (Black Incorporation Time). Cotton found that higher structure carbon blacks were incorporated in a shorter period of time [72] in contrast to earlier statements by Gesser et al [73] claiming the opposite effect. The time required to attain satisfactory dispersion, once the carbon black has been incorporated, decreases with increased "structure" since the aggregates are not as tightly packed together. Higher surface area gives stronger agglomerates which are more difficult to disperse. See table 2.2.

| Rubber property | Higher surface area | Higher structure | Higher loading |
|--------------------|---------------------|------------------|----------------|
| Incorporation time | Slight increase | Decrease | Increase |
| Dispersion time | Increase | Decrease | Not important |
| Viscosity | Increase | Increase | Increase |
| Die swell | Not important | Decrease | Decrease |

Table 2.2 - The effect of different grades and loading of carbon black on dispersive mixing.

2.7 Development of material properties during dispersive mixing.

As already stated the reinforcement effect of carbon black on a mixed compound causes a substantial improvement in a variety of vulcanisate properties such as tensile strength and dynamic mechanical properties. The reinforcement effect of carbon black shows up especially in its ability to increase the viscosity of a mixed compound dramatically depending on the type and loading of carbon black [74]. However the final properties of a mixed compound will not only depend on the amount and type of carbon black added to the polymer matrix but will also be influenced by the mixing conditions used to produce the mixed compound. The rate of decay of the agglomerate fractions in any particular interval is governed by the matrix viscosity, rotor speed and the residence time in the mixer [5,68,69], as each of these factors will directly affect the cumulative shear and stress history received by the compound in the mixer. Therefore any mixing parameter having an effect on these will have a direct effect on the final properties of the mixed compound.

2.7.1. Changes in the viscosity of the rubber compound during dispersive mixing.

The change in the rubber compound viscosity discussed in this section refer to the viscosity of the compound measured at constant temperature after mixing and does not refer to the temperature dependence of the viscosity of the material in the mixer.

Freakley and Clarke (nee Butler) [24,66] have done extensive work to study changes in the viscosity of a compound during dispersive mixing. The viscosity of the compound initially increases in the very early stages of mixing, reaches a maximum and then decreases. The viscosity increases to a maximum during incorporation as rubber penetrates into the carbon black. Their observations indicated that the reduction in viscosity of the compound, after reaching a maximum, comes from two contributory sources. The smaller contribution coming from mastication of the rubber and the larger from disagglomeration of the carbon black. The physical breakage of primary aggregates was not found to be a contributory source as the structure of the carbon black was not significantly changed by mixing. This was also observed by Boonstra and Medalia [75]. Similarly the reduction in the size of the agglomerates during dispersive mixing was not a significant contributory source [76].

Thirty years ago Medalia and Boonstra [77,78] proposed that in a carbon black/rubber system the rubber that penetrates within the agglomerates is immobilised and thus acts as part of the filler rather than part of the matrix. Therefore the rubber immobilised within the agglomerates should be included in the total volume fraction of filler in the compound and as a consequence the effective volume fraction will be higher than

expected. As dispersive mixing progresses agglomerates are broken down and immobilised rubber is released causing a reduction in effective volume fraction of filler and a consequent decrease in viscosity. Freakley and Clarke [66] proved this hypothesis quantitatively by showing that the relationship between effective filler volume fraction and relative viscosity for simple rubber/carbon black compounds is the same as the relationship between true volume fraction and relative viscosity. Relative viscosity, viscosity of the compound divided by that of the gum, was used to remove the effect of mastication on the viscosity of the compound. This was achieved by using the viscosity of the gum treated in a similar way to the compound and with an allowance made for strain rate amplification. Strain rate amplification of the gum was required since the presence of undeformable filler in the compound means that, for a given externally imposed strain, the rubber in a compound will experience a higher strain than the rubber in a filler-free gum. In a similar way the strain rate experienced by the elastomer in a compound will be higher than the strain rate externally imposed on the compound. Micrograph sections of samples were analysed to determine the effective volume fraction of agglomerates. It was found that the amount of immobilised rubber present in an agglomerate could be estimated using the DBPA value of the carbon black [66].

The Mooney viscometer [79] is traditionally used to measure the viscosity of rubber compounds. However the Mooney viscometer operates at shear rates which are too low to relate to actual processing conditions and hence the relevance of the instrument is questionable. The Negretti TMS biconical rotor rheometer (TMS rheometer) [10], used in this study, may be operated over a range of shear rates. This makes the

instrument very versatile, being able to obtain viscosity measurements which have relevance in certain forming operations.

2.7.2. Development of tensile properties during dispersive mixing.

Tensile strength, as measured using the British standard [80], improves rapidly with increased mixing time until a maximum is reached [74,81]. This is due to the disappearance of the large agglomerates and the improved dispersion of the aggregates of carbon black in the matrix. This improves the reinforcement effect because it increases the surface area of the carbon black in contact with the polymer matrix. Large agglomerates will act as stress concentrators, initiating cracks and magnifying true stresses that manifest themselves within the matrix when the bulk is deformed. Complex internal localised stress fields occur which result in premature rupture. Another property measured concurrently with tensile strength is elongation at break [80], calculated as the extension of a specified length of sample at rupture divided by the original length of this sample distance and expressed as a percentage. This property follows a similar trend as tensile strength with mixing time [74,81].

2.7.3. The Influence of the state of dispersion on dynamic mechanical properties.

Rubber is a viscoelastic material, that is its mechanical behaviour changes as a function of time. When a stress is applied to rubber it does not instantaneously take up the degree of strain corresponding to this stress. In fact in dynamic sinusoidal cycling the strain lags slightly behind the applied stress and vice versa. The phase

difference between the strain and stress is expressed in terms of a loss angle δ , see figure 2.5 [82].

The total stress measured is the sum of two stresses, the elastic stress (in phase with the strain) and the viscous stress (out-of-phase with the strain). Dynamic modulus is usually represented by a complex quantity, ie, the ratio of stress amplitude to strain amplitude (A/B). For tension and compression the complex modulus is given as [74,83]:

$$E^* = E + jE \quad (21)$$

The storage modulus (E) is the ratio of the amplitude of the in-phase stress component to the strain amplitude (C/B), and the loss modulus (E) is the ratio of amplitude of the out-of-phase component to the strain amplitude (D/B), see figure 2.5. The E measures the amount of energy stored and the E measures the energy dissipation into the rubber.

The loss angle δ between stress and strain is:

$$\tan \delta = E/E \quad (22)$$

It is defined as the ratio of energy loss (dissipation) to energy stored per cycle and is a measure of the hysteresis of the rubber.

STRESS & STRAIN

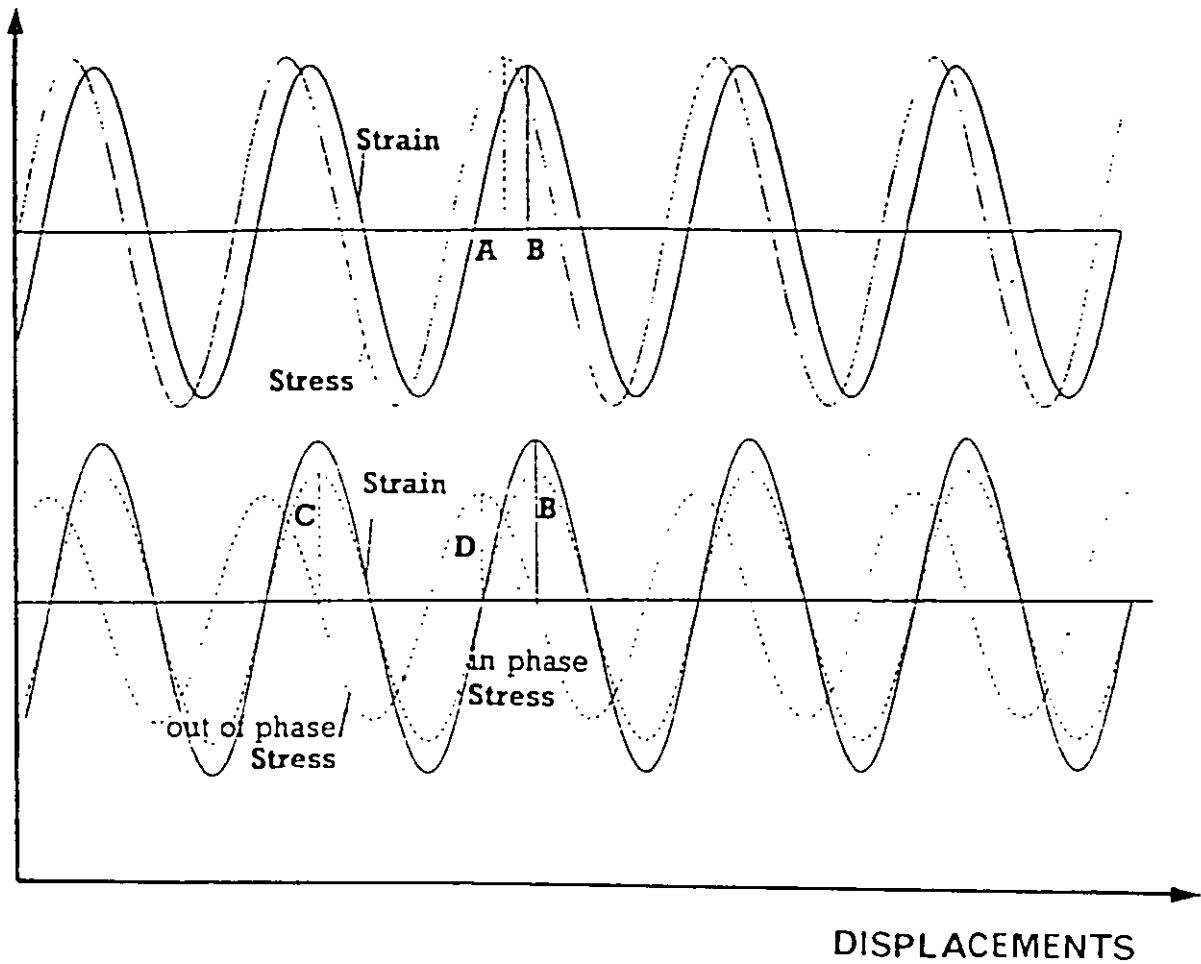


Figure 2.5 - Stress and strain.

- (a) Stress and strain as a function of time for sinusoidal deformation of rubber.
- (b) The stress sine wave resolved into two components: one in-phase with the strain and the other out-of-phase with the strain. The amplitudes of these two components determine the storage and loss modulus.

The principal qualitative effects of carbon black on the dynamic mechanical properties are [84,85]:

- i An increase in E' over the gum rubber.
- ii An increase in $\tan \delta$.
- iii Dependence of E' , E'' and $\tan \delta$ on amplitude.
- iv Different effects on dynamic properties from different grades of carbon black.

Unlike gum vulcanisates filled rubbers are very sensitive to amplitude. This phenomenon, known qualitatively for some 50 years, was brought into clear focus by the work of Payne in the 1960s [86,87]. The carbon black network structure is broken down at a high amplitude of cyclic straining regardless of the loading or interaggregate bond strength and the E' is governed by the individual carbon black aggregates. It is assumed the hysteresis (E'' or $\tan \delta$) results from the breakdown and re-formation of interaggregate bonds [86]. There is little breakdown of these bonds at low amplitude and thus little hysteresis. Considerable breakdown and re-formation of bonds take place at intermediate; thus hysteresis is high. Both E' and $\tan \delta$ continue to decrease at large amplitude; thus E'' can become quite low. A low value of E'' at high amplitude has been interpreted to suggest that the structure is broken down so intensively that structural re-formation is much slower than the cycle time. The decrease in $\tan \delta$ at high amplitudes indicates that less re-formation of interaggregate bonds take place than at intermediate amplitudes [86].

The amplitude dependence of dynamic mechanical behaviour is strongly influenced by the state of dispersion of a given carbon black with respect to both the size and

number of agglomerates and the mean number of contacts per aggregate [88]. The value of E' decreases with increased mixing time (ie dispersion). This effect is very pronounced in the poorly mixed/dispersed samples. The proposed reason for this is that in a well-dispersed compound the individual aggregates are well separated and hence the amplitude effect will be small [89].

The maximum in the plot of E'' versus strain amplitude indicates that there is a dynamic equilibrium between destruction and re-formation of the carbon black network [88]. Therefore as the dispersion of the carbon black increases the maximum in E'' decreases. The phase angle at intermediate and high amplitudes decrease with improved dispersion, especially during the initial stages of mixing [88].

In general natural rubber has low hysteresis, the actual value depending on the compound formulation [90]. Low hysteresis (high resilience) implies a low heat build-up. They are used widely in vibration isolation and shock absorption applications [91] due to the low hysteresis of rubber compounds and their capability of undergoing large recoverable deformations.

2.7.4. Other properties that are significantly dependent on the level of dispersion.

Other properties that are significantly dependent on the level of dispersion include hardness, tear strength and abrasion resistance. The level of dispersion required for any given rubber compound is predetermined by specification or application properties. As well as studying the properties of the rubber compound to determine

the state of dispersion it can also be measured directly using electrical resistance [31,92], microscopic techniques [93], surface roughness analysis [94] and electron microscopy [95].

In summary, the following properties of technological importance are influenced by the heterodistribution of carbon black are flow properties, crack growth resistance, heat build up, oil swell resistance, air permeation and electrical conductivity [96].

2.8 Modelling of the mixing process in the internal mixer.

Research work to model the mixing process in the internal mixer has intensified in the past decade. The models developed are directed towards an optimisation of:

- mixing technology and processing variables,
- geometry of the working elements,
- material properties of the raw material and the mixed compounds.

There are three main type of models that have been developed:

2.8.1 Modelling the flow.

The majority of the work has concentrated on the modelling the flow processes in the internal mixer [9,97,98,99,100,101,102]; more recently this has involved applying some finite element methods (FEM) [100].

2.8.2 Statistical models.

Statistical models have been developed to model the effect of mixer variables on material properties and mixer responses [39,103,104]. This involves undertaking a series of experiments to study the variables and then the generation of empirical equations using regression analysis. The debit side of this type of model is that the empirical nature of the relationships renders them specific to the mixer and the compound used for the relationships; as a consequence the resulting empirical equations are of limited use.

2.8.3 Energy Balance models.

There has been little research work done in this area, the only published work found was Menges & Grajewski [105], Grajewski & Sunder [106] and Michaeli & Sunder [107]. The models described in these papers predict the power and temperature development during mixing by trying to emulate the interactions between the major process parameters.

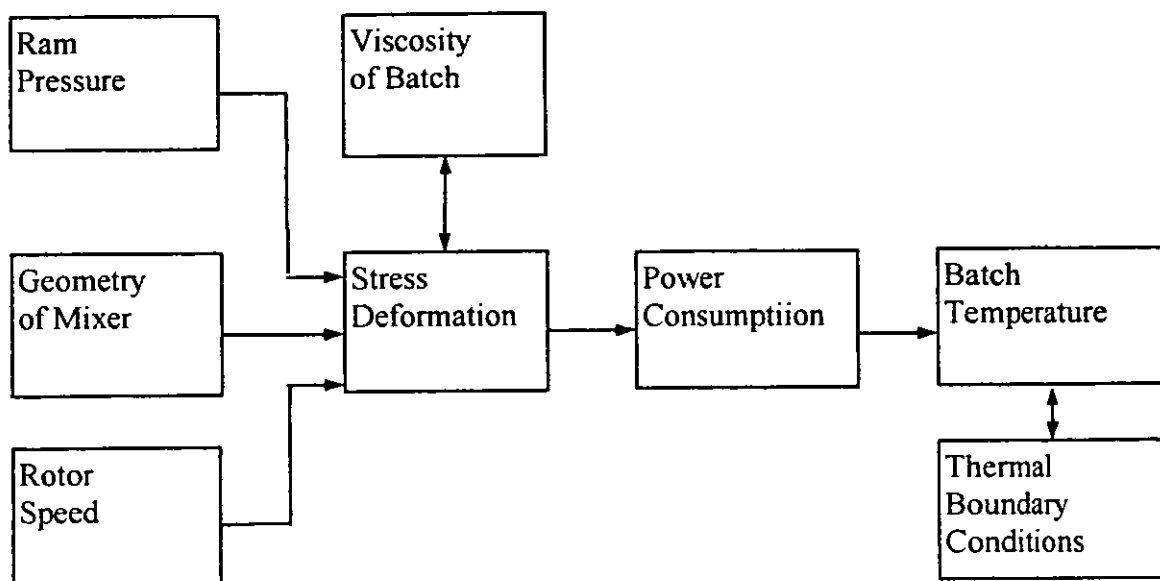


Figure 2.8 - The major process parameter interactions are summarised simplistically in the flow diagram above.

At any point in a mixing cycle it is the ram pressure, the mixer geometry, the fill factor, the rotor speed and the viscosity of the batch that effect the stress and strain history in the mixer [107]. These factors collectively determine the momentary power consumption and the temperature increase as a result of the input energy. The viscosity of the material in the mixer will be dependent on the cumulative stress and strain history received and the temperature of the batch. In addition to the cumulative energy dissipated into the system, the thermal boundary conditions will also affect the temperature of the batch [107].

Micheali and Sunder's paper [107], the more recent of the papers, describes a model that incorporates the research work from the two earlier papers. The model they describe predicts the temperature and power development in the material during mixing by setting up an energy balance after specific time intervals. This consists of

deducting the heat flow to the thermal boundaries (ie from the batch to the mixer body and rotors) from the power dissipated into the system after each specific time interval. From this balance the intrinsic energy and the material temperature after a specific time interval can be calculated. A new time iteration can then be started with the newly calculated material temperatures being incorporated to enable the temperature dependence of the viscosity of the material to be taken into consideration. The result of such a series of calculations are curves showing the development of power and temperature during mixing.

In order to determine the energy dissipated due to shear flow the mixer was divided into two sections referred to as volume elements. The two volume elements were (i) between the rotors and the chamber walls and (ii) between the rotors.

The average shear rate ($\dot{\gamma}$) is defined from the relative velocity (V_R) and the gap height (h).

$$\dot{\gamma} = \frac{V_R}{h} \quad (23)$$

In the volume element between rotor and chamber wall the rotor is assumed to be fixed, whereas the chamber wall moves with the circuit velocity over it. Individual gearing of the wings between the two rotors generates a relative velocity at constant rotor speed. In the space between the rotors the gap height and the mean shear rate involved are subject of the respective rotor position.

involved are subject of the respective rotor position.

The energy dissipated in each volume element is calculated using the following equation:

$$dE_{\text{diss},s} = \phi K(p) \gamma^{n-1} (X, \phi) dV \quad (24)$$

with:

$K(p)$ = temperature-dependent viscosity at shear rate 1 s^{-1}

ϕ = rotor speed

γ = shear rate

n = viscosity exponent

V = volume

X = rotor position

The relationship between viscosity and shear rate is approximated by a power law relationship and an Arrhenius equation is used to represent the temperature dependence on viscosity. The filling rate in each volume element has to be taken into consideration due to the fact that the mixer is partly filled. The fill rate distribution was determined by experiments in which the mixer chamber was opened and the material was removed in sections.

By totalling the dissipated power of both the volume elements the proportion of one rotor position can be calculated. Total power consumption during each time interval

can then be calculated by integration over all possible rotor positions.

In the model, the heat flow to the thermal boundary conditions was calculated by the employment of heat transfer coefficients. The heat transfer coefficient for the heat flow from the batch to the mixer body was determined from the geometry of the rotor and the chamber, from the rotor speed and from the thermodynamic properties of the batch. Whilst the heat transfer coefficient from the mixer body to the cooling water system was determined from the water throughput and the geometry of the cooling channels.

The authors [107] confirmed that this approach can accurately predict power and temperature development during mixing on both a Werner and Pfleiderer laboratory internal mixer (Gk-1,5E) and an Werner and Pfleiderer industrial mixer (Gk-110E) of 1.5 L and 110 L capacity respectively. However they have only studied mastication and not dispersive mixing. One of their first observations was that they were unable to predict the power consumption during the very early stage of mixing due to fluctuations in filling rate of the batch into the mixer.

CHAPTER THREE.

GENERAL EXPERIMENTAL DETAILS.

3.0. BR Banbury mixer.

All mastication/mixing was undertaken on a semi-automated laboratory Farrel BR Banbury mixer.

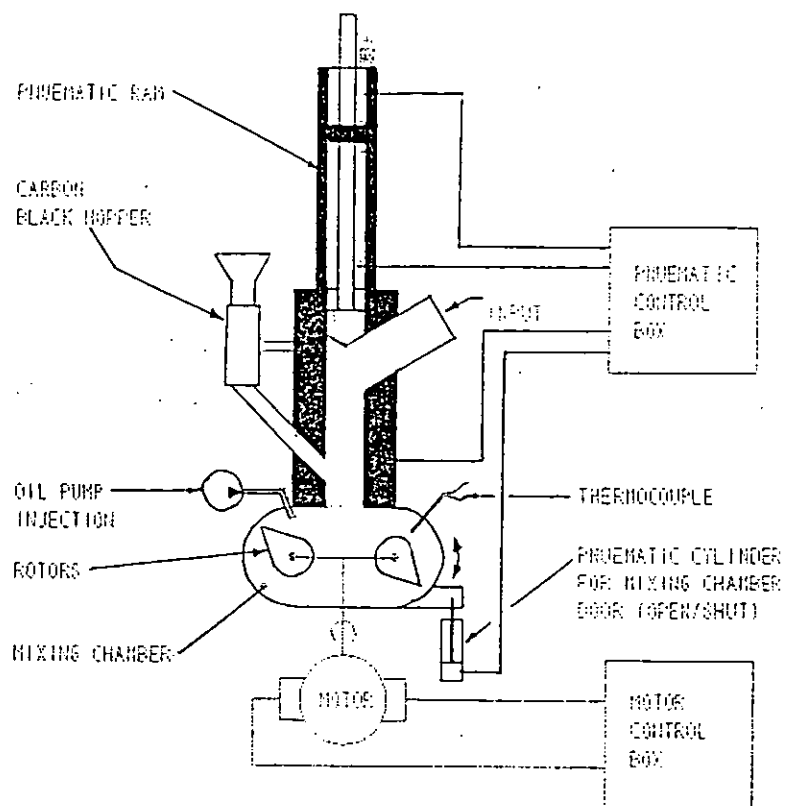


Figure 3.1 - Systematic diagram of the laboratory BR Banbury mixer.

The main specifications of the mixer are:

- Volume of 1.64 L.
- D.C. variable speed drive.
- A thermolator to control the circulating water temperature.
- J type thermocouples to measure both the temperature of the batch and the mixer body.
- Pneumatic control for operating the ram, drop door and to facilitate the automatic injection of carbon black and oil.
- Sensors and transducers to measure ram pressure (displacement) and power consumption.
- Computer control, using a 386 computer and Labtech Notebook 6.2 software [117], to enable efficient monitoring and control of the system. Rotor speed, batch and body temperature, power consumption and ram pressure (displacement) can be monitored throughout each mixing cycle. Rotor speed, ram movements, drop door, carbon black and oil injection can be automatically controlled.

3.1. Testing.

3.1.1. Negretti TMS biconical rheometer.

A Negretti TMS biconical rheometer was used to measure the shear stress of the experimental batches at different shear rates.

The TMS biconical rheometer is a variable speed rotational instrument. It has the basic configuration of the Mooney viscometer but differs mainly in its rotor design and the feeding of the material to be tested into the system. In the TMS biconical rheometer material is injected into the testing cavity by means of a transfer moulding system. This system offers several advantages: (i) the injection of material prior to testing allows precise dimensions of the cavity to be maintained; (ii) the hydrostatic pressure of the material in the cavity can be controlled; (iii) the system eliminates operator error during the filling of the samples [108]. The rotor is biconical for uniform shear rates over the rotor surface and grooved to prevent wall slip occurring during measurement.

The results from the TMS rheometer, as in chapter 4, are often given in terms of apparent viscosity. Apparent viscosity (η_a) is usually quoted as being the viscosity measured at a specified shear rate [37].

$$\eta_a = \frac{\tau}{\dot{\gamma}} \quad (3.1)$$

where η_a = apparent viscosity

τ = shear stress

$\dot{\gamma}$ = shear rate

When shear rate = 1 s^{-1} , η_a is referred to as the consistency constant (K).

| | | | |
|---------------|----------------------|---------------------|--------------|
| Temperature | Upper die | 100°C | |
| | Lower die | 100°C | |
| | Ram | 100°C | |
| Pre-heat time | 120 secs | | |
| Filling time | 120 secs | | |
| Test Mode | Varying shear stress | | |
| Sampling Rate | 10 readings/sec | | |
| No. of steps | 9 | | |
| Step | Time (sec) | Shear rate s^{-1} | Comment |
| 1 | 30 | 0.1 | Steady state |
| 2 | 30 | 0.2 | " |
| 3 | 30 | 0.6 | " |
| 4 | 18 | 1.0 | " |
| 5 | 15 | 1.5 | " |
| 6 | 12 | 4.0 | " |
| 7 | 9 | 10.0 | " |
| 8 | 6 | 25.0 | " |
| 9 | 4 | 50.0 | " |
| 10 | 3 | 100.0 | " |

Table 3.1 - The test sequence used for the TMS rheometer in chapter 4.

Similar conditions as in table 3.1 were used to determine the rate of disagglomeration in **chapter five** and for undertaking the investigative work in **chapter six**, except the testing procedure was 15 seconds at shear rates of 0.3, 1.0 and 3.0 s^{-1} . Also the filling time was minimised since the samples were placed around the rotor, rather than being injected. This was done to prevent any further disagglomeration taking place during testing. Care was taken to ensure the cavity was filled completely.

The test to test variation for the TMS rheometer used is estimated to be:

5% at shear rate 0.1 s^{-1}

3% at shear rate 1.0 s^{-1}

3.1.2. Monstanto Moving Die Rheometer (MDR).

A Monstanto MDR 2000 was used to study batch to batch variation in the final cured properties reported in chapter four.

The MDR is a rotorless curemeter which measures both elastic and viscous components of torque (modulus). Curemeters measure the change torque of a rubber compound with respect to time, ideally, at contact temperature. In an MDR the sample is sealed in a cavity formed by directly heated dies. The lower die oscillates at 1.66 Hz and the reaction torque is measured at the upper die [109,110].

The complex modulus (E^*) and the storage modulus (E') are recorded as a sine-function 16 times during each oscillation [14]. Using these values the micro-processor calculates the distance between the maximum storage modulus and a reference point (distance_a) and the distance between the maximum complex modulus and the same reference point (distance_b). The micro-processor then estimates $\tan\delta$ by using the equation:

$$\text{distance}_b - \text{distance}_a = \delta \quad (3.2)$$

| | |
|----------------------|---------------------------------|
| Die temperatures | 177 °C |
| Test time | 3 mins |
| Data points measured | maximum torque dNm (M_H) |
| | minimum torque dNm (M_L) |
| | $\tan \delta$ at Maximum torque |
| | scorch time secs (TSI) |

nb: scorch time = time to reach a rise of 1 dNm above the initial minimum torque.

Table 3.2 - The test procedure used for the MDR.

The test to test variation for the MDR rheometer used is estimated to be:

$$M_H = 1.5\%$$

$$M_L = 1.5\%$$

$$\tan \delta = 5.4\%$$

$$TSI = 1.8\%$$

CHAPTER FOUR.

AN INVESTIGATION TO STUDY THE EFFECT OF MIXING PARAMETERS ON THE EFFICIENCY OF MASTICATION.

4.0 Objectives.

This work was designed to improve the understanding of how mixing parameters affect the efficiency of the mastication of natural rubber in the internal mixer.

The investigation was conducted in three distinct parts:-

Part One: To evaluate how the rotor speed, water temperature and mixing time influence the efficiency of mastication. This also enabled the analysis of the correlation between rotor revolutions and mastication.

Part Two: To analyse the effect of fill factor on mastication.

Part Three: To determine how variation in the initial viscosity of the premasticated grade of raw rubber effects the final properties of a N660 carbon black/natural rubber compound.

4.1 General experimental details.

All mastication/mixing was undertaken on a semi-automated laboratory Farrel BR Banbury (see section 3.0).

All experimental work was undertaken on a premasticated grade of SMR L natural rubber. It was essential that the viscosity of the natural rubber used for experiments in part one and two was consistent. This was achieved by storing sufficient sheets from one bale of rubber to complete the experiments. Each sheet selected was checked for consistency by taking three samples for Mooney viscosity testing (see section 3.1.1).

After each batch was dumped the temperature of the rubber was measured using a hand held temperature probe to obtain an accurate final temperature value.

The apparent viscosity (η_a) of each batch was measured using a Negretti TMS biconical rheometer, as discussed in section 3.1.1. The efficiency of mastication was expressed in terms of the reduction of the apparent viscosity. In part three, when mixed rubber compounds were produced, a Monstanto MDR 2000 curemeter was used to study batch to batch variation in the final cured properties, as discussed in section 3.1.2.

An experimental design and optimising program developed by the Avon Rubber Company was used to undertake regression analysis of the results [118]. This

program selects the best regression equation by means of a Tukey's criterion (see Appendix 1).

4.2 Part One - The effect of mixing time, water temperature and rotor speed on the efficiency of mastication.

4.2.1 Experimental procedure.

4.2.1.1 Experiment One.

A central composite experimental design was produced which varied the conditions for mastication. The design consisted of a three variable, two level, full factorial design with star points and six centre points.

| Batch no. | *Name | Rotor Speed | Time | Water Temp |
|-----------|-------|-------------|-------------|-------------|
| 1 | HHH | +1 | +1 | +1 |
| 2 | HHL | +1 | +1 | -1 |
| 3 | HLH | +1 | -1 | +1 |
| 4 | LHH | -1 | +1 | +1 |
| 5 | HLL | +1 | -1 | -1 |
| 6 | LLH | -1 | -1 | +1 |
| 7 | LHL | -1 | +1 | -1 |
| 8 | LLL | -1 | -1 | -1 |
| 9 | VLMM | $-\sqrt{2}$ | 0 | 0 |
| 10 | VHMM | $+\sqrt{2}$ | 0 | 0 |
| 11 | MVLM | 0 | $-\sqrt{2}$ | 0 |
| 12 | MVHM | 0 | $+\sqrt{2}$ | 0 |
| 13 | MMVL | 0 | 0 | $-\sqrt{2}$ |
| 14 | MMVH | 0 | 0 | $+\sqrt{2}$ |
| T5-20 | MMM | 0 | 0 | 0 |

* Name ordering: Rotor speed/mixing time/water temperature.

Table 4.1 - Experimental design for part one, experiment one.

This gave a total of twenty batches to be masticated. This design enabled non-linear regression analysis to be conducted on results and for all interactions between variables to be studied.

| Variables | Values for points | | | | |
|--------------------|-------------------|----|----|-----|-------------|
| | $\sqrt{-2}$ | -1 | 0 | +1 | $\sqrt{+2}$ |
| Rotor speed (rpm) | 30 | 43 | 75 | 107 | 120 |
| Mixing time (secs) | 0 | 26 | 90 | 154 | 180 |
| Water temp (°C) | 20 | 27 | 45 | 63 | 70 |

The fill factor used for each batch was 56%.

Table 4.2 - Defined ranges used in part one, experiment one.

All twenty batches were masticated in series. The batches were mixed in increasing temperature order, to reduce waiting time for water temperature changes. To check that there was no gradual build up in temperature from batch to batch the body thermocouples were monitored after each batch to ensure that the next batch was not mixed until it had reached the set water temperature value.

4.2.1.2. Experiment Two.

In addition, a smaller second experiment was undertaken to study whether the efficiency of mastication is dependent on rotor speed if the total number of rotor revolutions is constant.

In the experiment rotor speed was varied from 60 ---> 120 rpm and mixing time was altered accordingly, so that each batch received 90 rotor revolutions. Water temperature was maintained at 45 C and the fill factor again was 56%.

4.2.2. Results for part one.

4.2.2.1. Results for experiment one.

| Batch | Name | Final temp °C | η_a at $\dot{\gamma}$ 0.1 s ⁻¹ kPa.S | η_a at $\dot{\gamma}$ 1.0 s ⁻¹ kPa.S |
|-------|------|---------------|---|---|
| 1 | HHH | 120 | 588.8 | 109.65 |
| 2 | HHL | 103 | 549.5 | 107.15 |
| 3 | HLH | 94 | 776.2 | 131.83 |
| 4 | LHH | 100 | 660.7 | 117.49 |
| 5 | HLL | 76 | 724.4 | 123.03 |
| 6 | LLH | 73 | 831.8 | 128.82 |
| 7 | LHL | 80 | 575.4 | 107.15 |
| 8 | LLL | 49 | 776.2 | 141.25 |
| 9 | VLMM | 75 | 724.4 | 123.03 |
| 10 | VHMM | 118 | 602.6 | 112.2 |
| 11 | MVLM | *25 | 871.0 | 134.9 |
| 12 | MVHM | 109 | 588.8 | 109.65 |
| 13 | MMVL | 84 | 588.8 | 109.65 |
| 14 | MMVH | 115 | 679.1 | 120.23 |
| 15 | MMM1 | 97 | 631.0 | 114.82 |
| 16 | MMM2 | 97 | 645.7 | 114.82 |
| 17 | MMM3 | 97 | 645.7 | 114.82 |
| 18 | MMM4 | 97 | 645.7 | 114.82 |
| 19 | MMM5 | 97 | 631.0 | 114.82 |
| 20 | MMM6 | 97 | 631.0 | 112.2 |

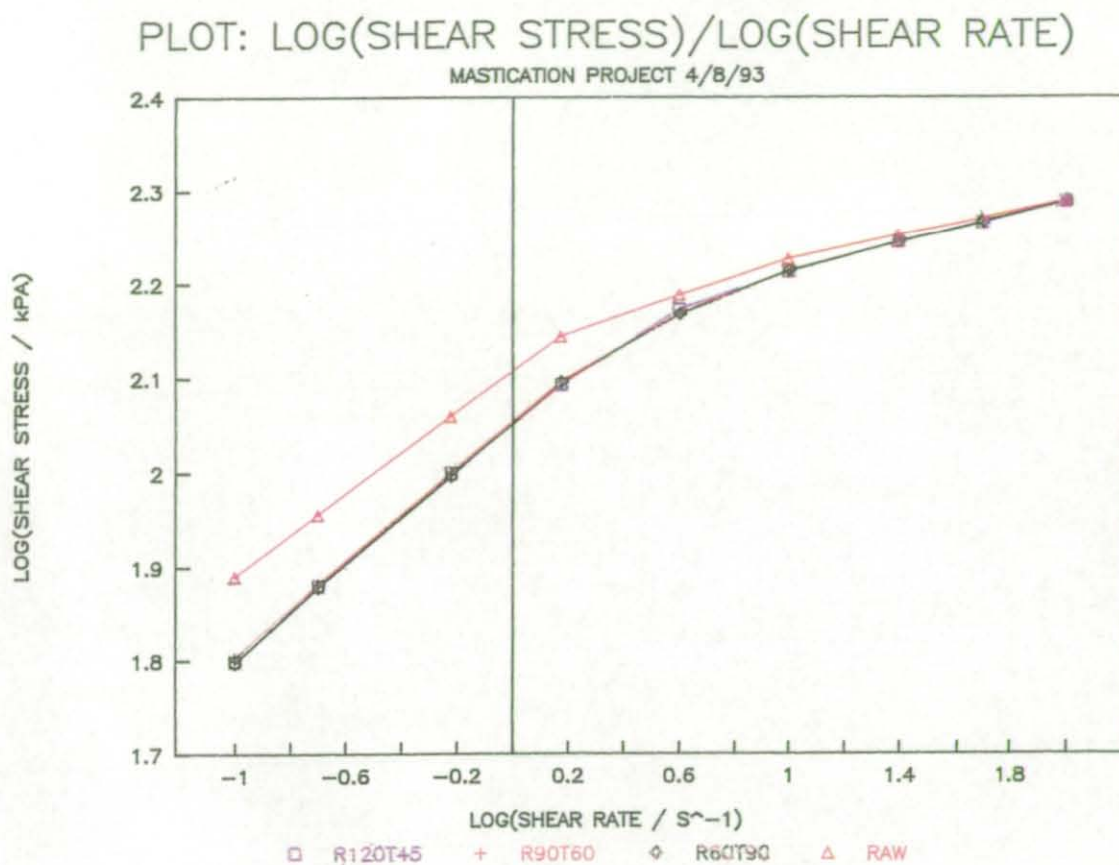
nb: Final batch temperature measured using hand held probe.

* Not mixed.

** Naming system the same as before: Rotor speed/mixing time/water temperature.

Table 4.3 - TMS biconical rheometer results and final dump temperature for part one, experiment one.

4.2.2.2. Results for experiment two.



nb: R120T45 = rotor speed at 120 rpm and mixing time at 45 secs

Figure 4.1 - TMS results for part one, experiment two.

4.2.3. Regression analysis of the results.

The statistical package revealed no significant correlations between the input parameters, therefore regression analysis using all the parameters was valid.

Abbreviations used: Mixing time = M

Rotor speed = S

Water temperature = W

Rotor revolutions = R

The empirical model used was a second order polynomial function which has the form:

$$y = \beta_0 + \beta_1 M + \beta_2 S + \beta_3 W + \beta_{11} M^2 + \beta_{22} S^2 + \beta_{33} W^2 + \beta_{12} MS + \beta_{13} MW + \beta_{23} SW \quad (4.1)$$

For a definition of the coefficient R-squared see Appendix 1.

The "best" regression equations generated -

For η_a :

$$\text{at } 0.1 \text{ s}^{-1} = 637 - 94.3M + 42.7M^2 - 31.3S + 29.7W + 9.45S^2 - 6.38MS \quad (42)$$

R-squared = 98.7%

$$\text{at } 1.0 \text{ s}^{-1} = 115 - 9.71M + 3.85M^2 - 3.13S + 2.01W + 1.85S^2 + 2.0WM + 1.75WS \quad (43)$$

R-squared = 91%

For % difference between the η_a before and after mastication:

$$\text{at } 0.1 \text{ s}^{-1} = 26.8 + 10.8M - 4.89M^2 + 3.6S - 3.4W - 1.06S^2 + 0.738WS \quad (44)$$

R-squared = 98.7%

$$\text{at } 1.0 \text{ s}^{-1} = 13.7 + 7.31M - 2.91M^2 + 2.35S - 1.51W - 1.41S^2 - 1.51WM - 1.31WS \quad (45)$$

R-squared = 91.1%

For temperature of the rubber at dump:

$$T = 96.9 + 19.1M + 12.7S^2 - 13.7M + 10.2W + 2.52W^2 \quad (46)$$

R-squared = 92.4%

Regression analysis on the results from experiment one was also undertaken in terms of rotor revolutions (mixing time * rotor speed).

| Variables | Values for points | | | | |
|-------------------|-------------------|----|-------|-----|-------------|
| | $-\sqrt{2}$ | +1 | 0 | +1 | $+\sqrt{2}$ |
| Rotor revolutions | 0 | 40 | 137.5 | 235 | 275 |
| Water temp °C | 20 | 27 | 45 | 63 | 70 |

Table 4.4 The defined ranges used when time and speed were expressed in terms of rotor revolutions.

The "best" regression equations generated were.

For η_a :

at $0.1 \text{ s}^{-1} = 612 - 96.1R + 54.8R^2 + 29.7W - 7.77W^2$ (4.7)

R-squared = 97.4%

at $1.0 \text{ s}^{-1} = 112 - 9.65R + 5.6R^2 + 2.01W$ (4.8)

R-squared = 87%

A selection of Cartesian line graphs to illustrate the results.

These two dimensional graphs show apparent viscosity (at a shear rate 1 s^{-1}) on the y-axis. One of the three variables is on the x-axis and its relationship with another variable is represented by graphing numerous lines of the physical properties with different levels of the variable. The remaining variable was kept constant at its centre point.

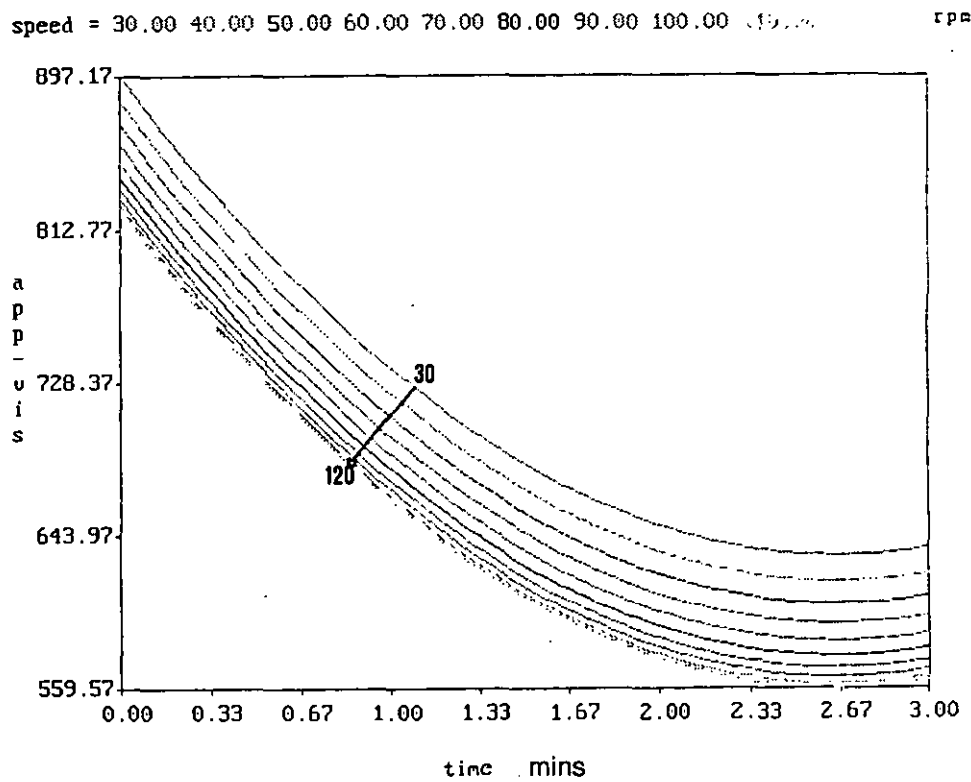


Figure 4.2 - Rotor speed/mixing time.

speed = 30.00 40.00 50.00 60.00 70.00 80.00 90.00 100.00 110.00 120.00 rpm

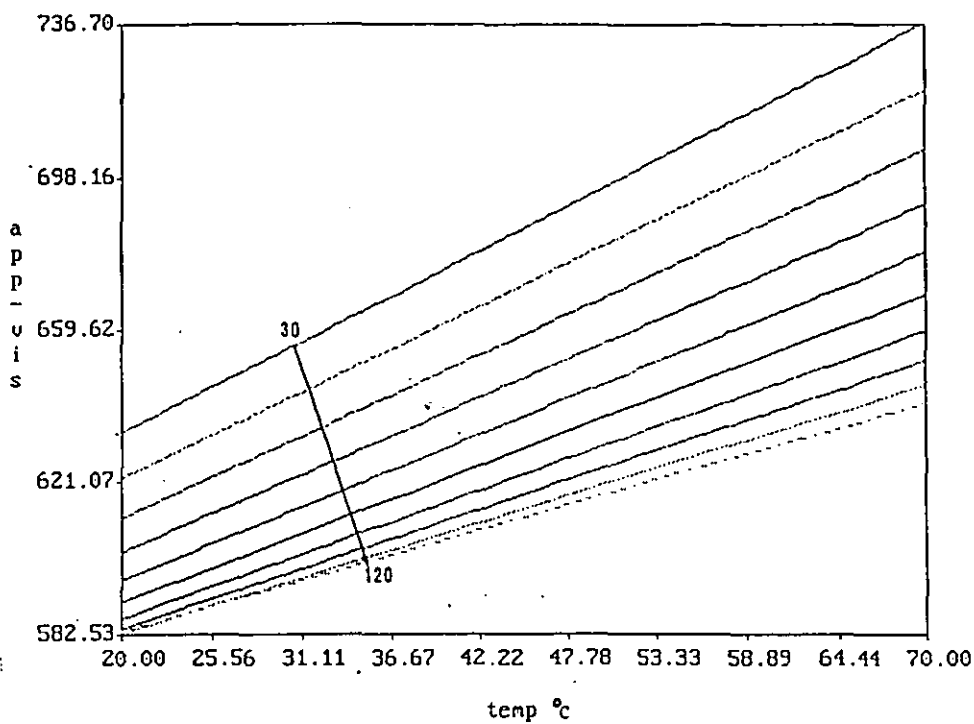


Figure 4.3 - Rotor speed/water temperature.

time = 0.00 0.33 0.67 1.00 1.33 1.67 2.00 2.33 2.67 3.00 mins

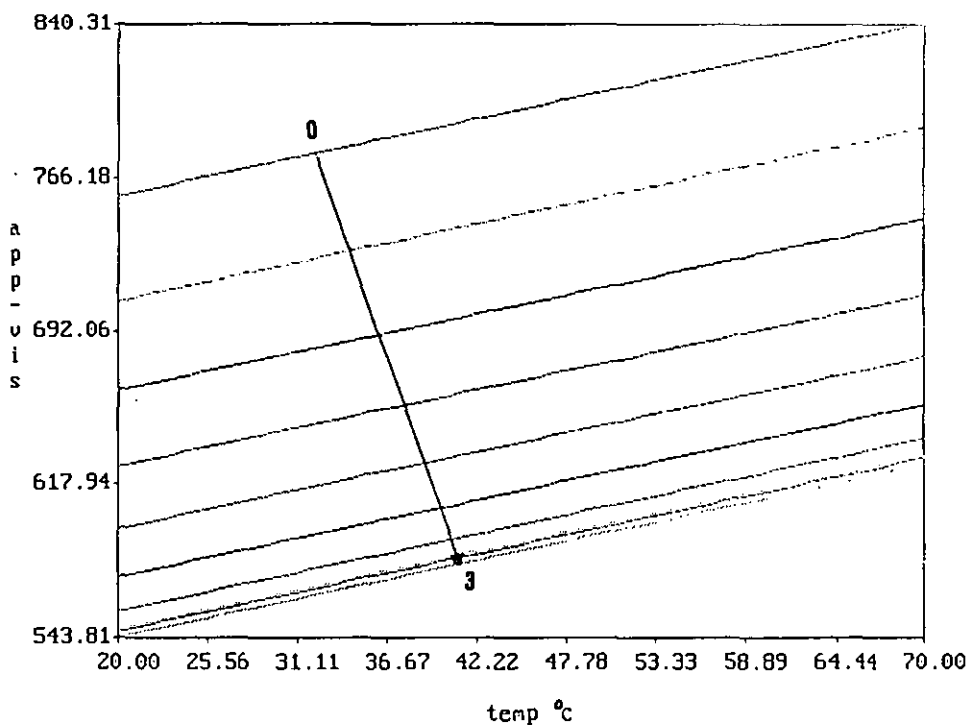


Figure 4.4 - Mixing time/water temperature.

4.2.4. Summary of findings in part one.

Ranking for Full factorial

HHL, LHL, HHH, LHH, HLL, HLH, LLL, LLH

—————▶
Increased final viscosity
ie reduced mastication efficiency

As anticipated from previous findings [56,58], it was found that rotor speed water temperature and mixing time all have an effect on the efficiency of mastication. The most effective combination was when rotor speed and mixing time were high and water temperature was low; under these optimum conditions it was possible to reduce the η_a of the natural rubber used by 37%. At the other end of the scale the least effective combination was when rotor speed and mixing time was low and water temperature was high, under these conditions it was only possible to reduce the η_a of the natural rubber by 5%. The reason for this was that the optimum combination of parameters would have resulted in the natural rubber receiving the largest cumulative amount of shearing stress whilst the worst combination would have been exposed to the least. From the temperature results it can be seen that, because of the low volume to surface area ratio in the Farrel BR Banbury, the final temperature of some batches was above 115°C so the effect of thermo-oxidative mastication would have been a factor in this experiment (see section 2.6.1.)[47].

4.2.4.1. The effect of mixing time.

The regression analysis showed that the mixing time was the most dominant variable over the ranges studied. It was also shown that the rate at which viscosity decreases becomes progressively slower as mixing time increases until eventually a steady state is reached. From the results it was calculated that approximately 30% of the reduction in η_a occurred in the first 30 seconds of mixing (see figure 4.2 & 4.4). This is because the conditions for cold mastication are superior at the early stages of a mixing cycle.

4.2.4.2. The effect of rotor speed.

It was found that as rotor speed increased step changes had progressively less effect on the efficiency of mastication (see figure 4.2 & 4.3).

4.2.4.3. The effect of water temperature.

Under the experimental conditions employed, it was found that water temperature had a linear response with respect to η_a (see figure 4.3 & 4.4). It was observed that there was some interaction between rotor speed and water temperature. Step changes at low rotor speeds have more of an effect on the efficiency of mastication at high water temperatures rather than at lower water temperatures. However at high rotor speeds water temperature has significantly less effect. This must be directly related to the variation in rubber temperature achieved under the different conditions. The results

suggest that at low rotor speeds step increases in water temperature progressively move the temperature of the rubber into the region where mastication is at a minimum. This is due to the characteristic U shape curve for mastication with respect to temperature (see figure 2.3). Whilst at high rotor speeds, irrespective of water temperature, the temperature of the rubber is much more likely to be sufficient for thermo-oxidative breakdown to occur.

4.2.4.4. The effect of the mixing parameters on the dump temperature of the batch.

Regression analysis was also undertaken between the final rubber temperature after mastication and the three variables. It was found that the final temperature of the rubber is dependent on all three variables and also that there is no interaction between the variables. Mixing time was shown to have the most significant effect. Rotor speed had a linear relationship with final rubber temperature whilst the other variables had a quadratic relationship.

4.2.4.5. Rotor revolutions.

A correlation between the results from experiment one for η_a (at shear rate 0.1 s^{-1}) and 'total' number of rotor revolutions produced a R-squared value of 97.4%. This shows that the number of rotor revolutions received correlates well with the efficiency of mastication.

In experiment two it was found that if the same number of rotor revolutions was undertaken and the rubber temperature at dump was approximately the same, (in this experiment between 90 and 92°C) a consistent reduction in viscosity was achieved independent of rotor speed (see figure 4.1).

4.3. Part Two - The effect of fill factor on the efficiency of mastication.

4.3.1. Experimental procedure.

A two level experimental design was produced which examined the effect of fill factor and mixing time on the efficiency of mastication and their interaction.

| Batch no. | Fill factor | Mixing time |
|-----------|-------------|-------------|
| 1 | +1 | +1 |
| 2 | +1 | -1 |
| 3 | -1 | +1 |
| 4 | +1 | -1 |
| 5 | 0 | 0 |

Table 4.5 - Experimental design for part two.

This resulted in five batches needing to be masticated.

| Variables | Values for points | | |
|--------------------|-------------------|----|-----|
| | -1 | 0 | +1 |
| Fill factor (%) | 35 | 55 | 75 |
| Mixing time (secs) | 30 | 75 | 120 |

Rotor speed and water temperature were maintained at 75 rpm and 45°C

Table 4.6 - The defined ranges used in part two.

4.3.2. Results for part two.

| Batch no. | Final temp °C | η_a at $\dot{\gamma}$ 0.1 s ⁻¹ kPa.s | η_a at $\dot{\gamma}$ 1.0 s ⁻¹ kPa.s |
|-----------|---------------|--|--|
| 1 | 120 | 588.8 | 104.7 |
| 2 | 91 | 691.8 | 112.2 |
| 3 | 86 | 602.6 | 107.2 |
| 4 | 71 | 741.3 | 120.2 |
| 5 | 100 | 645.7 | 117.5 |
| RAW | | 776.2 | 125.9 |

nb: Final temperature of batch measured using hand held probe.

Table 4.7 Results for part two.

4.3.3 Regression analysis of the results.

The statistical package revealed no significant correlations between the two input parameters therefore regression analyses using both the parameters was valid.

Abbreviations used:

Fill factor = F

Mixing time = M

Shear rate = $\dot{\gamma}$

The "best" regression equations generated.

For η_a :

$$\text{at } 0.1 \text{ s-l} = 654 - 60.4F - 15.8M + 8.93FM \quad (4.9)$$

$$R\text{-squared} = 99.5\%$$

$$\text{at } 1.0 \text{ s-l} = 112 - 6.47F - 1.3M + 0.193F^2 \quad (4.10)$$

$$R\text{-squared} = 100\%$$

For % difference between the η_a of the rubber before and after mastication at:

$$\text{at } 0.1 \text{ s-l} = 15.7 + 7.77F + 2.04M - 1.13FM \quad (4.11)$$

$$R\text{-squared} = 97.9\%$$

$$\text{at } 1.0 \text{ s-l} = 10.9 + 4.96F + 0.99M - 0.2FM \quad (4.12)$$

$$R\text{-squared} = 99.9\%$$

For temperature of the rubber at dump:

$$T = 100 + 13.5F + 11M - 8F^2 \quad (4.13)$$

$$R\text{-squared} = 96.3\%$$

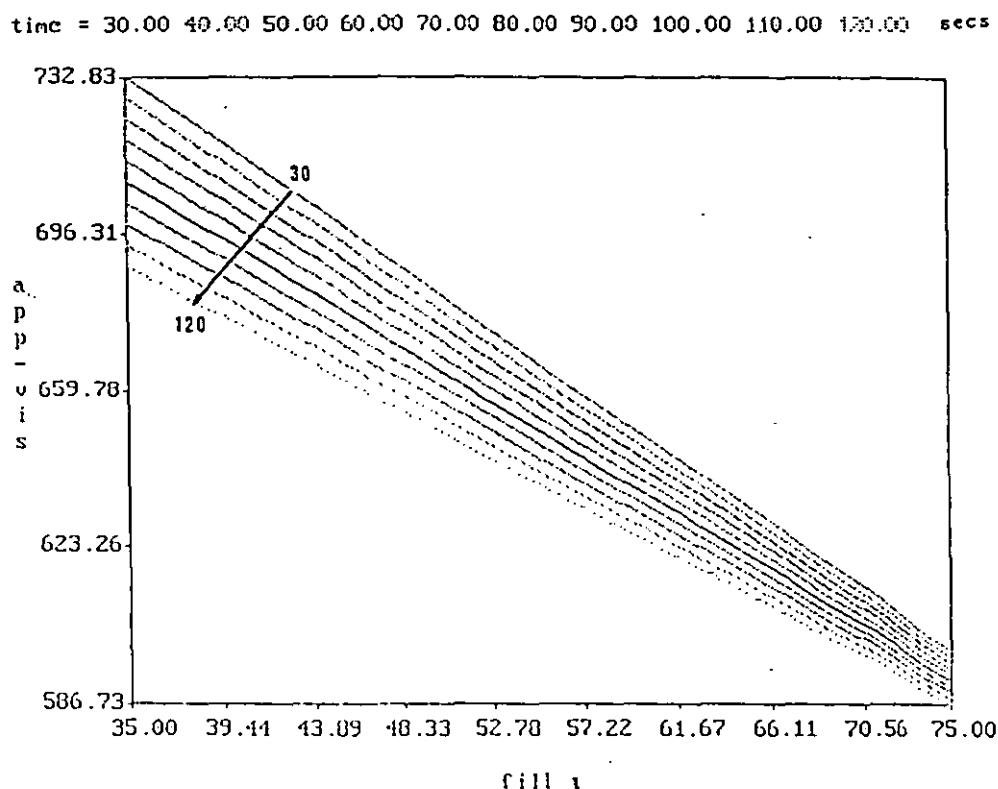


Figure 4.5 - A Cartesian line graph illustrating the relationship between fill factor and mixing time.

4.3.4. Summary of findings in part two.

The results indicate that fill factor has a greater effect on the efficiency of mastication than mixing time, therefore indicating that fill factor is the most significant parameter of those studied. For the laboratory mixer fill factor has a linear relationship with apparent viscosity over the range covered (see figure 4.5). As a very rough "rule of thumb" it was found that for the laboratory Farrel BR Banbury a 10% increase in fill factor caused a 3.5% reduction in apparent viscosity. Figure 4.5 also indicates some interaction between the two variables, as fill factor increases then the effect of variation in mixing time reduces.

4.4. Part Three - A study to determine how variation in the initial viscosity of the premasticated grade of SMR L natural rubber affects the final properties of the rubber compound.

Natural rubber is not a consistent material. There are inconsistencies from tree to tree, plantation to plantation and from country to country. Compounders and rubber technologists have for some considerable time suggested the inconsistency in the initial viscosity of natural rubber as a possible source of final property variation. As a consequence it was decided to add this section to the mastication response project. The objectives were:

- (i) To study the variation in viscosity of premasticated SMR L natural rubber.
- (ii) To mix batches in the laboratory Farrel BR Banbury, using raw rubber with different initial viscosity, to determine what level of variation would persist after mastication, single stage mixing and passing through a simulated two-roll mill train.

4.4.1. Experimental procedure.

Over a period of three months samples of premasticated SMR L natural rubber were collected at random. A batch was prepared from each of the samples collected using a single stage mixing cycle. The mixing conditions were selected using simulation rules developed within the Teaching Company project, to enable simulation by the laboratory Farrel BR Banbury and a 16" laboratory mill of mixing and milling in a factory system comprising of a Carter 3D Banbury mixer and an 80" two roll mill [111]. The details of both the mixing and the milling cycle used in this experiment are specified below. The rubber compound produced contained 27 phr of a N660 carbon black and a traditional sulphur curing system.

The mixing conditions selected comprised:

(1) Mixing procedure (Single Stage).

| | |
|-----------------------|------------------------|
| Total Mixing time | 300 secs |
| Mastication time | 70 secs |
| Sulphur addition time | 194 secs |
| Lab fill factor | 65% |
| Rotor speed | 40 -70 rpm at 245 secs |
| Water temperature | 40C |
| Ram pressure | 80 psi |

(2) Milling procedure.

| Time (secs) | Action |
|-------------|----------------------------------|
| 0 | Feed batch onto mill |
| 0 - 180 | Allow rubber to pass through nip |
| 180 - 200 | Unload mill |

Repeat a further three times

Parameters.

| | |
|-----------------------|----------------------------|
| Nip setting | 4 mm |
| Roll temperature | 45 C |
| Band thickness | 260 mm |
| Front/back roll speed | 12.0/14.5 rpm respectively |

Two sets of seven batches were mixed:

Set one - the rubber was removed from the Banbury after mastication.

Set two - the rubber was mixed, and then milled.

Testing:

Samples from of each of the seven sheets were collected for TMS biconical rheometer testing.

Set one - TMS biconical rheometer testing.

Set two - TMS biconical rheometer and MDR curemeter testing both after mixing and milling.

4.4.2. Results for part three.

| | Incoming SMR L to Special. Mixing | | After Mast. | | After Mixing. | | After Mill Train | |
|--|--|-----|----------------|-----|------------------|-------------------------|---------------------|-------------------------|
| Results | Mean Val. | StD | Mean Val. | StD | Mean Val. | StD | Mean Val. | StD |
| TMS | | | | | | | | |
| η_a at $\dot{\gamma}$ 0.1 s ⁻¹ kPa.s | 894 | 107 | 661 | 57 | 479 | 31 | 281 | 13 |
| η_a at $\dot{\gamma}$ 1.0 s ⁻¹ kPa.s | 133 | 10 | 114 | 6 | 88 | 4 | 64 | 2 |
| MDR | | | | | | | | |
| M _L dNm | | | | | 1.3 | .06 | .91 | .03 |
| M _H dNm | | | | | 11 | .22 | 10.7 | .14 |
| Tan δ | | | | | .022 | 1 * 10 ⁻³ | .021 | 4 * 10 ⁻⁴ |
| TS1 secs | | | | | .45 | 2 * 10 ⁻² | .44 | 0 |

nb: for defintion of standard deviation (StD) see appendix 1.

Table 4.8 - The test results showing the mean and standard deviation of the batches as they progressed through the laboratory simulation of the mixing process.

4.4.3. Summary of findings in part three.

It was calculated that the variation in η_a (at $\dot{\gamma}$ 0.1 s⁻¹) between the samples collected was approximately 12.07%.

As the rubber progressed through the mixing process the amount of variation between the batches reduced to the extent that the difference between the properties measured with the MDR curemeter and TMS biconical rheometer were not significantly greater than the test variation (see sections 3.1.1. and 3.1.2.). The reduction in variation was most significant during the first 70 sec mastication stage when the standard deviation was reduced by just under 50%.

4.5. Recommendation for the control of mastication for single stage mixing.

As stated in section 2.2, rubber compounds are traditionally mixed using a two stage mixing process rather than a more economical single stage process for two main reasons:-

- (1) The amount of work put into the mixing process is significantly reduced in a single stage process which makes it more difficult to get consistent physical properties from batch to batch.
- (2) The risk of the compound scorching when the curatives are added in a single stage process due to the sharp rise in batch temperature during the initial stages of

mixing.

The rotor revolution results suggest that a satisfactory way to control the mastication stage of mixing, to overcome both these problems, would be to mix to a designated number of rotor revolutions to ensure consistent reduction in viscosity from batch to batch and then control the temperature profile of the mix by altering the rotor speed. This would enable the rubber to be masticated to a specified viscosity and temperature.

It must be recognised however that this recommendation comes from work done on a laboratory Banbury mixer. In a production internal mixer, where the efficiency of heat transfer is severely reduced due to the ratio of mixer surface area to chamber volume being much smaller, it may not be possible to control temperature sufficiently by changing rotor speed.

CHAPTER FIVE

DEVELOPMENT OF A PREDICTIVE MODEL FOR THE RUBBER MIXING PROCESS.

5.0 Introduction.

Objective: To develop an initial computerised model that can predict the rubber temperature and power traces during mixing in an internal mixer, depending on the materials and mixing parameters.

As already stated in the Introduction, this investigation was not in the original statements of objectives but was evolved during the project. There are substantial pressures on the rubber industry to reduce costs whilst still maintaining quality. If the mixing process can be fully quantified and predictions made about performance, then major advances are possible in the development of mixing cycles. A predictive model would remove the need to perform expensive time consuming experiments each time more data is required since by simulating the mixing process the computer program would quickly enable optimum mixing cycles in terms of both quality and productivity to be determined. Consequently this would reduce lead times for new compounds and improve overall productivity.

The investigation into the effect mixing parameters, in an internal mixer, have upon

the efficiency of mastication (detailed chapter four) suggested that the development of a predictive model was viable. The mastication study illustrated that each of the mixing parameters (water temperature, rotor speed, mixing time and fill factor) have an effect on the mixing conditions which is significant, repeatable and that the effect of each of parameter could be isolated from each other. The mixing data collected during the mastication was used as the main source of data to develop an initial predictive model.

This chapter discusses the development of an initial predictive model for a laboratory BR Banbury mixer (see section 3.0) for the mastication of a premasticated SMR L natural rubber and dispersive mixing with 27 phr of N660 carbon black.

5.1. Benefits of a predictive model.

(1) Batch thermocouples in internal mixers are subjected to both steady-state errors and transient errors relating to poor thermal response (see section 2.4). A predictive model would enable the prediction of true batch temperature rise during the mixing process. A compounder/rubber technologist could then, given the maximum temperature to which a compound could safely be mixed and subsequently processed, use the model to set the processing parameters between these limits and maximise the mixing performance.

(2) By having the ability to predict both power and temperature changes during mixing it would be possible to predict the state of mix of a compound during mixing

and therefore establish the minimum effective mixing cycle required to achieve a desired state of mix.

(3) If the model was fully utilised it would be possible to incorporate a scaling system between different sizes of mixer. The effects of mixing compounds in different size mixers could then be examined with the view of maximising throughput at lowest possible cost.

5.2 Overall development of the model.

The model operates by predicting the energy supplied and lost in the mixing process as a function of material and machine behaviour. From these predictions the energy absorbed into the system by the mixing action can be estimated and this estimation can then be used to determine the temperature rise in the rubber. The model is iterative, each iteration based on changes that occur in one rotor revolution.

5.2.1 Operation of model.

Temperature rise in the rubber is described as a function of the energy absorbed from the mixing action (dW).

Each rotor revolution iteration is calculated in the following way:

Let R = a single rotor revolution

Total energy generated in R rotor revolutions = dW (input)

where dW (input) = average applied rotor torque (TQ) during R revolution * angular displacement.

Therefore as working in one rotor revolution iterations

$$dW \text{ (input)} = \text{average TQ during R revolution} * 2\pi \quad (5.1)$$

The applied rotor torque is estimated after the completion of each rotor revolution; an average torque during R rotor revolution is calculated using the previous estimated torque value ie at the end of R-1 rotor revolution.

$$dW \text{ (input)} = ((TQ(R) + TQ (R-1))/2) * 2\pi \quad (5.2)$$

Energy lost to the mixer body and the rotors = dW (lost)

The dW during R rotor revolution is therefore

$$dW = dW \text{ (input)} - dW \text{ (lost)}. \quad (5.3)$$

Temperature rise during R rotor revolution = dT,

$$\text{where } dT = dW / \text{heat capacity of materials} \quad (5.4)$$

The rise in batch temperature after R rotor revolution is calculated by adding the dT to the previous cumulative total. The cumulative rise in rubber temperature is calculated by adding together the calculated dT for each rotor revolution undertaken.

This initial predictive model was developed on a spreadsheet using Supercalc software [119]. The advantage of using a spreadsheet format was that the effect of each of the terms could be clearly studied throughout each mixing cycle.

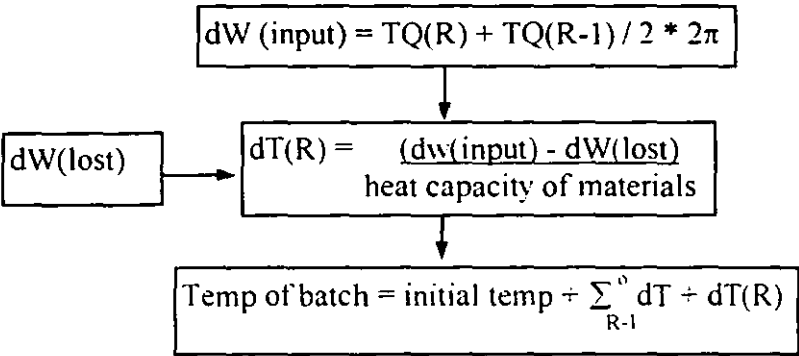


Figure 5.1 A flow chart of the overall model.

5.3 Development of the part of the model for predicting the energy generated (dW (input)).

5.3.1 During Mastication.

For simplicity the model was initially developed to predict only the energy generated during mastication.

As already stated

$$dW \text{ (input)} = \text{average rotor torque (TQ) during R revolution} * 2\pi. \quad (5.1)$$

The TQ is determined after the completion of each rotor revolution as a function of rotor speed, compound viscosity, batch temperature, fill factor and a machine factor.

$$TQ = f(\text{rotor speed, rate of mastication, batch temperature, fill factor, machine factor}) \quad (5.5)$$

When the model is running, it is the terms for the rate of mastication and rubber temperature that reduce the rotor torque to simulate the reduction in viscosity and the increase in batch temperature. The rest of the terms set the initial conditions.

Relationships and constants for these different factors were largely determined from the results of the mastication investigation (detailed in section 4.2).

The plots generated to determine the constants and details of additional mixing cycles undertaken are detailed in Appendix 2. Table 5.3 on page 113 shows the constants calculated.

5.3.1.1 Effect of speed.

The change in rotor torque (TQ) in the mixer was assumed to have a "power-law" relationship with rotor speed [37,107].

$$TQ = K M_a (\text{rotor speed})^n \quad (5.6)$$

The consistency constant K is equal to the initial apparent viscosity of the raw rubber as measured at a shear rate ($\dot{\gamma}$) of 1 s^{-1} in a Negretti TMS biconical rotor rheometer (for test procedure see 3.1.1).

The power-law index n was calculated from the slope of the plot $\log(\text{rotor torque})$ vs $\log(\text{rotor speed})$ obtained from the Farrel BR Banbury. The magnitude of the n value calculated in this way was approximately the same as the average n value calculated from plotting $\log(\dot{\gamma})$ vs $\log(\tau)$, obtained from the TMS biconical rheometer, for all the mastication mixes studied.

A machine factor (M_a) was derived as a constant of proportionality for the relationship between the consistency constant of the power-law equation and rotor speed. It was altered slightly from mix to mix to take into consideration that when the ram is lowered the temperature of the batch will be slightly different depending upon the water temperature and rotor speed during loading, which in turn will result in the torque being slightly different.

$$M_a = 0.00291e^{-0.02 (\text{temp of batch at ram down} - 25)} \quad (5.7)$$

The temperature at ram down was calculated using the following equation.

$$\text{temp. at ram down} = 25.8 + 0.239 (\text{rotor speed rpm}) + 0.210 (\text{water temp } ^\circ\text{C}) \quad (5.8)$$

This equation was generated by undertaking a small factorial experiment which varied the water temperature and rotor speed during the loading of the rubber. The rubber was then dumped immediately as the ram was lowered and the temperature of the rubber measured using a hand held probe. This equation assumes the loading of the rubber and the lowering of the ram always takes 30 seconds.

It was also necessary to establish the "minimum value (mv)" of rotor torque for the Farrel BR Banbury as the torque remained constant at this value. This was necessary otherwise the predicted torque value would continue decreasing due to the format of the model. The mv value was calculated from the minimum torques achieved in the series of mixes.

5.3.1.2 Effect of batch temperature.

The effect of batch temperature on rotor torque (TQ) was modelled by assuming a similar relationship to the temperature dependence of apparent viscosity (η_a) of a polymer i.e.

$$\eta_a = Ae^{-bT} \text{ where } A \text{ and } b \text{ are constants and } T \text{ is temperature [37].}$$

It was therefore represented in the following way:

$$TQ_{\text{final}} = TQ_{\text{initial}} e^{-bT} \quad (59)$$

The constant b , the batch temperature constant, for this model was determined by plotting $\ln(\text{rotor torque})$ vs batch temperature. Data was obtained from short mixing cycles undertaken in the Farrel BR Banbury.

5.3.1.3 Effect of mastication.

The effect of mastication on TQ was estimated by establishing a relationship between η_a/η_{ai} and the number of rotor revolutions undertaken, where η_{ai} is the initial apparent viscosity of the rubber and η_a is the apparent viscosity after R rotor revolutions. The values of η_a were determined at a shear rate of 1 s^{-1} in a Negretti TMS biconical rheometer (for test procedure see 3.1.1). A linear relationship was produced when $1/(\eta_a/\eta_{ai})^2$ vs number of rotor revolutions was plotted. The rate of mastication with rotor revolutions was expressed in the form:

$$\eta_a/\eta_{ai} = \sqrt{\frac{1}{d(R) + y_0}} \quad (510)$$

Where d is the slope of the plot, denoted mastication constant one and y_0 is $1/(\eta_a/\eta_{ai})^2$ when the number of rotor revolutions equals 0, denoted mastication constant two. In this model, for simplicity, it is assumed that the reduction in viscosity is only dependent on the number of rotor revolution undertaken and independent of other mixing conditions.

5.3.1.4 Effect of fill factor.

The relationship between fill factor and rotor torque (TQ) was given as:

$$TQ = Ge^{x(\frac{FF}{100})} \quad (511)$$

Where G and x are constants calculated using experimental data obtained from the Farrel BR Banbury. The fill factor constant, x, equals the slope of the plot Ln(rotor torque) vs fill factor.

5.3.2 During dispersive mixing.

A series of mixes were undertaken to study dispersive mixing when 27 phr of N660 carbon black was added to the masticated rubber. The details of these mixes are given in Appendix 2.

No attempt was made to model the power and temperature trace during the loading of the carbon black when the ram was up. Due to the relatively low loading of carbon black in this initial model the "second power peak" (see section 2.6.2.1.) occurred almost as soon as the ram was fully lowered. It was assumed that carbon black incorporation had occurred at this point and it was not necessary to model filler incorporation in this initial model.

The changes made to the mastication model to include dispersive mixing comprise:

- (1) A separate function for the reduction in viscosity due to disagglomeration of the carbon black (see section 5.3.2.1).
- (2) Reduction of the effect of mastication to take into account that immobilised rubber within the carbon black agglomerates would not be available for mastication. The rubber available for mastication would equal $1 - \text{effective filler fraction}$ (see section 5.3.2.2).
- (3) The constant K and the power index value n were altered to take into consideration the addition of carbon black (see section 5.3.2.3).

5.3.2.1 Determination of the rate of disagglomeration (in terms of rotor revolutions).

Disagglomeration results in a reduction in viscosity by causing a decrease in the effective volume fraction of filler in the compound (see section 2.7.1). It is not possible to examine the disagglomeration process in the absence of mastication. However the effect of mastication on the viscosity of the compound was isolated from the effect of disagglomeration by studying values of relative shear stress rather than apparent viscosity. Relative shear stress (RS) is determined, in this project by dividing the shear stress of the compound, as measured at a shear rate of 1 s^{-1} using

a Negretti TMS bioconical rheometer (for test procedure see 3.1.1), by that of the rubber masticated under similar mixing conditions. As with the rate of mastication it was assumed that the reduction in viscosity due to disagglomeration was only dependent on the number of rotor revolutions and independent of other mixing conditions.

The rubber and the carbon black were mixed in a series of stages to obtain the relationship between relative shear stress vs rotor revolutions (see appendix two for details). The rubber was initially masticated and then the carbon black was added. After a short period of mixing the compound was discharged and a sample of approximately 25g was taken. The remainder of the compound was then fed back into the mixer for the second stage of mixing. The compound was repeatedly discharged from and replaced into the mixer until seven samples had been taken. The shear stress of the samples was then measured on the Negretti TMS biconical rheometer at a shear rate of 1 s^{-1} (see section 3.1.1). To calculate RS the rubber was then masticated under the same conditions as those used for the mixed compound.

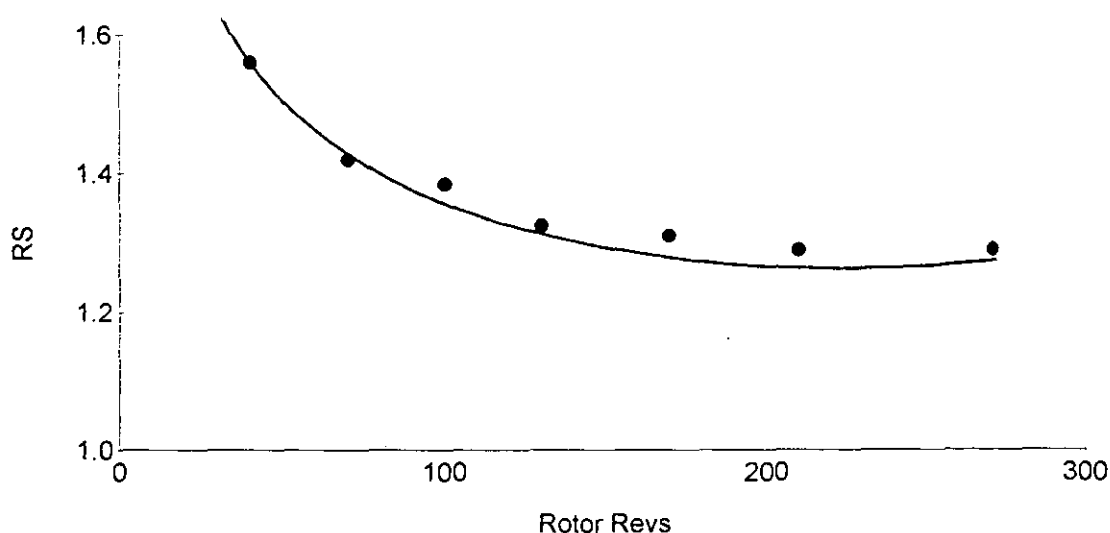


Figure 5.2 - RS vs rotor revolutions.

By plotting $\ln(RS)$ vs rotor revolutions the following relationship was produced (see figure 5.3). For simplicity no allowance has been made for the rubber mastication mixes to increase either the mixing time of the batch or the strain rate at which the shear stress was measured to take into consideration strain amplification (see section 2.7.1).

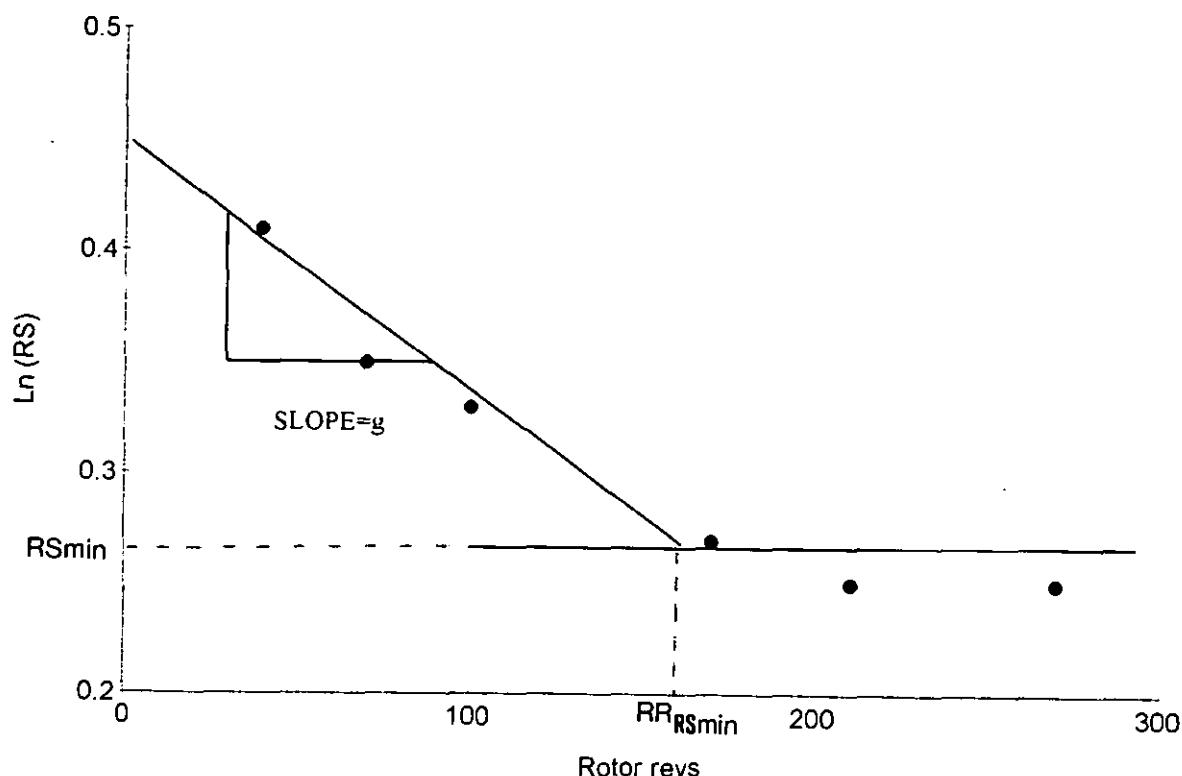


Figure 5.3 - $\ln(RS)$ vs rotor revolutions.

g = Rate of disagglomeration.

RS_{min} = Minimum RS achievable under mixing conditions.

RR_{RSmin} = Number of rotor revolutions to RS_{min} .

The term $e^{-g(RR)}$ was added into the model to take account of the effect of disagglomeration on viscosity, where RR equals the number of rotor revolutions after

the carbon black was incorporated. RS_{min} and $RR_{RS_{min}}$ can also be estimated from this graph. When $RR_{RS_{min}}$ have been undertaken, the model assumes that the maximum amount of disagglomeration possible in the internal mixer has been achieved and that no further reduction on viscosity will occur due to disagglomeration.

5.3.2.2 Determination of the effective filler volume.

The effective volume fraction of filler includes the carbon black itself plus the rubber which is immobilised within the agglomerates. In order to determine the effective volume fraction of filler in a compound it is first necessary to ascertain the amount of immobilised rubber present in an agglomerate. The DBPA value (see section 2.5.2.) for the carbon black can be used to determine the amount of immobilised rubber in an agglomerate [63].

The volume fraction of immobilised rubber in an agglomerate (σ)

$$= \text{DBPA} / [\text{DBPA} + (100/P_{cb})] \quad (512)$$

where DBPA = DBPA value ($\text{cm}^3/100\text{g}$)

P_{cb} = Density of carbon black (gcm^{-3})

The effective volume fraction of filler at different stages of the mix was calculated using the equation [63]:

$$\phi_e = (\phi_a * \sigma) + \phi_t \quad (513)$$

where ϕ_e = effective volume fraction of filler,

ϕ_a = volume fraction of agglomerates,

ϕ_t = volume fraction of carbon black (as calculated from the true density of carbon black).

The volume fraction of agglomerates can be calculated by determining the morphology of thin sections of samples using a video camera and monitor attached to a light microscope. However, as this is a long and tedious process it was decided not to undertake this procedure but to estimate the maximum and minimum effective volume fractions and then use the curve produced for rate of disagglomeration to determine the reduction in effective filler volume with rotor revolutions (see figure 5.2 on page 84). The maximum effective volume fraction was estimated with the assumption that at 0 secs of dispersive mixing 100% of the carbon black is in the form of agglomerates, whilst the minimum effective volume was taken to equal the true volume fraction of carbon black. Thus it was assumed that complete disagglomeration was achieved in the mixer.

5.3.2.3. Changing the consistency constant K and the power index value n.

The decrease in the consistency constant K for the compound (K_c) as mixing progresses was determined using the following equation [112]. The TMS biconical rheometer results from the mastication investigation discussed in section 4.2 were used to determine K_{rr} .

$$K_c = K_{rr} (1 + \alpha_1 \phi t + \alpha_2 \psi + \alpha_{11} \phi t^2 + \alpha_{22} \psi^2 + \alpha_{12} \phi t \psi) \quad (514)$$

where ϕt = volume fraction of carbon black

K_{rr} = K initial - reduction due to mastication

ψ = Specific surface area of carbon black ($m^2/100g$)

$\alpha_1, \alpha_2, \alpha_{11}, \alpha_{22}, \alpha_{12}$ = Constants

$$\alpha_1 = -.1024$$

$$\alpha_2 = 0.3094 * 10^{-2}$$

$$\alpha_{11} = 13.54$$

$$\alpha_{22} = -0.3028 * 10^{-5}$$

$$\alpha_{12} = 0.01610$$

It was initially intended that the power index (n) for the compound (nc) would be calculated using the following equations [112].

$$\frac{d(\log \eta_r)}{d(\log \gamma)} = n^1 + \beta_1 \phi t + \beta_2 \psi + \beta_{12} \phi t \psi \quad (515)$$

$$nc = 1 - \frac{d(\log \eta_r)}{d(\log \gamma)} \quad (516)$$

where: n^1 = the slope of the plot $\log \eta_g$ vs $\log \gamma$

ψ = specific surface area of carbon black ($m^2/100g$)

η_r and η_g = apparent viscosity of the compound and gum respectively

ϕt = volume fraction of carbon black

$\beta_1, \beta_2, \beta_{12}$ = constants

However the resulting value calculated was found to be too low to give the appropriate second peak in torque when the carbon black was added. The reason for this is perhaps due to the fact that this equation was generated for predicting viscosity measurements from a TMS biconical rheometer whilst in this investigation a relationship between rotor torque and speed in a Farrel BR Banbury was required. In a Farrel BR Banbury more complex flows occur, involving both transient and elongational flows. The correct relationship was obtained from plotting log (second power peak in torque) vs log (rotor speed) in a similar manner as in the initial mastication model (see section 5.3.1.1.).

5.4. Development of the part of the model for predicting the energy lost from the mixer (dW (output)).

The investigations for this part of the model resulted in the development of another sub-model referred to as the heat transfer model. The heat transfer model, like the predictive model, determines the true temperature profile of the rubber in the mixer by calculating the energy balance between the energy supplied to and lost from the system. However the heat transfer model uses actual power traces to determine the energy supplied and therefore cannot be used independently of mixing data. This approach was taken since it enabled one part of the energy balance equation, the energy output part of the model, to be developed and verified separately from the total predictive model. The heat transfer model calculates the energy going out of the mixer by determining the heat flow from the rubber to the mixer body and the rotors. The heat flow in turn is determined by the employment of heat transfer coefficients.

Initially it was decided to undertake a large statistical analysis using the mixing data from the mastication response project (see section 4.2) and from the mixing cycles used to develop the energy input part of the model (see appendix two) to analyse the effect mixing parameters have on the temperature profile. The relationships between the variables were then used to aid in the development of the heat transfer model.

This part of the investigation was therefore in two parts:

Part One: Statistical analysis.

Part Two: Validation of the heat transfer model.

5.4.1. Statistical analysis.

The statistical package Minitab Statistical Software [120] was used for the analysis. The first thing that became apparent was the inaccuracy of the batch thermocouple in the laboratory BR Banbury mixer. The thermocouple in the laboratory mixer is attached to an end plate and protrudes into the centre of the mixer. Figure 5.4 compares the final dump temperatures measured by the thermocouple with those measured by the hand held probe taken to provide a true value of temperature. If there was no difference between the two forms of measurement they would lie on the 45° line which is designated the direct line. This was observed not to be the case; the thermocouple in the mixer measured consistently lower than the true values measured and also there was a significant scatter in the level of error. It is believed, from previous studies [42], that the errors are caused by the poor thermal conductivity of the rubber, the large heat capacity of the batch thermocouple and the heat conduction

from the batch thermocouple through its supporting structure. Both the batch and the mixer thermocouples in the BR laboratory are J type thermocouples.

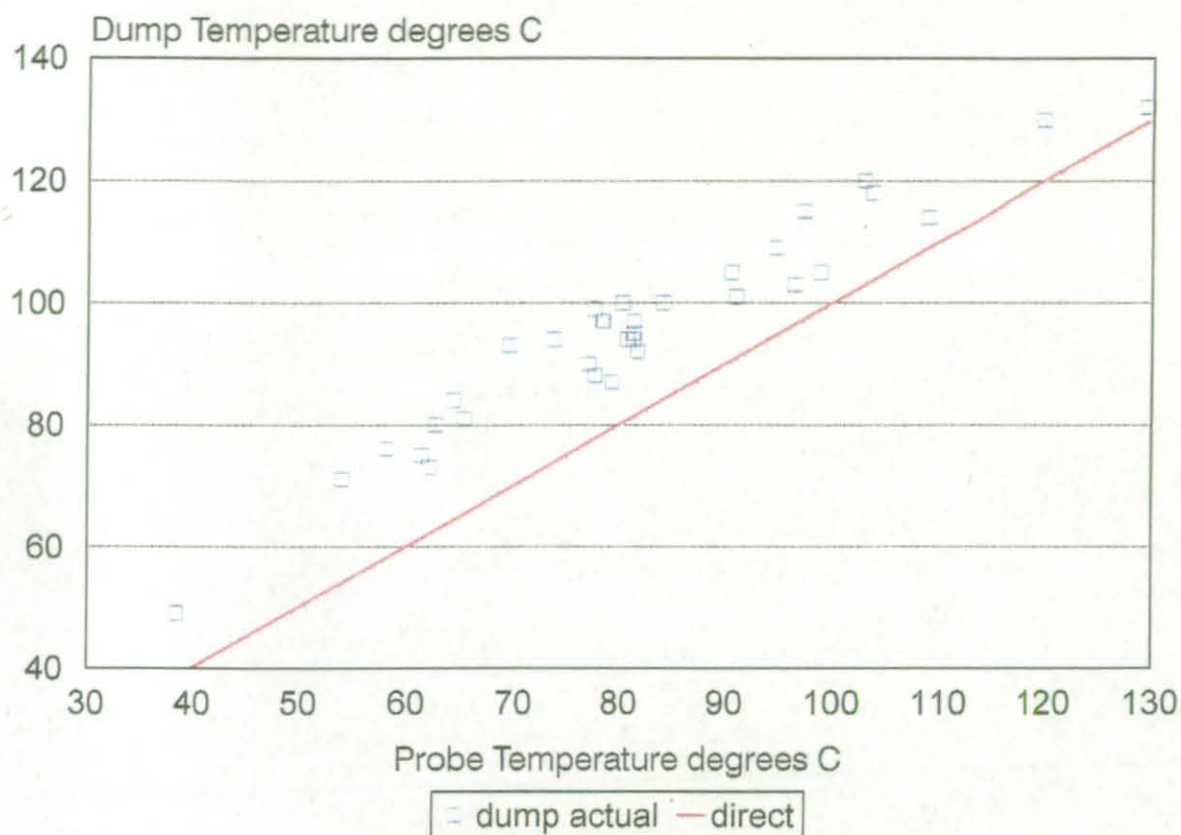


Figure 5.4 - Measured dumped rubber vs probe.

By correlating the final batch thermocouple values with the true temperatures values, the following regression equations were generated to significantly improve the accuracy of the actual temperature profile. It was found that the level of errors was reduced further if individual equations were made for the gum and carbon black filled mixes.

For gum:

$$\text{Rubber temp} = -215 + 71.3 \log (\text{batch therm.}) \quad (517)$$

$$\text{R-squared} = 96.8\%$$

For carbon black filled:

$$\text{Rubber temp} = 29.8 + 0.78 (\text{batch therm.}) \quad (518)$$

$$\text{R-squared} = 95.4\%$$

For a definition of the adjusted correlation coefficient, R-squared, see Appendix 1.

At the time of formulation it was anticipated that these regression equations would be compound dependent (see section 6.6) as the rate of heat transfer from the batch to the thermocouple is dependent on the loading of carbon black. The efficiency of heat transfer from the rubber to the thermocouple improves with the addition of carbon black due to the improved thermal conductivity. Figure 5.5 illustrates the improvements achieved by using independent regression equations for the gum and black filled rubbers.

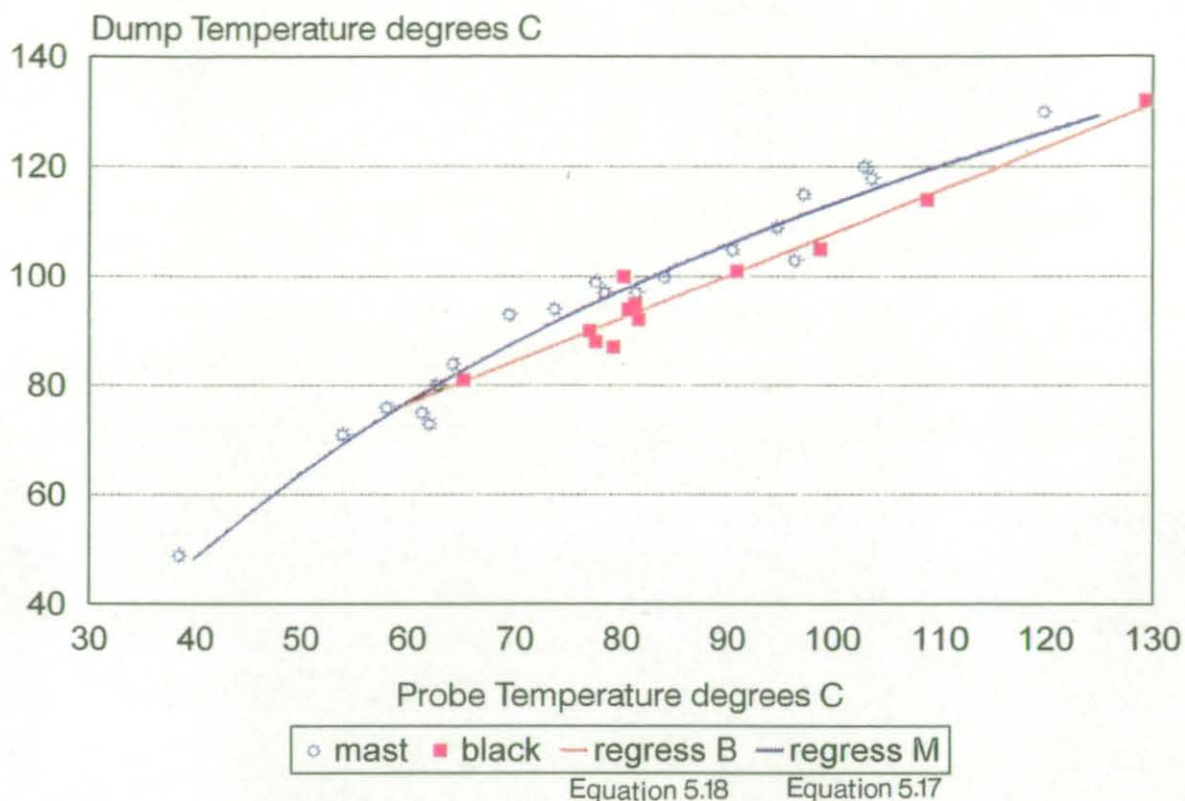


Figure 5.5 - Improved prediction of final dump temperature using regression equations.

To determine the effect other mixing parameters have on the temperature profile of the rubber the following parameters for each of the mixes were analysed:

- (1) Mixing time (secs).
- (2) Energy input (integral of power * time / heat capacity of materials) (J).
- (3) Final power / heat capacity of the materials (W).
- (4) Initial temperature of the mixer as measured by the mixer thermocouple (°C).
- (5) Final temperature of the mixer body as measured by the mixer thermocouple (°C).
- (6) Heat capacity of the materials (JK^{-1}).

- (7) Rotor speed (rps).
- (8) Final batch temperature as measured by the batch thermocouple in the mixer (°C).
- (9) The final true temperature of the batch measured using the hand held probe (°C).

The first statistical analysis undertaken was to generate the best linear regression equations (BREG), using the Minitab to determine the true final temperature of the batch using the other mixing variables. For an explanation of how the software does this and definitions for the standard error of estimate (Std) and the adjusted correlation coefficient (R-squared) see Appendix 1.

| No. of variables | c1 | c2 | c3 | c4 | c5 | c6 | c7 | c8 | s | R-sq |
|------------------|----|----|----|----|----|----|----|----|------|------|
| 1 | | | | | | | | X | 5.4 | 90.4 |
| 1 | | X | | | | | | | 12.8 | 46.7 |
| 2 | | | | | | | X | X | 4.9 | 92.3 |
| 2 | X | | | | | | | X | 5.2 | 91.3 |
| 3 | | | | X | | | X | X | 4.6 | 93.1 |
| 3 | | | | | X | | X | X | 4.6 | 93.1 |
| 4 | | X | X | | | | X | X | 4.4 | 93.8 |
| 4 | | | X | X | | | X | X | 4.5 | 93.5 |
| 5 | | | X | X | | X | X | X | 4.2 | 94.2 |
| 5 | X | X | X | | | | X | X | 4.3 | 94.1 |
| 6 | | | X | X | X | X | X | X | 4.2 | 94.3 |
| 6 | X | X | X | | | X | X | X | 4.2 | 94.2 |
| 7 | X | X | X | X | X | X | X | X | 4.1 | 94.4 |
| 7 | | X | X | X | X | X | X | X | 4.2 | 94.3 |
| 8 | X | X | X | X | X | X | X | X | 4.2 | 94.2 |

Definition of columns c1 - c8, the units are the same as listed on page 93.

c1 = Mixing time

c2 = Total energy

c3 = Final power / heat capacity

c4 = Initial mixer temperature (mixer thermocouple)

c5 = Final mixer temperature (mixer thermocouple)

c6 = Heat capacity

c7 = Rotor speed

c8 = Final batch thermocouple reading

Table 5.1 - The best linear regressions generated by the minitab, using the BREG function.

A correlation analysis was also undertaken to assess the association between the variables. For a definition of the measurement of correlation see Appendix 1.

| | c1 | c2 | c3 | c4 | c5 | c6 | c7 | c8 |
|----|-------|-------|-------|-------|------|-------|------|------|
| c2 | .432 | | | | | | | |
| c3 | -.370 | .602 | | | | | | |
| c4 | -.180 | -.412 | -.303 | | | | | |
| c5 | -.094 | -.188 | -.169 | .968 | | | | |
| c6 | .195 | -.178 | -.409 | .443 | .489 | | | |
| c7 | -.309 | .634 | .840 | -.095 | .065 | -.235 | | |
| c8 | .128 | .541 | .384 | .428 | .631 | .469 | .571 | |
| c9 | -.037 | .474 | .466 | .451 | .627 | .397 | .664 | .944 |

Same column definitions as for table 5.1, note c9 = final true temperature of the batch

Table 5.2 - A correlation of the variables.

5.4.1.1. Summary of findings from the statistical analysis.

From table 5.1 the best linear fit would be the first choice when five variables had been picked. This equation had the lowest s value and the highest R-sq without both the start and final mixer temperatures being present in the equation. The software warned against using an equation with both the start and final mixer temperature being included because they are highly correlated as illustrated in table 5.2. The regressions suggested in table 5.1 significantly improved the accuracy of predicting the dump temperature of the rubber. However, due to the way these regressions were produced, they were not as efficient at simulating the shape of the temperature profile as the separate probe regression equations for the batch during mastication (5.17) and dispersive mixing (5.18). This often results in the final true temperature of the batch being predicted prematurely in the mixing cycle.

The most significant variable, as expected, was the final true temperature of the batch and this was followed by rotor speed. From table 5.1 it can be seen that the software very quickly picked up rotor speed as an important variable. This is most likely to be because the speed correlates well with the energy input into the system as confirmed in Table 5.2. However rotor speed also controls the rate at which the mixer body is exposed to new rubber surfaces. This observation led to the heat transfer coefficient in the heat transfer model being made speed dependent.

It was noted that particularly good correlations were observed between:

- (1) Initial mixer temperature and rotor speed.
- (2) Initial and final mixer temperatures.
- (3) The batch thermocouple and the actual temperature of the rubber at dump.

It was expected that this statistical analysis would lead to the development of an algorithm that would be an improvement on equations 5.17 and 5.18 using both the batch thermocouple and the mixer body thermocouple to predict the temperature profile. However, from table 5.1, it can be seen that when the software had the option of picking two variables it did not pair the batch thermocouple with the mixer thermocouple, suggesting that there is very little connection between them. The reason for this is likely to be because of their relative positions to each other. As already stated the batch thermocouple is attached to an end plate and protrudes out between the two rotors whilst the mixer thermocouple is attached to the sideframe of the mixing chamber. This means that they are spatially far apart in the mixer and also

their relative access to the cooling water system differs greatly. Therefore their ability to transfer heat from their respective supporting structure to the cooling water system is substantially different.

Moore and Brett [42] (see section 2.4) reported a study to determine how batch thermocouple predictions could be improved. They found monitoring of rubber temperature could be improved by measuring the temperature gradient between thermocouples. However in their work the thermocouples were in close proximity to each other. The preceding statistical analysis shows that if the thermocouples are far apart no benefit is obtained by trying to relate their readings.

5.4.2. Validation of the heat transfer model.

As already stated the heat transfer model, like the predictive model, is basically an energy balance model; it operates by predicting the amount of energy absorbed into the system in a one second interval. This prediction is then used to estimate the temperature rise in the rubber. The energy supplied is taken from the power input with corrections made to take into consideration energy lost in the drive system. The energy lost from the system is determined by predicting the heat flow from the rubber to the mixer body and rotors.

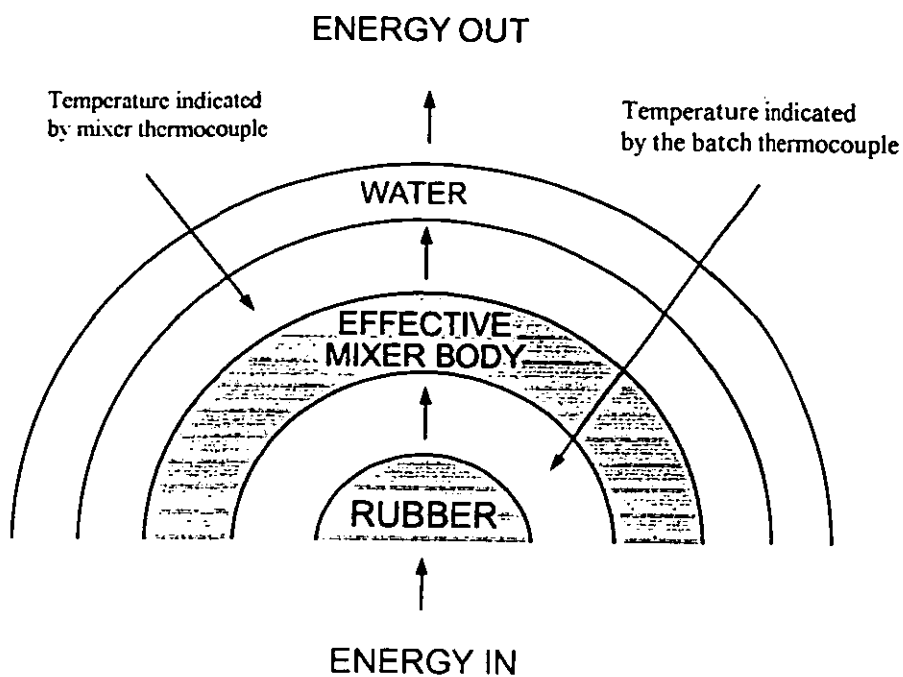
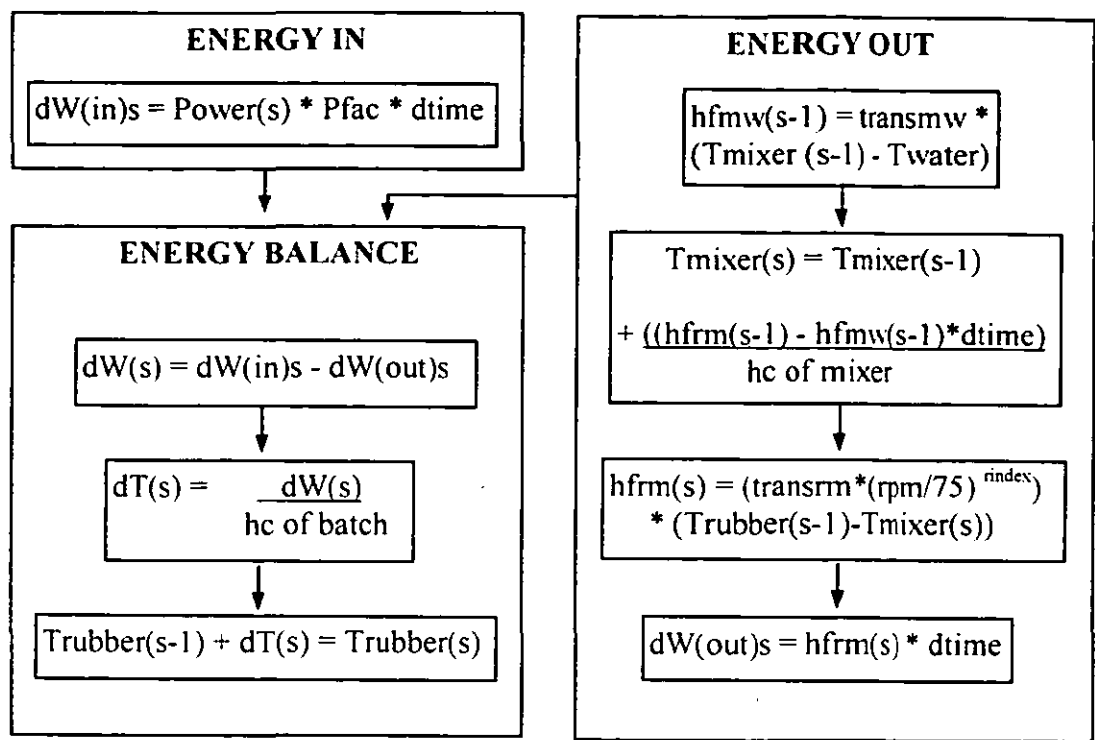


Figure 5.6 - A simplified diagram of how the model works. It also indicates the temperatures measured by the batch thermocouple and the mixer thermocouple.

5.4.2.1. Operation of the model



| | |
|---------|--|
| Pfac | = power converted to heat (%) |
| dTime | = interval of time = 1 |
| hfmw | = heat flow mixer to the water (W) |
| transmw | = heat transfer coefficient from mixer to the water |
| T | = temperature (°C) |
| s | = a second interval |
| hc | = heat capacity (JK ⁻¹) |
| hfrm | = heat flow rubber to mixer (W) |
| tranrm | = heat transfer coefficient from the rubber to the mixer |
| rindex | = index for the dependence of transrm on rotor speed |
| dT | = rise in temperature (°C) |
| dW | = energy absorbed (J) |

Figure 5.7 - Overall flow chart of the heat transfer model.

The rotors and the mixer body masses are combined to form "an effective mixer body" for the purpose of this analysis.

To predict the heat flow from the rubber to the effective mixer body it was thought necessary to account for the following parameters.

- (1) The heat capacity of the effective mixer body (hc of mixer JK^{-1}).
- (2) The heat transfer coefficient from the rubber to the effective mixer body ($transrm$). The value of this constant depends on:
 - (i) Whether the carbon black has been added.
 - (ii) On the rotor speed, as expressed by a speed index ($rindex$)
- (3) The heat transfer coefficient from the effective mixer body to the water ($transmw$).

These constants were deduced by sequentially varying each parameter and selecting the combination which gave the lowest sum of squares of errors on the final measured rubber temperatures. This process was repeated until there was no further improvement in the fit. It was found that the value of each parameter was significant showing that all the terms in the model are necessary. The heat transfer coefficients in this model are not in the classical engineering form but are terms for the combined effect of thermal conductivity and mode of contact.

It should be noted that the speed indices used to express the effect of rotor speed on heat transfer vary significantly from 0.74 during mastication to 1.61 during dispersive

mixing. An index of 1 would suggest that the heat transfer is controlled by the replacement of rubber in contact with the effective mixer body at each rotor revolution. An index less than 1 suggests that normal thermal conductivity is having an effect. Whilst an index of greater than 1 suggests that either the flow of rubber is more fractured or that slippage increases at higher rates [37]. Both result in more rapid exposure of the rubber to the effective mixer body. The use of an index greater than 1 in this model has been validated statistically; the index of 1.61 gives a sum of squares of errors of 216 for 13 mixes whereas an index of 1 gives a sum of 397. Therefore the high index is justified.

Other known parameters required to generate the model are:

- (5) Mixer power profile (power W).
- (6) Heat capacity of rubber compound (H_c of materials JK^{-1}).
- (7) Time of carbon black incorporation (secs). In this initial model, like the predictive model, this was assumed to occur as soon as the ram was lowered (see section 5.3.2).
- (8) The proportion of power converted to heat in the batch (P_{fac} %) [115].
- (9) The set water temperature (t_{water} $^{\circ}\text{C}$).

5.4.2.2. Development of the model.

Originally the constants 1, 2, and 3 (as identified on page 101) were deduced by running the model and getting least square fits when compared with both the final true rubber temperature and the final mixer thermocouple readings. This assumed that the temperature of the effective mixer body could be reflected by the values recorded by the mixer thermocouple attached to the sideframe of the mixing chamber. However this assumption was re-examined after finding that a better optimisation could be achieved for the final rubber temperature if the mixer thermocouple readings were ignored. This finding was consistent with the failure to develop an adequate algorithm for predicting the temperature of the rubber, using the relationship between the mixer thermocouple and the batch thermocouple (see section 5.4.1.1.). It suggested that the temperature of the effective mixer body is not uniform which is consistent with previous findings (see figure 5.10) [115]. The resulting constants for 1, 2 and 3 suggest the the effective mixer body is hotter than indicated by the mixer thermocouple. The reason for this is likely to be due to the position of the mixer thermocouple. The design of a Farrel BR Banburys means the ability to transfer heat from the rotors, the end plates and the drop door to the cooling water is less than that of the main sideframe of the mixing chamber where the mixer thermocouple is situated. With this concept in mind the constants 1, 2, and 3 were again deduced in a similar manner as before but only utilising least square fits using the final true batch temperatures and assuming that the effective mixer body temperature will be hotter than indicated by the mixer thermocouple.

To validate the heat transfer model the predicted rubber temperatures generated were used to simulate the response of the batch thermocouple in the mixer. This was achieved using a thermocouple algorithm that works in a similar manner to the main part of the model (see equation 5.19). The constants for this algorithm were similarly generated by running the algorithm and getting least squared fits on the final batch thermocouple values. The temperature values indicated by the batch thermocouple, as illustrated in figure 5.6, are between the mixer temperature and the rubber temperature.

The thermocouple algorithm uses the predicted rubber temperatures, simulated using the heat transfer model, to predict the temperatures indicated by the batch thermocouple in the mixer.

$$T_p(s) = T_p(s-1) + \frac{((\text{transrp} * (\text{Trubber}(s) - T_p(s-1))) - (\text{transpm} * (T_p(s-1) - T_{pst})))}{\text{hc of therm.}}$$

Where

s = time (secs)

T_p = predicted batch thermocouple values (°C)

Trubber = predicted temperature of the rubber determined using the heat transfer model (°C)

T_{pst} = initial batch thermocouple value (°C)

transrp1 = heat transfer coefficient from rubber to batch thermocouple before addition of carbon black = 0.4

transrp2 = heat transfer coefficient from rubber to batch thermocouple after addition of carbon black = 0.6

transpm = heat transfer coefficient from thermocouple to effective mixer body
= 0.1

hc of therm. = heat capacity of batch thermocouple = 10

As already stated the temperature values indicated by the mixer thermocouple are between the mixer temperature and the water temperature (figure 5.4). For this reason the predicted temperature profile of the effective mixer body in the proceeding graphs has been reduced depending on the water temperature (5.20). This was undertaken to show that the temperature rise of the effective mixer body, as generated by the heat transfer model, is the same as that indicated by the mixer thermocouple.

The following equation uses the effective mixer body temperature, simulated by the heat transfer model, to predict the temperature indicated by the mixer thermocouple.

$$T_m = (T_{\text{mixer}} * wf) + (T_{\text{water}} * (1-wf)) \quad (5.20)$$

Where

T_m = predicted mixer thermocouple values (°C)

T_{mixer} = predicted effective mixer body temperature simulated by heat transfer model (°C)

wf = conversion factor = .32 [115]

T_{water} = set water temperature (°C)

5.4.2.3. Examples of temperature profiles produced from the heat transfer model.

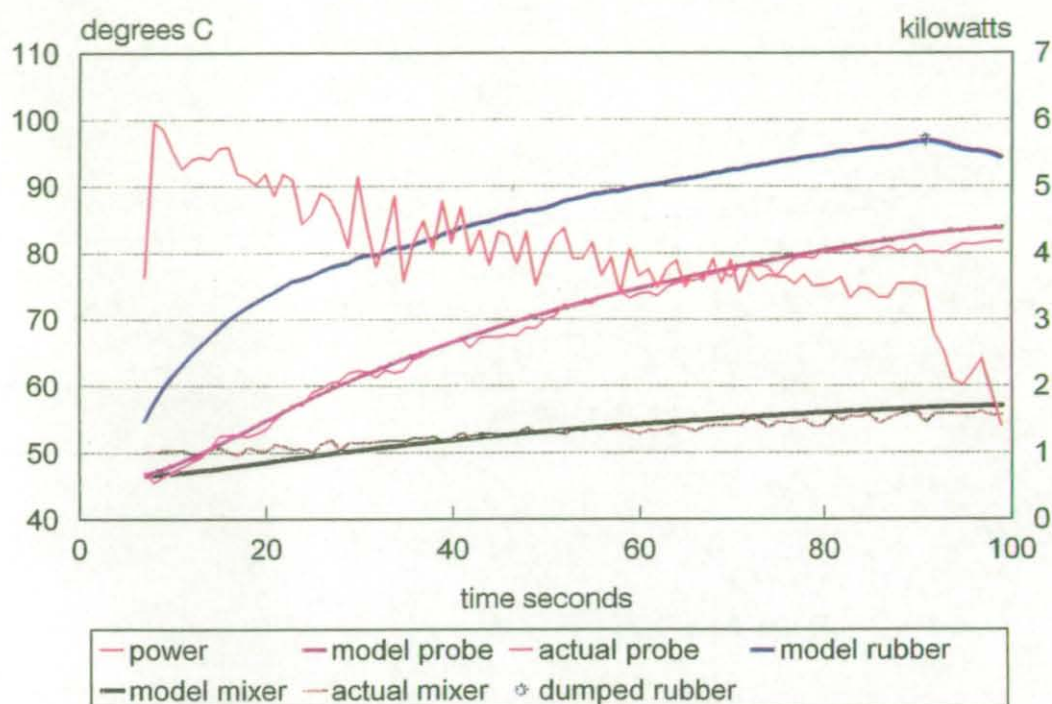


Figure 5.8 - A predicted temperature profile using the heat transfer model.

Figure 5.8 shows a predicted temperature profile during mastication; the batch thermocouple profile predicted by the thermocouple algorithm is very close to the actual measurements. The shape of the predicted and actual mixer thermocouple measurements also correspond closely. The temperature profile predicted by the heat transfer model for the rubber is also shown. At dump, the predicted temperature 97°C matches the temperature actually measured. Finally the power trace is shown so the amount energy being put into the system can be compared with the temperature traces.

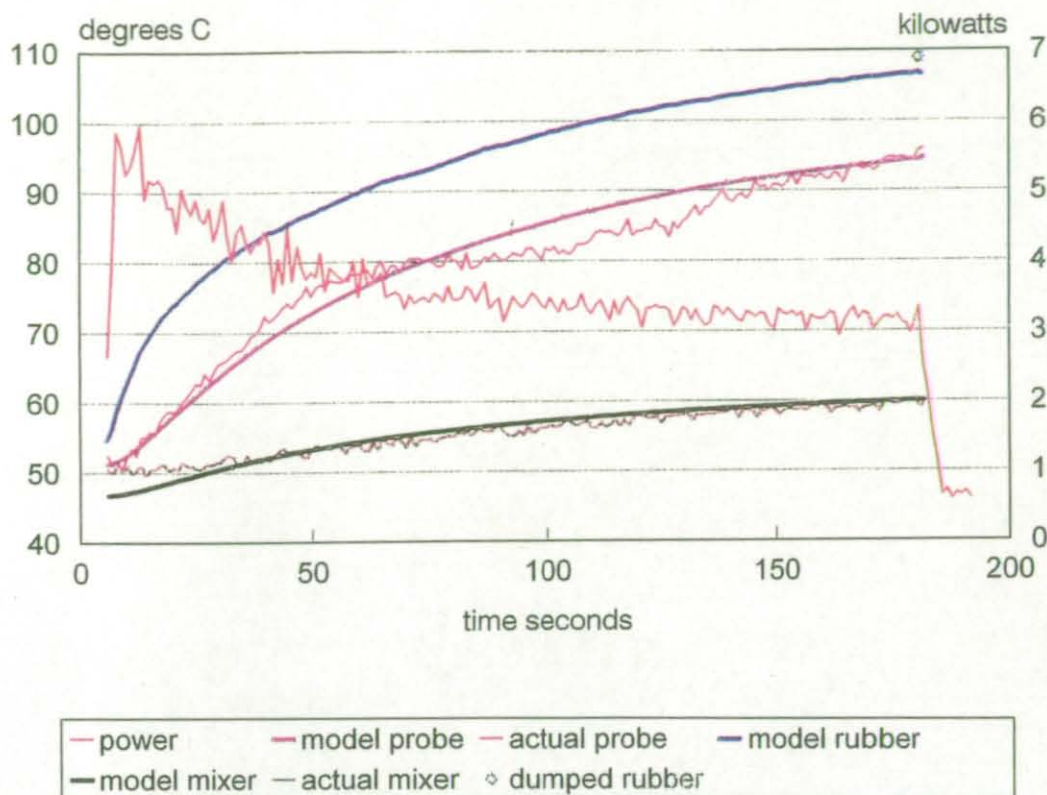


Figure 5.9 - A second temperature profile using the heat transfer model.

Most of the mastication cycles analyzed produce similar matches but some have definite steps in the batch thermocouple profile illustrated by figure 5.9. There is nothing in the power traces to anticipate such steps. However in a previous study [115], see figure 5.10, when batch J type thermocouples were fitted in the ram, the door and in each sideframe of a laboratory mixer it was found that for half the time the two sideframe readings coincided with each other but for the remainder the two deviated from each other by up to 5C. These deviations were likely to be due to disturbances in the circulation of the rubber. The deviations in our study are not greater than those found in the previous study and hence the discrepancies between

the predicted and batch thermocouple temperatures have to be accepted as being due to the undesirable location of the batch thermocouple.

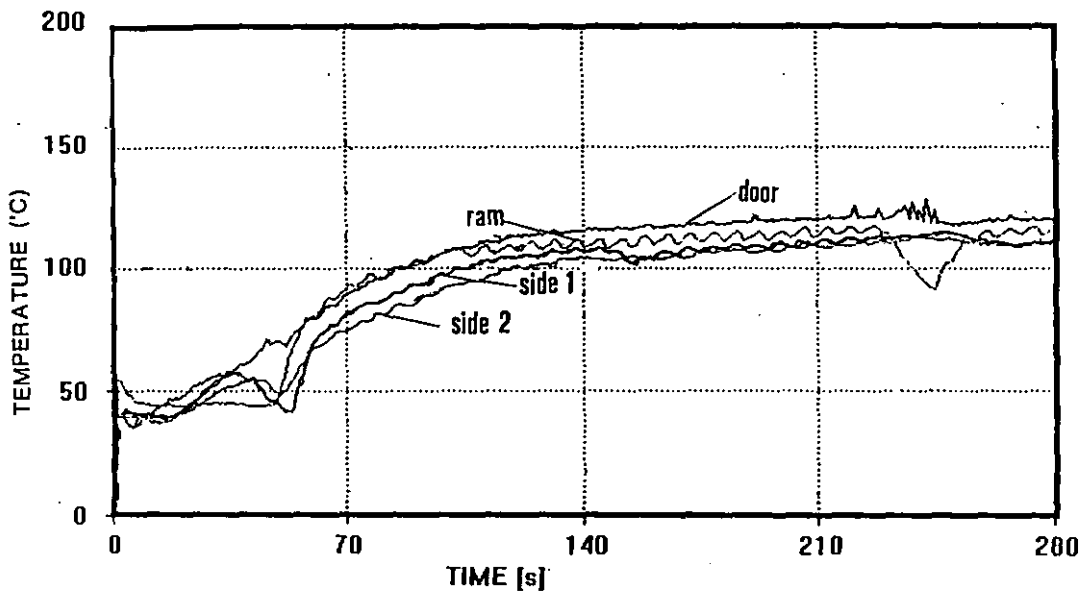


Figure 5.10 - A graph comparing the temperature measurements from thermocouples located in different parts of a Banbury mixer. These results come from a previous study [115].

It was also found in this study, that the temperature measured at the door was about 10°C hotter than the sideframes and that it produced a much more steady trace when compared to the other thermocouples. This observation was consistent with the temperature readings from the batch thermocouple in the Farrel BR Banbury and verifies that the necessary assumptions made about the effective mixer body in the heat transfer model were correct.

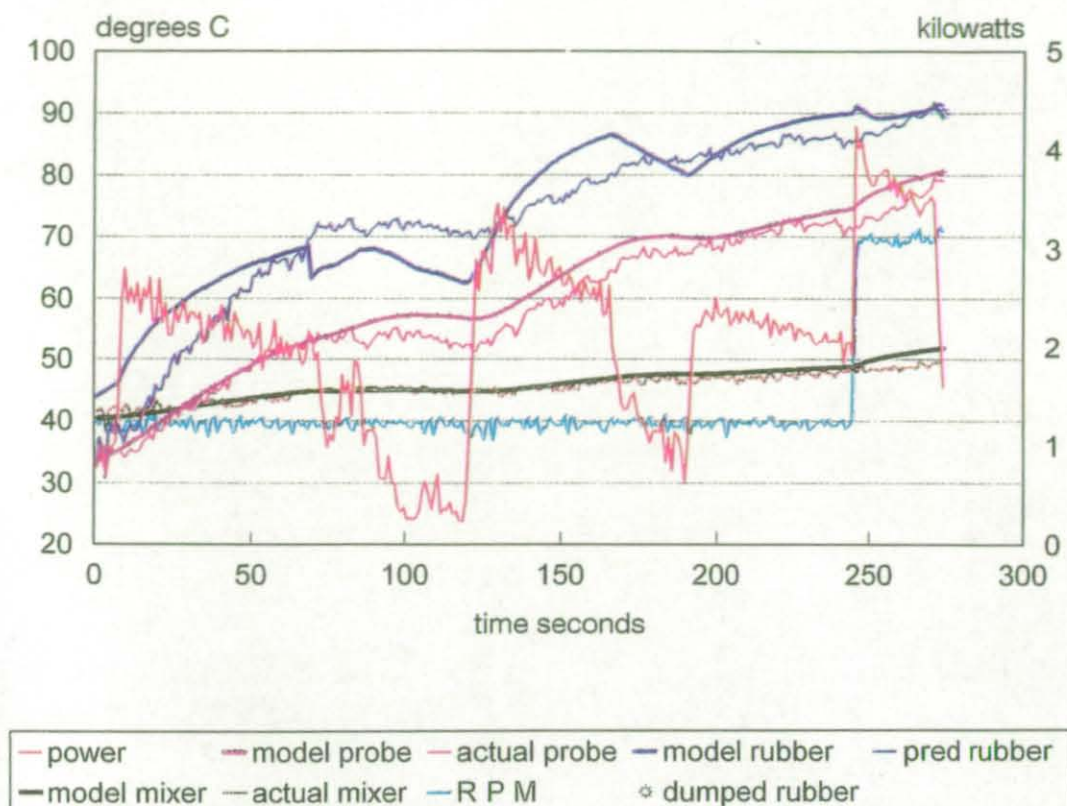


Figure 5.11 - A third temperature profile using heat transfer model.

Figure 5.11 shows a complete mix with a speed increase at the end of the cycle. The temperature profile of the rubber estimated using the thermocouple regression equations (5.17 & 5.18) is also shown. The batch temperature rose sharply at the start. At the end of the mastication period the ram was raised and the carbon black added. This produced an immediate step down in the batch temperature due to the introduction into the mix of the carbon black at 20°C. On dropping the ram the power picked up again with a further rise in temperature. Near the end of the cycle the speed was increased causing a small increase in the rubber temperature. This rise was not large as, due to the high speed index, the heat transfer from the rubber to the

mixer was also substantially increased.

The predictions produced using the probe algorithm and the actual probe temperatures followed each other reasonably well apart from during the ram up periods when the batch circulation in the mixer was seriously disturbed.

The temperature of the rubber predicted by the thermocouple regression equations can also be followed. At the point of carbon black addition there is a change from the non-linear gum rubber equation (5.17) to the linear carbon black one (5.18). The thermocouple regression equations are generally not as responsive as the temperature profile suggested by the heat transfer model.

5.4.2.4. Accuracy of the heat transfer model at simulating the temperature profile of the rubber compound.

The heat transfer model successfully estimated the dump temperature of 85% of the mixes analysed within $\pm 6^{\circ}\text{C}$ of the actual value.

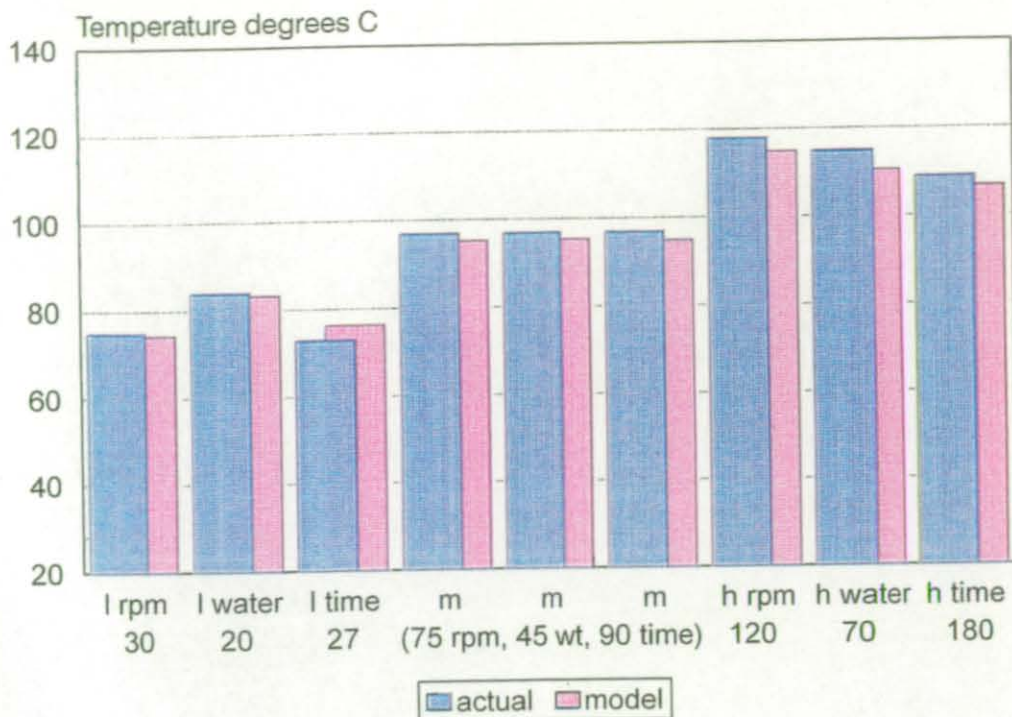


Figure 5.12 - Illustrates the ability of the model to predict the actual dump temperatures under extreme mixing conditions.

See Appendix 2 for a table comparing the actual and predicted dump temperatures of the other batches using the heat transfer model. The same table also compares the actual and predicted measurements of the batch thermocouple (predicted using equation 5.19) and the mixer thermocouple (predicted using equation 5.20).

5.5. Coefficients for initial predictive model.

The part of the heat transfer model predicting the energy going out of the system was then combined with the model for predicting the energy going into the system to produce an initial predictive model. The heat transfer model calculates the energy going out of the system by predicting the heat flow from the batch to the effective mixer body. The methodology for producing the heat transfer model is discussed in section 5.4.2. The energy going into the system is predicted by determining the rotor torque as a function of rotor speed, compound viscosity, batch temperature, fill factor and a machine constant. The methodology of determining the rotor torque is discussed for mastication in section 5.3.1. and for dispersive mixing in section 5.4.2. A flow chart of the model is shown in figure 5.1.

| Coefficient | Value | Definition | Detailed in: |
|------------------------------|-----------------------------|---|--------------|
| For dW(input) | | | |
| K | 131830 | Consistency constant | 5.3.1.1 |
| n | 0.233/0.2 | Power-law index | " |
| M_a | equation 5.7 | Machine constant | " |
| mv | 370/389 | Min rotor torque value Nm | " |
| -b | -0.007 | Batch temperature constant | 5.3.1.2. |
| d | 0.0034 | Mastication constant 1 | 5.3.1.3. |
| yo | 1.045 | Mastication constant 2 | 5.3.1.3. |
| x | 0.0185 | Fill factor constant | 5.3.1.4. |
| -g | -0.0014 | Rate of disagglomeration | 5.3.2.1. |
| RR_{RSmin} | 160 | Number of rotor revs to RSmin | " |
| * σ | 0.618 | | 5.3.2.2. |
| ** Kc | $Krr * 1.355$ | Vol. fract. immobilised rubber Consistency constant comp | 5.3.2.3 |
| For dW(output) | | | |
| transrm | 170/203.4 | Heat trans. coef. batch to mixer | 5.4.2.1. |
| transmw | 49 | Heat trans. coef. mixer to water | " |
| rindex | 0.74/1.61 | Speed index | " |
| hc mixer | 4314 | Heat capacity of mixer | " |
| Pfac | 0.85 | Prop. power converted to heat | " |
| hc of *** rubber black | mass kg*1900 mass kg*900 | | |

* $\sigma = 0.618$ since $P_{cb} = 1.8 \text{ gcm}^{-3}$ and $DBPA = 90 \text{ cm}^3/100\text{g}$

** $Kc = Krr * 1.355$ since $\phi t = 0.119$ and $\psi = 36 \text{ m}^2/\text{g}$

*** heat capacity in JK^{-1}

NB: When there are two values the first is for mastication and the second is for dispersive mixing. Further details of how these specific constants were calculated see Appendix 2.

Table 5.3 - Coefficients for initial predictive model.

5.6. Accuracy of the predictive model at simulating the temperature profile of the rubber compound.

| Speed rpm | Water Temp. (°C) | Fill Factor (%) | Mixing Time (secs) | +/- Actual (°C) |
|--------------|------------------------|-----------------------|--------------------------|-----------------------|
| 43 | 63 | 56 | 154 | +2 |
| 43 | 27 | 56 | 154 | -5 |
| 107 | 27 | 56 | 154 | +6 |
| 107 | 63 | 56 | 154 | -4 |
| 43 | 27 | 56 | 26 | +5 |
| 43 | 63 | 56 | 26 | +4 |
| 107 | 63 | 56 | 26 | +2 |
| 107 | 27 | 56 | 26 | +2 |
| 30 | 45 | 56 | 90 | -1 |
| 75 | 20 | 56 | 90 | +1 |
| 75 | 70 | 56 | 90 | -3 |
| 107 | 27 | 45 | 154 | -5 |
| 75 | 45 | 35 | 30 | 0 |
| 75 | 45 | 56 | 90 | 0 |
| 75 | 45 | 56 | 180 | -2 |
| 75 | 45 | 75 | 120 | +2 |

Table 5.4. - Temperature predictions using the initial mastication model.

| Speed (rpm) | Water Temp.(C) | Mast. Time(secs) | Disp. Time(secs) | +/- Actual(C) |
|----------------|-------------------|---------------------|---------------------|------------------|
| 40 | 40 | 70 | 60 | +6 |
| 40 | 40 | 70 | 150 | -3 |
| 40 | 27 | 70 | 190 | -2 |
| 40 | 40 | 70 | 265 | +1 |
| 60 | 40 | 50 | 180 | +1 |
| 100 | 40 | 60 | 120 | +4 |
| 80 | 40 | 40 | 120 | +1 |

Table 5.5 - Temperature predictions using the initial dispersive model.

The temperature profile of over 90% of the mixing cycles are within +/- 5°C of the measured final dump temperatures.

5.7 Accuracy of the predictive model at simulating the power traces of the rubber compound.

The torque profiles simulated can be converted to give predicted power consumption profiles. The power predictions were increased to take into consideration that not all of the power consumed would have been converted to heat, some of it was lost in the gearing system. The P_{fac} term from the heat transfer model was used for this purpose (see section 5.4.2.1). Examples of the power traces predicted can be seen in figures 5.13 to 5.17. The predictive model can predict the power consumption of 90% of the mixes within 7% of the actual.

5.8 Some examples of the profiles produced using the predictive model.

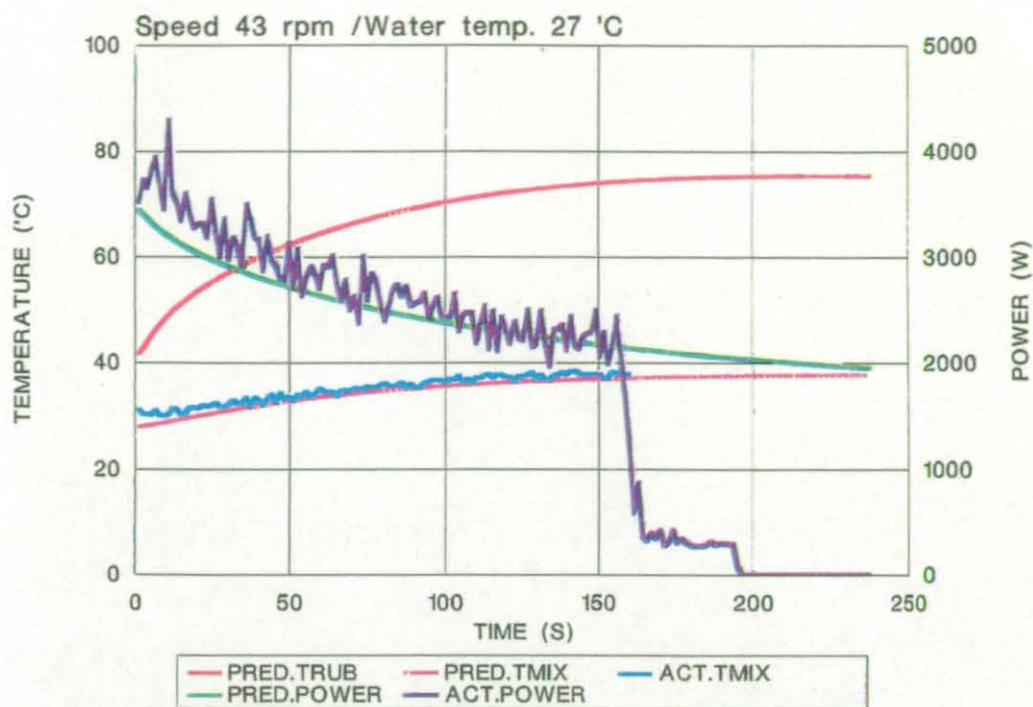


Figure 5.13 - The predictive model simulating temperature and power traces during mastication - rotor speed 43 rpm/water temperature 27°C.

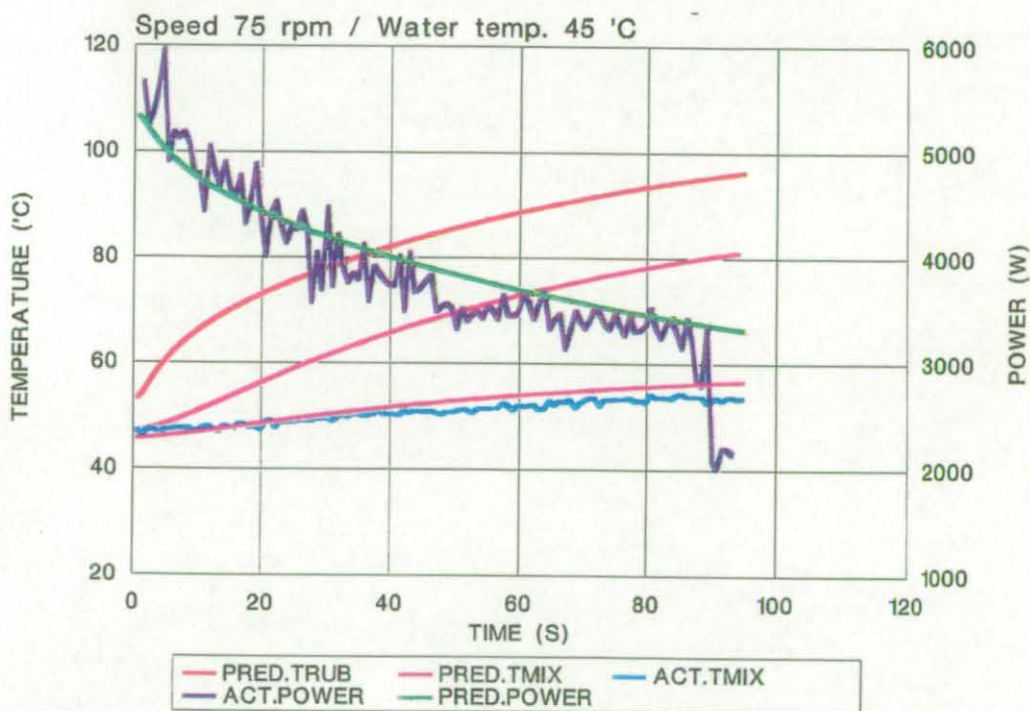


Figure 5.14 - The predictive model simulating temperature and power traces during mastication - rotor speed 75 rpm/water temperature 45°C.

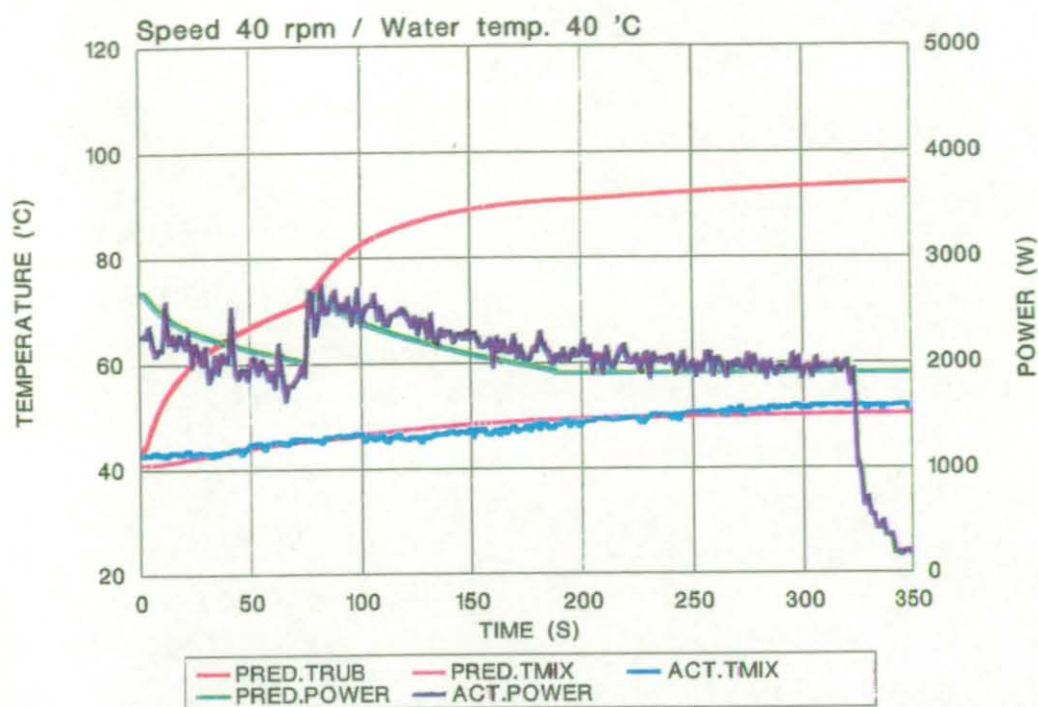


Figure 5.15 - The predictive model simulating temperature and power traces during mastication and dispersive mixing - rotor speed 40 rpm/water temperature 40°C.

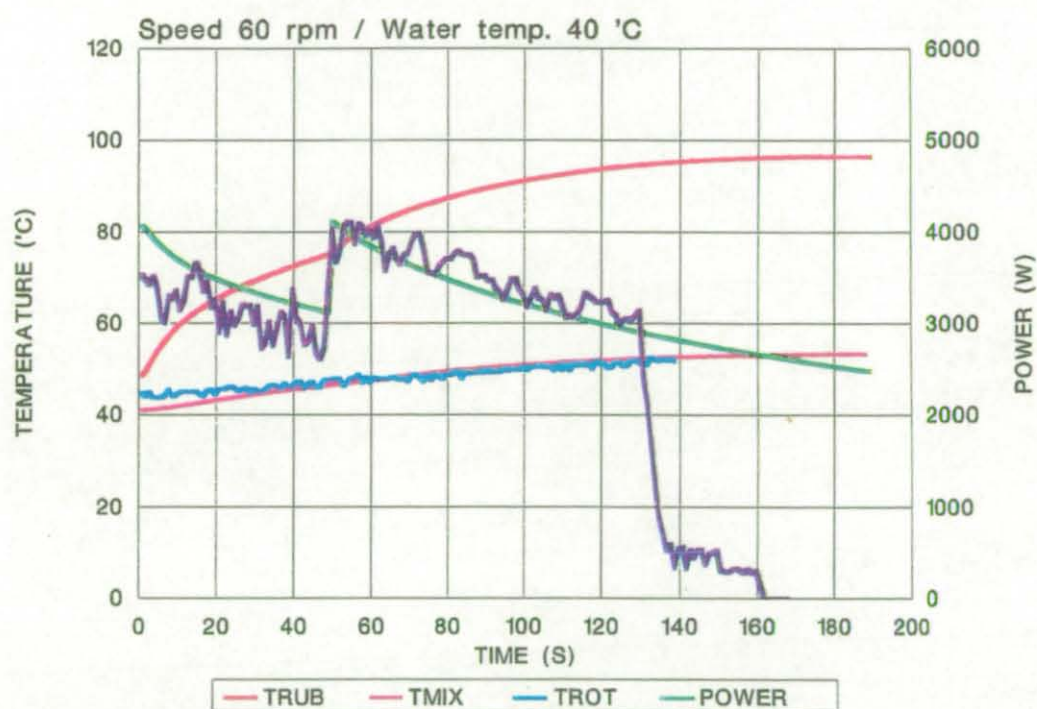


Figure 5.16 - The predictive model simulating temperature and power traces during mastication and dispersive mixing - rotor speed 60 rpm/water temperature 40°C.

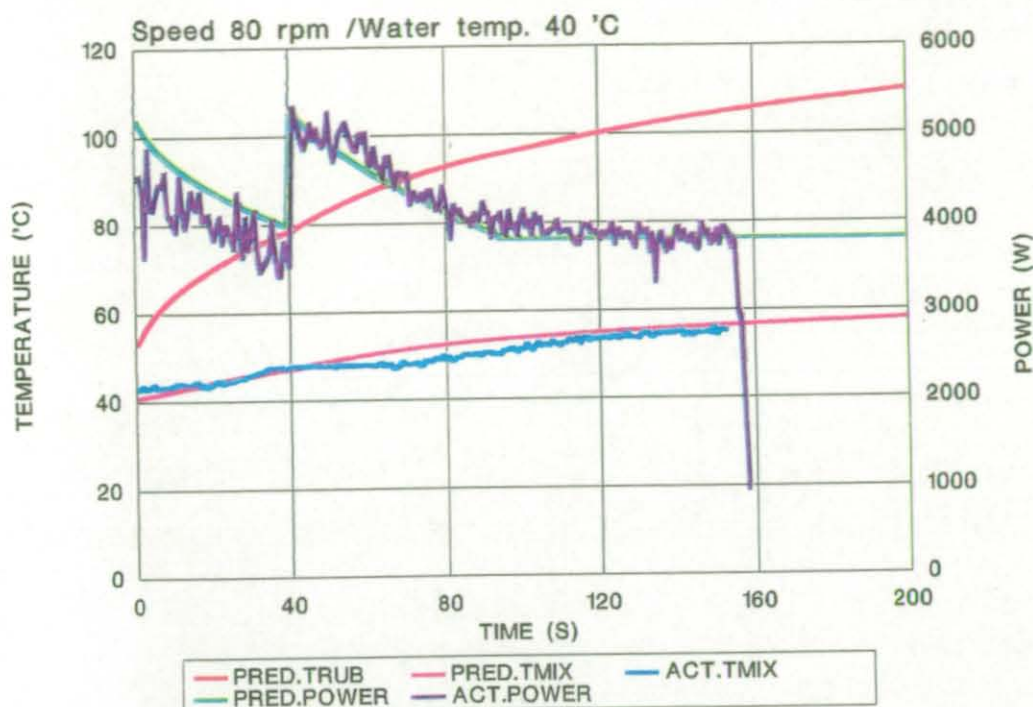


Figure 5.17 - The predictive model simulating temperature and power traces during mastication and dispersive mixing - rotor speed 80 rpm/water temperature 40°C.

5.9 A initial study into the way oil additions would affect the predictive model.

Hydrocarbon oils are used widely in rubber compounds and are expected to influence mixing performance. An initial study has been carried out to establish what effect the addition of aromatic process oil would have on the power profiles of the premasticated SMR L natural rubber/35 phr N660 carbon black compound. A slightly higher loading of 35phr of carbon black was used rather than 27 phr in the initial predictive model to prevent extensive wall slip at the high loading of oil [37].

5.9.1 Experimental details

Six batches were mixed with loadings of the aromatic process oil varying from 0 to 10 phr in 2 phr increments. The mixing cycle used is:

| | |
|-----------------------|---------------------------|
| Mixing time | 300 secs |
| Mastication time | 70 secs |
| Sulphur addition time | 194 secs |
| Fill factor | 65% |
| *Rotor speed | 40 --> 70 rpm at 245 secs |
| Water temperature | 40°C |

nb - The sharp increase in the power profiles towards the end of the mixing cycle is due to step increases in the rotor speed.

5.9.2 Observations from the experiment.

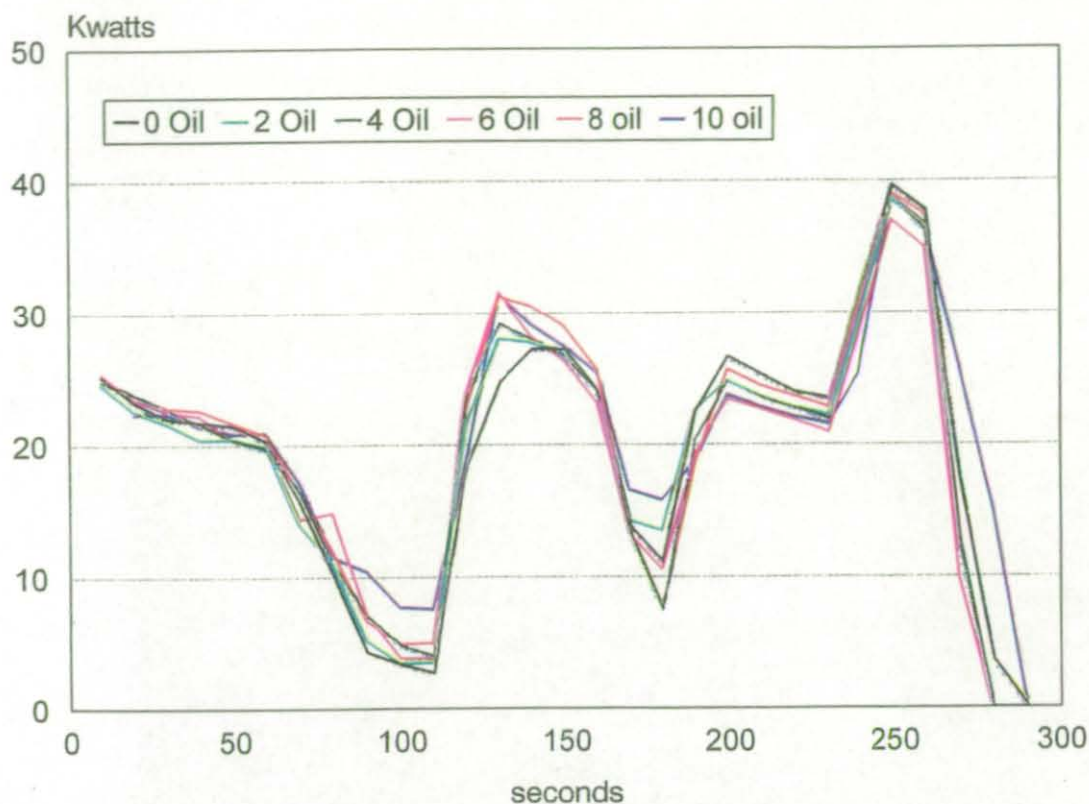


Figure 5.18 - Showing smoothed power profiles of six batches that differ only in the phr of oil added to them.

Smoothed power traces from these seven mixes are shown in figure 5.18. The power profiles were found to alter very little with changes in oil loading. It was therefore decided that the variation was not significant enough to warrant any changes to this initial model. The only difference noted was that the time for carbon black incorporation was reduced by approximately 12 seconds with the addition of oil from 0 to 4 phr, demonstrating that the oil was acting as a surfactant therefore allowing more rapid incorporation. At oil levels greater than 4 phr no further improvement was shown, suggesting that 4 phr of oil was sufficient for a monolayer coating of oil on the surface of the carbon black.

CHAPTER SIX.

DEVELOPMENT OF A MATERIAL DATABASE FOR THE PREDICTIVE MODEL.

6.0 Introduction.

Objective: To develop a material database containing all the coefficients that would enable the predictive model to simulate the batch temperature and power profiles for dispersive mixing of a wide range of carbon blacks/SMR L natural rubber compounds

To enable the initial predictive model developed for a laboratory Farrel BR Banbury mixer (see chapter 4) to be rendered generally useful, the coefficients required for the model to function needed to be determined for a wide range of materials . To initiate the development of a material database it was decided to undertake a large experimental design to determine coefficients for a wide range of carbon blacks at different loadings. The carbon blacks were characterised in terms of both structure (DBPA) and surface area (CTAB). The grade of natural rubber, premasticated SMR L, used was as in the previous work.

For the model to function fully it is necessary to determine how the following coefficients, identified in Chapter 5, alter depending on the type and loading of carbon

black added to the masticated rubber:

- (1) Rate of disagglomeration (g)
- (2) Maximum disagglomeration achievable in the Banbury mixer (RS_{min}).
- (3) Number of rotor revolutions required before reaching maximum disagglomeration ($RR_{RS_{min}}$).
- (4) Rate of reduction in effective filler volume (ϕ_e)
- (5) Effect of rotor speed in terms of the consistency constant (K) and the power-index (n).
- (6) Effect of compound temperature on torque which is represented by the batch temperature constant (-b).
- (7) The number of rotor revolutions before complete incorporation of the carbon black.
- (8) Effect of fill factor which is represented by the fill factor constant (x).
- (9) The heat transfer coefficients from the rubber to the mixer (transm).

It was decided that to keep the experiment to a practical size the effect of fill factor would not be investigated in the initial experiment. A term for the number of rotor revolutions before complete incorporation of the carbon black was not been included in the initial model due to the rapidity of incorporation (see section 5.3.2). However, a new term is proposed in anticipation of the longer incorporation times due to the high loadings of carbon black to be investigated for the material database. It was anticipated that the rest of the coefficients identified in chapter 5 would not have to be altered.

6.1 Experimental Design.

The statistical package 'Algorithm for construction of experimental designs' (ACED) [121] was employed to produce a D-optimal design intended to cover all interactions between the primary variables necessary to determine the coefficients listed above for a wide range of carbon blacks.

6.1.1. The Defined ranges of the experiment.

(1) Type of carbon black.

The carbon blacks being used were: N220, N326, N330, N339 N539, N660, and N772.

| Carbon Black | DBPA ml/100g | CTAB m ² /g |
|--------------|-----------------|---------------------------|
| N220 | 114 | 110 |
| N326 | 72 | 83 |
| N330 | 102 | 83 |
| N339 | 120 | 94 |
| N539 | 111 | 41 |
| N660 | 90 | 38 |
| N772 | 65 | 33 |

Table 6.1 - Specifications of carbon blacks used.

(2) Loading.

20 --> maximum phr

The maximum loading was calculated with the assumption that the maximum effective volume fraction of filler at the point of incorporation should not exceed 0.6. A maximum of 0.6 for the laboratory Banbury mixer was estimated by experimenting with the maximum loading of carbon black the mixer could accommodate without stalling the motor. The effective volume fraction (ϕ_e) of filler includes the true volume fraction of carbon black plus the rubber which is immobilised within the agglomerates. As discussed in the last chapter ϕ_e can be estimated using 5.13 [66].

The volume fraction of immobilised rubber in an agglomerate (σ) was estimated for each carbon black depending on its DBPA value, using equation 5.12 [66]. The maximum effective volume fraction of filler was estimated with the assumption that at the point of incorporation 100% of the black is in the form of agglomerates.

$$\text{Volume fraction of black in an agglomerate} = (1 - \sigma) \quad (61)$$

$$\text{Volume of immobilised rubber in an agglomerates } (\sigma r) = \quad (62)$$

$$\frac{\text{True volume fraction of black } (\phi_t) * \sigma}{(1 - \sigma)}$$

where ϕ_t is calculated from the true density of carbon black.

$$\text{So volume fraction of agglomerates } (\phi_a) = \phi_t + \sigma r$$

The maximum loading for each of the carbon blacks was calculated using equation 6.1 and 6.2. In the experimental design three loadings of each carbon black was entered into the ACED program. A minimum loading of 20 phr, a maximum loading and a mean loading.

| Carbon Black | Maximum Loading phr |
|--------------|---------------------|
| N220 | 45 |
| N326 | 45 |
| N330 | 50 |
| N339 | 45 |
| N539 | 50 |
| N660 | 60 |
| N772 | 75 |

Table 6.2 - The maximum loadings calculated for each carbon black.

(3) Water temperature.

Three water temperatures were entered into the experimental design, 20, 45 and 70 °C.

(4) Rotor speed.

Three rotor speeds were entered into the experimental design, 30, 60 and 90 rpm.

(5) Number of rotor revolutions for dispersive mixing.

Three levels of rotor revolutions were also entered into the experimental design. The actual values depended on the loading and type of carbon black. The maximum

number of rotor revolutions in each case was intended to be used to determine the maximum disagglomeration achievable in the BR Banbury mixer.

| Carbon Black | Load phr | Minimum | Middle | Maximum |
|--------------|----------|---------|--------|---------|
| N220 | 20 | 50 | 165 | 320 |
| | 32.5 | 70 | 208 | 385 |
| | 45 | 90 | 250 | 450 |
| N326 | 20 | 50 | 165 | 320 |
| | 45 | 70 | 208 | 385 |
| | 70 | 90 | 250 | 450 |
| N330 | 20 | 50 | 165 | 320 |
| | 35 | 70 | 208 | 385 |
| | 50 | 90 | 250 | 450 |
| N339 | 20 | 50 | 165 | 320 |
| | 32.5 | 70 | 208 | 385 |
| | 45 | 90 | 250 | 450 |
| N539 | 20 | 50 | 140 | 270 |
| | 35 | 70 | 175 | 320 |
| | 50 | 90 | 210 | 370 |
| N660 | 20 | 50 | 140 | 270 |
| | 40 | 70 | 175 | 320 |
| | 60 | 90 | 210 | 370 |
| N772 | 20 | 50 | 140 | 270 |
| | 47.5 | 70 | 175 | 320 |
| | 75 | 90 | 210 | 370 |

Table 6.3 - Number of rotor revolutions of dispersive mixing undertaken.

By joining all combinations of the input variables a total of 567 experimental points was obtained. From this the software produced an experimental design, consisting of 45 of these candidate points from which it was anticipated that the relationships listed in section 6.0. could be determined. For full details of the 45 mixes undertaken see appendix three.

6.1.2. Additional experimental details.

To minimise material variation the premasticated SMR L natural rubber used throughout the experiment was taken from a single bale of rubber.

The fill factor after the carbon black addition was kept constant at 60%.

The mastication stage for each mix was kept constant at 40 rpm for 70 secs. However due to the inherent time lag on the cooling system it was not possible to keep to a constant water temperature during mastication. Consequently the water temperature was set to the temperature as indicated in the experimental design throughout the mixing cycle.

It was found necessary to do a "sweep down" to ensure full incorporation of all the carbon black at the higher loadings. This involved raising the ram and opening the feed hopper door. A brush was then used to sweep any loose black from the feed hopper down into the mixing chamber. For consistency a "sweep down" was done for each batch, when $\frac{4}{5}$ of the minimum number of rotor revolutions had been

undertaken for a particular carbon black loading. The "sweep down" occupied a total of 20 seconds and the rotor revolutions during this period were not counted in the total due to the much reduced mixing efficiency when the ram is raised.

An interval of at least twenty minutes was allowed between each mixing cycle so that start conditions were constant. The power consumption, the mixer thermocouple and the batch temperature probe values were monitored at one second intervals throughout each mixing cycle. The final temperature of the batch was measured using a hand held temperature probe. The viscosity of the mixed compounds were measured using the Negretti TMS biconical rheometer (for test procedure see section 3.1.1). The final batch temperature measured using the hand held probe and the viscosity results for the 45 mixes are detailed in Appendix 3.

6.1.3. Statistical Analysis.

Multiple regression analysis was done using the Minitab Statistical Software [120]. A series of 'best regression equations (BREG)' was produced in the form of second order polynomial equations (same format as equation 4.1). The optimum regression equation was chosen by taking the equation with the highest adjusted correlation coefficient (R-squared) and the lowest standard error of estimate (s). See Appendix 1 for further details on BREG function, R-squared and s.

| Variables | abbrev -iations | -1 | 0 | +1 |
|--------------------------|--------------------|-----|------|-----|
| CTAB (ml/g) | ctab | 33 | 72 | 110 |
| DBPA (m ² /g) | dbpa | 65 | 93 | 120 |
| Speed (rps) | rps | 0.5 | 1.0 | 1.5 |
| Water (°C) | W | 20 | 45 | 70 |
| Rotor revs | RR | 50 | 250 | 450 |
| Black (phr) | load | 20 | 47.5 | 75 |

Table 6.4 - Defined ranges used for equation (unless stated)

6.2 Observations from the experiment.

6.2.1. The mastication stage of the mixing cycle.

It was observed that whilst the power traces during the mastication phase of the mixing cycle were consistent when a high water temperature and fill factor were combined there was significant scatter when a low water temperature and fill factor were combined. Four batches at low fill factor and water temperature were masticated to establish whether this scatter was due to inconsistency in the rate of mastication or due to the inability to accurately monitor under these mixing conditions. They were masticated using the same mixing regime as in the experiment and their viscosity measured using the TMS bioconical rheometer.

The results were:

Shear stress at 1 s^{-1} - mean: 114.5

std deviation batch to batch: 5.05

The low level of variation (see section 3.1.1) showed that the reduction in viscosity was consistent batch to batch therefore indicating that the monitoring of power consumption is not consistent under these conditions. This likely due to voids in the mixing batch leading to poor circulation and slippage in the mixing chamber (see section 2.2.1.2 and 2.2.1.4.) This observation means that although the rate of mastication can be modelled accurately under these conditions the modelling of power consumption cannot.

6.2.2. Early stage of mixing after addition of carbon black.

The power profiles measured for each mixing cycle were converted to torque profiles and these were then smoothed by taking an average over every five points measured (ie every five seconds). It was found that even after smoothing there was a significant amount of disorder in the initial part of the mixing cycle, after the addition of carbon black. This was shown in two ways:

(i) During development of a regression equation for predicting the number of rotor revolutions required for carbon black incorporation, as a function of mixing conditions, carbon black type and loading. In this project incorporation is assumed to be completed at the point where the smoothed torque profile starts decreasing after

reaching a maximum. The best regression equation generated (6.3) had an adjusted correlation coefficient (R-sq) of 63.5% which is not statistically significant.

No. of R before incorporation

$$= 25.7 - 12.9\text{ctab} - 8.63(\text{rps})^2 - 3.58(\text{dbpa} \cdot \text{load}) - 3.76(\text{ctab} \cdot \text{RR}) - 2.33(\text{rps} \cdot \text{W}) + 3.38(\text{rps} \cdot \text{RR}) \quad (6.3)$$

$$\text{R-squared} = 63.5\%$$

(ii) Secondly, during regression analysis of the smoothed values of torque monitored during mixing. A regression equation (6.4) produced to fit torque values after 35 rotor revolutions (after ram down) as a function of the all mixing variables had a R-squared of 69% when optimised. A similar regression equation (6.5), taking torque values after 105 rotor revolutions, had a R-squared of 91%.

Ln torque after 35 rr

$$= 6.64 + 0.124(\text{load}) - 0.0442(\text{rps}) - 0.0756(\text{W}) - 0.847(\text{load})^2 + 0.04(\text{rps} \cdot \text{W}) + 0.058(\text{load} \cdot \text{W}) + 0.0484(\text{dbpa} \cdot \text{W}) \quad (6.4)$$

$$\text{R-squared} = 69\%$$

Ln torque at end of each mixing cycle

$$= 6.361 + 0.202(\text{load}) - 0.129(\text{RR}) - 0.068(\text{W}) + 0.053(\text{dbpa}) \quad (6.5)$$

$$\text{R-squared} = 91\%$$

Both (i) and (ii) indicate that accurate modelling of the power consumption during the early stages of mixing after the introduction of the carbon black is not possible, since the process itself is not consistent

6.3 Analysis undertaken to determine how reduction in viscosity attributed to the disagglomeration process alters depending on the mixing conditions, type and loading of carbon black.

As explained in 5.3.2.1 the effect of disagglomeration on viscosity is calculated in the predictive model by determining the relationship between $\ln(\text{relative shear stress})$ (RS) and number of rotor revolutions. In addition the reduction in effective filler fraction with increasing rotor revolutions is also estimated from this relationship (see section 5.3.2.2). It was therefore decided that if the relationship between $\ln(\text{RS})$ and the number of rotor revolutions could be quantified with respect to changes in mixing condition, type and loading of carbon black then development of a material database for carbon black would have largely been achieved. Therefore future work was concentrated upon this objective.

6.3.1 Coefficients required for the effect of disagglomeration in the databases.

g = rate of disagglomeration

RS_{\min} = minimum RS achievable under particular mixing conditions.

$RR_{RS_{\min}}$ = Number of rotor revolutions to RS_{\min} .

see figure 5.3.

6.3.2. Determining RS for the 45 mixes.

6.3.2.1 - Initial method.

Experimental work was undertaken to determine reduction in the shear stress of the natural rubber under different mixing conditions. In this study, due to lack of information on effective filler fraction, no allowances have been made to increase either the mixing time of the elastomer or the strain rate at which the shear stress was measured to take into consideration strain amplification (see section 2.7.1). The determination of the reduction in the shear stress of the natural rubber under the different mixing conditions, was initially attempted by masticating the NR (fill factor 60% consistent with compound) in a series of stages at the three different water temperatures (20, 45 and 70 °C) using the same procedure used in the development of the initial model (see appendix two). The rubber was masticated for X amount of time then discharged and a sample of approximately 25g taken (sufficient for Negretti TMS biconical rheometer testing). The remainder of the masticate was then fed back into the mixer for a second stage of mixing. The masticate was repeatedly discharged from and replaced into the mixer until nine samples had been taken, the final sample being taken after 450 rotor revolutions. The viscosity of each of the samples collected was then measured using the same procedure as used for the compounds (for test procedure see section 3.1.1). From these results a series of plots of shear stress (1 s^{-1}) vs rotor revolutions for the elastomer was produced at different water temperatures. These plots were then used to predict the RS of the 45 carbon black mixes at dump. The RS values calculated, for the 45 mixes, using this method are detailed in

Appendix 3.

However regression to fit these results as a function of the other variables produced an equation which suggested that RS increased with increased rotor revolutions. This is inconsistent with previous findings (see section 4.3.4.6 and [63]).

$$RS = 2.72 + 0.189(dbpa) + 0.522(ctab) + 1.13(load) - 0.154(W) + 0.162(RR) + 0.4(ctab*load)(6.6) - 0.115(ctab*W)$$

R-squared 93%

Comparing the reduction in shear stress of the natural rubber vs rotor revolutions at different water temperatures with the observations made in chapter 4.3.4.4 highlighted the fact that temperature has a large effect on the efficiency of mastication.

| No. of rotor revolutions | Shear stress after mast. at Water temp. 20°C (Kpa) | Shear stress after mast. at Water temp. 70°C (Kpa) |
|--------------------------|--|--|
| 50 | 99 | 108 |
| 450 | 65 | 92 |

Table 6.5 - Comparing reduction in shear stress at 1 s⁻¹ when masticating at different water temperatures.

This observation identified that the error was due to the reduction in shear stress of the elastomer being larger than would have been achieved during the mixing conditions of the majority of the carbon black mixes. This was because the discharge and replacement regime employed in the mastication experiment enabled the elastomer to be masticated under cooler conditions therefore giving greater mechanical rupture of primary bonds, since the level of shear forces exerted by the rotors on the compound would have been greater [59,60].

However, it should also be taken into consideration that the elastomer in the highly loaded carbon black compounds mixed for a long time at high speed and high water temperature reached batch temperatures in the region of 130 - 140°C. In these mixes the level of mastication due to oxidative scission (hot mastication) would have been significant [59,61]. It was therefore decided to determine the reduction in viscosity of the elastomer as a function of not only the number of rotor revolutions but also in terms of heat history received.

6.3.2.2. Second method.

An equation was developed to relate reduction in elastomer viscosity (shear stress at 1 s^{-1}) as a function of rotor revolutions undertaken and heat history received.

Experimental data was used from the mastication project discussed in section 4.2.1 (18 mixes). In addition an extra 12 mastication mixing cycles were undertaken. This was done for two reasons; firstly because the initial mastication project did not cover the wide range of mixing conditions in this experiment and secondly to undertake some long mixing cycles at high water temperatures (90°C) so the effect of oxidative scission could be studied. These mixes are detailed in Appendix 3.

As discussed in chapter 5 (see section 5.4.1) the readings from the batch thermocouple are inaccurate to get improved temperature values for each of the 30 mixes equation 5.18 was employed. Each of the adjusted temperature profiles were assessed at one second intervals to get a measure of the efficiency of both types of mastication.

(1) The efficiency of the mechanical rupture of primary bonds in the Farrel BR Banbury mixer would be dependent on both the number of rotor revolutions undertaken and heat history received. Equation 6.7 [114] was used to assess this type of mastication, the equation basically increases the value of X at high rotor speed and low batch temperature when the conditions for mechanical rupture of primary bonds are predominate (see section 4.3.4):

$$\sum_1^R \left(\frac{\text{Rotor revs per sec}}{\text{Rubber temp}} \right) = X \quad (6.7)$$

Where R = number of rotor revolutions in mixing cycle.

(Not using defined ranges in table 6.4.)

(2) Oxidative scission only occurs in the Farrel BR Banbury mixer at high batch temperature (see section 4.3.4). Equation 6.8 [114] was used to assess the rate of oxidative scission, the equations assumes that no oxidative scission occurs below 80°C Above 80°C Y is increased as the batch temperature becomes higher:

$$\sum_1^R \text{ If rubber temp} > 80^{\circ}\text{C then (Rubber temp}-80)^3 = Y \quad (6.8)$$

Where R = number of rotor revolutions in mixing cycle.

(Not using defined ranges in table 6.4.)

Regression analysis was then undertaken to generate an equation to fit the viscosity of the 30 masticates at dump (shear stress at 1 s^{-1}) using the terms X and Y.

Initially the following equation was generated:

$$\text{Shear stress of elastomer at } 1 \text{ s}^{-1} = 125 - 7.9X + 2.24(X - 1.84)^2 - 0.00416 (Y)^2/1000000 \quad (6.9)$$

R-squared = 92.8%

(Not using defined ranges in table 6.4.)

The batch temperature profiles of the 45 carbon black mixes were assessed in a similar manner to produce values for X and Y. Equation 6.9 was then employed to estimate the shear stress of the natural rubber in the carbon black filled compound thereby separating the effects of disagglomeration from that of mastication. Examination of the relationship between the shear stress of the natural rubber in the compound and rotor revolutions showed that after a large number of rotor revolutions equation 6.9 predicts an increase in viscosity. The reason for this is that to give the best-fit relationship the statistical package has been forced to opt for the $(X - 1.84)^2$ term therefore making it conform to a parabola. In reality it has long been established that a plot of elastomer viscosity and mixing time will become increasingly level. To overcome this an exponential term was introduced to replace the power term. The final equation generated was:

$$\text{Shear stress of elastomer at } 1 \text{ s}^{-1} = 99.4 - 0.00149(Y^2/1000000) + 32.7\exp(-X/1.7) \quad (6.10)$$

R-squared = 92.8%

(Not using defined ranges in table 6.4.)

The shear stress values for the natural rubber were then calculated, using equation

6.10 for each of the 45 carbon mixes at dump. These were then used to re-determine the RS values (See Appendix three for full details).

Multiple regression was then undertaken to fit these RS values as a function of the mixing variables.

$$RS = 2.11 + 0.372(DBPA) + 0.459(Ctab) + 1.19(load) + 0.0801(W) + 0.232(load^2) + 0.342(dbpa*load) + 0.343(ctab*load) + 0.086(W*RR) + 0.106exp^{-RR} \quad (6.11)$$

R-squared = 96.5%

An exponential term was added to represent rotor revolutions, this was done for the same reasons as in equation 6.10 and its introduction improved the fit of the equation.

The equation generated to represent RS as a function of all the mixing variables did indicate a significant reduction in RS with an increase in rotor revolutions (t-ratio 4.89). Also an interaction between temperature and rotor revolutions was found to be significant (t-ratio 3.09). However, although the CTAB of the carbon black and the loading were found to be the most significant terms in the equation (t-ratio 14.54 and 19.82 respectively), the regression analysis did not find an interaction between them and rotor revolutions. This made it impossible to assess how g , RS_{min} , RR_{RSmin} alter depending on type and loading of carbon black. For example RR_{RSmin} will be consistent at a particular water temperature. The reason the experiment was not sufficient discriminating was probably due to several contributing factors. The main reason however is likely to be because the experiment was relatively small when considering the wide range of mixing variables. In particular there was insufficient

variation in the number of rotor revolutions undertaken with a lot of the mixes either being very short or very long.

6.4. Determining the coefficients for the effect of disagglomeration using the torque values.

An alternative to the viscosity approach would be to use the torque profiles to quantify the disagglomeration process. In other words to use the torque profiles to create more viscosity results. The advantage of using the torque profiles is that they give continuous information on the state of mix (one result per second throughout each mixing cycle).

It might be expected that there would be a high level of correlation between viscosity and torque at the end of the mixing cycle after taking into consideration batch temperature and rotor speed. Surprisingly however a regression analysis fitting final torque values as a function of rotor speed, dump temperature of compound (measured using hand held probe) and compound viscosity (shear stress 1 s^{-1}) generated an equation which was not statistically significant as it had an R-squared value of only 49.5%.

$$\text{Torque at end of mixing cycle} = 660 + 36.5\text{rps} - 3.68(\text{dump temp.}) + 1.25(\text{viscosity}) \quad (6.12)$$

$$\text{R-squared} = 49.5\%$$

(Not used defined ranges in table 6.4)

Examination of the separate regressions for torque (6.5) and viscosity (6.13) against

the experimental design variables showed that viscosity is highly influenced by CTAB whilst it has an insignificant effect on torque.

$$\begin{aligned} \text{Viscosity of compound} &= 242 + 26.1(\text{dbpa}) + 48.6(\text{ctab}) + 0.109(\text{load}) - 24.3\text{RR} \\ (\text{shear stress at } 1 \text{ s}^{-1}) &- 0.78(W)^2 + 22.1(\text{dbpa} * \text{load}) + 33.9(\text{ctab} * \text{load}) \end{aligned} \quad (613)$$

$$R\text{-sq} = 93.5\%$$

Some of the strong interactions between the carbon black and the rubber take time to develop after mixing [116]. The CTAB [1] is a measure of the surface area and hence the quantity of interactions, therefore it exerts a substantial influence on compound viscosity. In contrast the DBPA level affected both the torque and viscosity. The DBPA [1] is a measure of the shape of the aggregates and therefore affects both. The poor correlation between viscosity and torque meant it was not feasible to determine the coefficients for disagglomeration using the torque profiles.

6.5. Generation of a series of regression equations to predict torque and temperature profiles.

Due to insufficient data it was not possible to determine the coefficients for the effect of disagglomeration required for the predictive model. However to use the calculated data, it was decided that the data should be analysed to produce a series of regression equations to establish the effect material and mixing parameters have on the torque and temperature profile during dispersive mixing. This was a completely new approach and the resulting regression equations cannot be related to the predictive model and are specific to the Farrel BR Banbury mixer used.

6.5.1. Generation of regression equation for torque profiles.

Regression analysis on the carbon black mixes was undertaken after 105, 155, 205, 255, and 305 rotor revolutions of dispersive mixing. In addition to this an analysis was also undertaken to predict the torque profiles of the natural rubber in these carbon black mixes. In other words, to predict the torque profiles of a gum natural rubber batch if it was masticated under the same conditions as the carbon black mixes.

6.5.1.1. Analysis to predict the torque profile of the natural rubber in the carbon black mixes.

An algorithm was generated [114] and optimised using the torque profiles of the mastication mixes detailed in 6.3.2.2. To simulate the torque profiles the algorithm has terms for rotor revolutions, batch temperature and rotor speed. As data was collected every second during each of the mastication mixes the algorithm simulates the torque profile in one second intervals.

R = number effective rotor revolutions during t.

$$= R_{(t-1)} + (rps / (temp_{(t)}/100)) \quad (6.14)$$

where

t = seconds of mastication mixing (ie since the ram down)

temp = temperature of the batch calculated using regression equation 5.18

rps = rotor revolutions per second

Batch temperature was included in the calculation, to determine effective rotor revolutions, to take into consideration that as the batch gets hotter the shear stress generated during each rotor revolution would be reduced.

$$\text{Algorithm to predict torque} = \frac{(to1 * ((1-R/to2) + to3) * \text{EXP}(-\text{temp}_{01}/to4) * (rps * 2)^{to5})}{2\pi} \quad (6.15)$$

during mastication

where

to = constant

to1 = 1820

to2 = 6930

to3 = 67300

to4 = 21.8

to5 = .2425

The best-fit constants were deduced by sequentially varying each constant and selecting the combination which gave the lowest sum of squares of errors on the measured torque at 20 second intervals throughout each of the 30 mastication batches. This process was repeated over progressively lower ranges until there was no further improvement in the fit.

Equation 6.15 was then used to predict the torque profile of the rubber in each of the 45 carbon black mixes.

6.5.1.2. Generation of separate regression equations.

Separate regression equations were generated after 105, 155, 205, 255 and 305 rotor revolutions of dispersive mixing for the carbon black mixes. Regression equations were also generated from the simulated torque profiles of the natural rubber in the carbon black mixes. However, these were taken after 152, 202, 252, 302 and 352 rotor revolutions to take into consideration that the rubber received 47 rotor revolutions of mastication (40 rpm for 70 sec) before the carbon black was added. The earliest regression equation was taken after 105 rotor revolutions of dispersive mixing to avoid the complication of taking values during the "sweep down" (see section 6.1.2.) and to ensure the measured torque profiles are systematic (see section 6.2.2.). Therefore not all the carbon black mixes could be used to generate the regression equation. The number of mixes used to generate each regression equation is indicated in table 6.7. The last regression equation was generated after 305 rotor revolutions since after this point there were insufficient data points for any regression equation to be statistically sound.

The only terms used to produce the regression equations using the BREG function (see appendix one) were carbon black loading (phr), water temperature (°C), rotor speed (rps), CTAB value (m^2/g), DBPA value ($\text{ml}/100\text{g}$), CTAB value * carbon black loading and DBPA value * carbon black loading. This produced equations with highly significant R-squared values and therefore a full second order polynomial regression analysis was not undertaken.

6.5.2. Generation of regression equations for batch temperature profiles.

The regression equation for the batch thermocouple (equation 5.18) was used to determine the batch temperature profile during each of the carbon black mixes. Regression analysis on these temperature profiles was then undertaken after 105, 155, 205, 255, and 305 rotor revolutions in a similar manner as the regression equations generated for the torque profiles.

6.5.3. Regression equations generated.

| Profile | *RR | Regression equation | R-sq | No.of Mixes |
|---|-----|---|------|-------------|
| Carbon black torque | 105 | $590 + 1.06(\text{load}) - 2.80(W) - 60.5(\text{rps}) + 0.0510(\text{dbpa} * \text{load})$ | 94.7 | 25 |
| | 155 | $517 + 0.8869(\text{load}) - 1.74(W) - 40.9(\text{rps}) + 0.0343(\text{dbpa} * \text{load}) + 0.00694(\text{ctab} * \text{load})$ | 92.9 | 25 |
| | 205 | $512 + 1.12(\text{load}) - 1.43(W) - 50.7(\text{rps}) + 0.0324(\text{dbpa} * \text{load})$ | 89.4 | 25 |
| | 255 | $461 + 0.67(\text{load}) + 0.036(\text{ctab}) - 1.35(W) + 0.0276(\text{dbpa} * \text{load}) + 0.0080(\text{ctab} * \text{load})$ | 85.4 | 20 |
| | 305 | $567 - 0.867(\text{dbpa}) - 1.36(W) - 35.2(\text{rps}) + 0.0396(\text{dbpa} * \text{load})$ | 87.2 | 16 |
| torque produced by rubber in carbon black mix | 105 | $575 + 0.439(\text{ctab}) - 2.93(W) + 43(\text{rps}) - 0.0156(\text{ctab} * \text{load})$ | 93.2 | 25 |
| | 155 | $590 - 2.18(W) + 16.6(\text{rps}) - 0.0164(\text{dbpa} * \text{load})$ | 80.2 | 25 |
| | 205 | $609 - 2.24(W) - 0.0124(\text{dbpa} * \text{load}) - 0.00664(\text{ctab} * \text{load})$ | 82.3 | 25 |
| | 255 | $631 - 2.31(W) - 19(\text{rps}) - 0.0161(\text{dbpa} * \text{load})$ | 79.8 | 20 |
| | 305 | $692 - 1.23(\text{dbpa}) + 0.852(\text{ctab}) - 2.33(W) - 22.5(\text{rps}) - 0.0231(\text{ctab} * \text{load})$ | 84 | 16 |
| batch temp. in carbon black mixes | 105 | $59.9 + 0.0710(\text{dbpa}) + 0.489(W) + 13.9(\text{rps}) + 0.000588(\text{ctab} * \text{load})$ | 95.6 | 25 |
| | 155 | $57.8 + 0.423(W) + 19.4(\text{rps}) + 0.00218(\text{dbpa} * \text{load}) + 0.000625(\text{ctab} * \text{load})$ | 97 | 25 |
| | 205 | $53.6 + 0.433(W) + 23.6(\text{rps}) + 0.00236(\text{dbpa} * \text{load}) + 0.000664(\text{ctab} * \text{load})$ | 97.5 | 25 |
| | 255 | $50.6 + 0.441(W) + 26.4(\text{rps}) + 0.0022(\text{dbpa} * \text{load}) + 0.00119(\text{ctab} * \text{load})$ | 98.8 | 20 |
| | 305 | $48.2 + 0.456(W) + 28.6(\text{rps}) + 0.00234(\text{dbpa} * \text{load}) + 0.00073(\text{ctab} * \text{load})$ | 93.1 | 16 |

* No of rotor revolutions of dispersive mixing

Defined ranges in table 6.4 were not used.

Table 6.6 - Regression equations to predict torque and temperature profile.

6.5.4. The effect of material and mixing parameters on the torque and temperature profiles during dispersive mixing.

Figures 6.1 to 6.10 illustrate the effect material and mixing parameters have on torque and temperature profile during dispersive mixing. Each of these graphs show the effect of altering one parameter whilst the others are held constant.

The constant value used to generate the graphs for:

| | |
|----------------------|------------------------|
| Rotor speed | = 1 rps |
| Water temperature | = 45°C |
| Carbon black loading | = 40 phr |
| DBPA | = 90 ml/100g |
| CTAB | = 45 m ² /g |

6.5.4.1 Effect of material parameters.

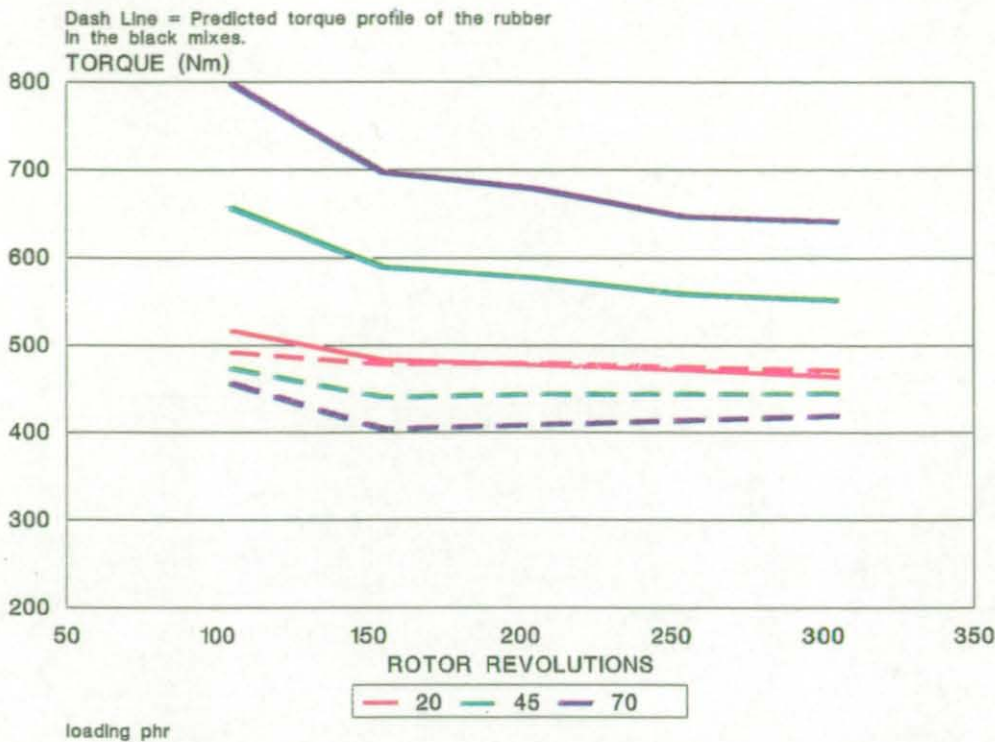


Figure 6.1 - The effect of the carbon black loading on the torque profile.

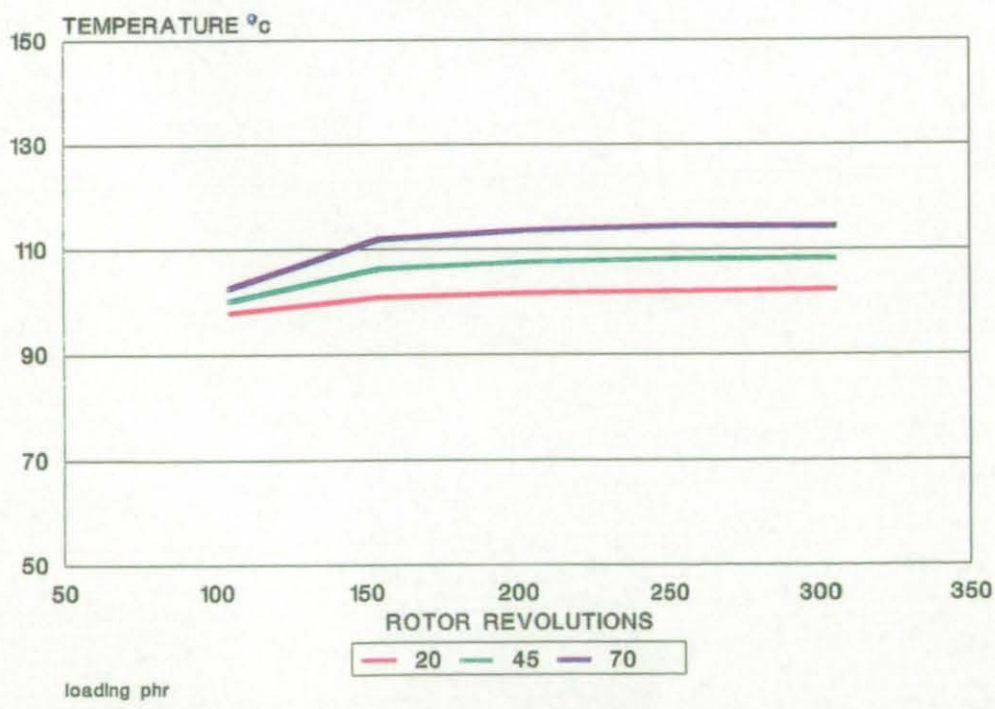


Figure 6.2 - The effect of the carbon black loading on the batch temperature profile.

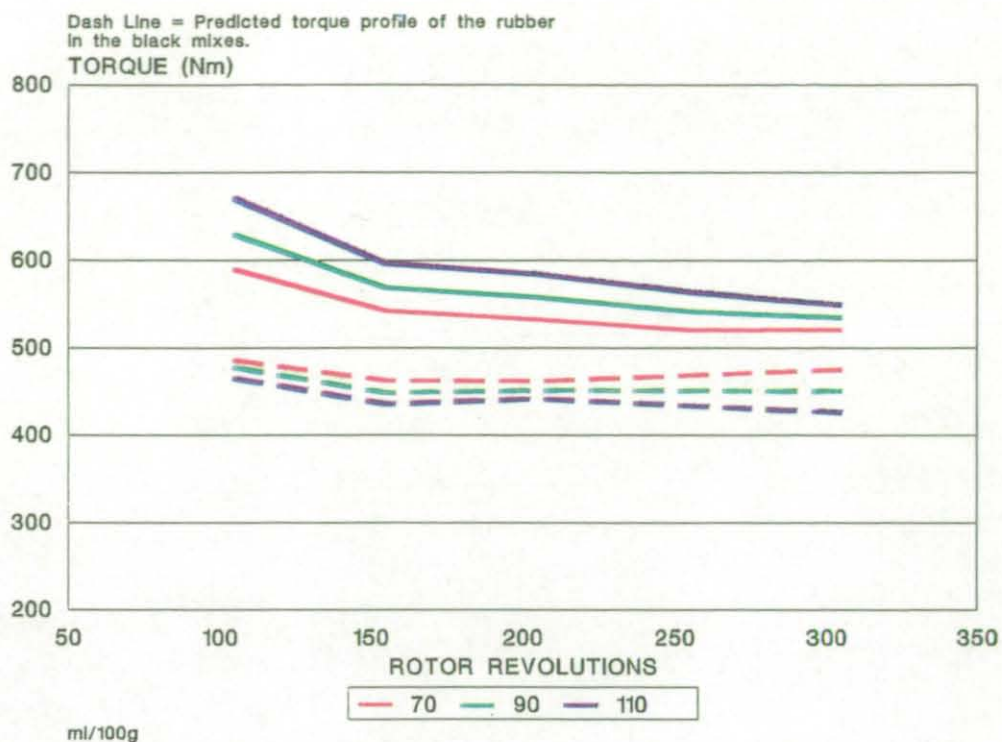


Figure 6.3 - The effect of the DBPA value of the carbon black on torque.

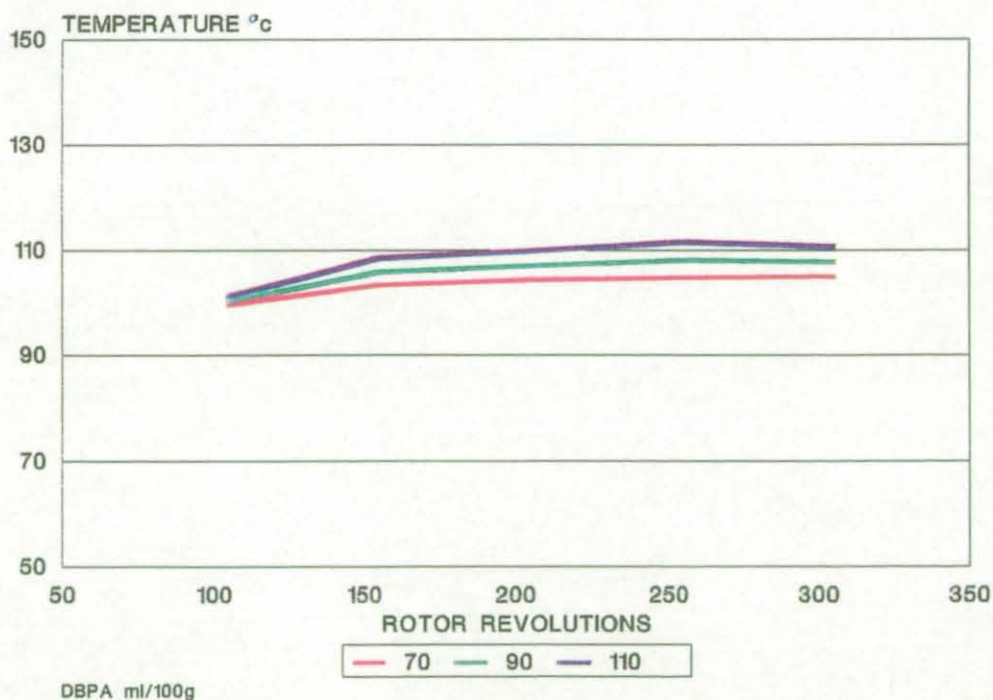


Figure 6.4 - The effect of the DBPA of the carbon black on the batch temperature profile.

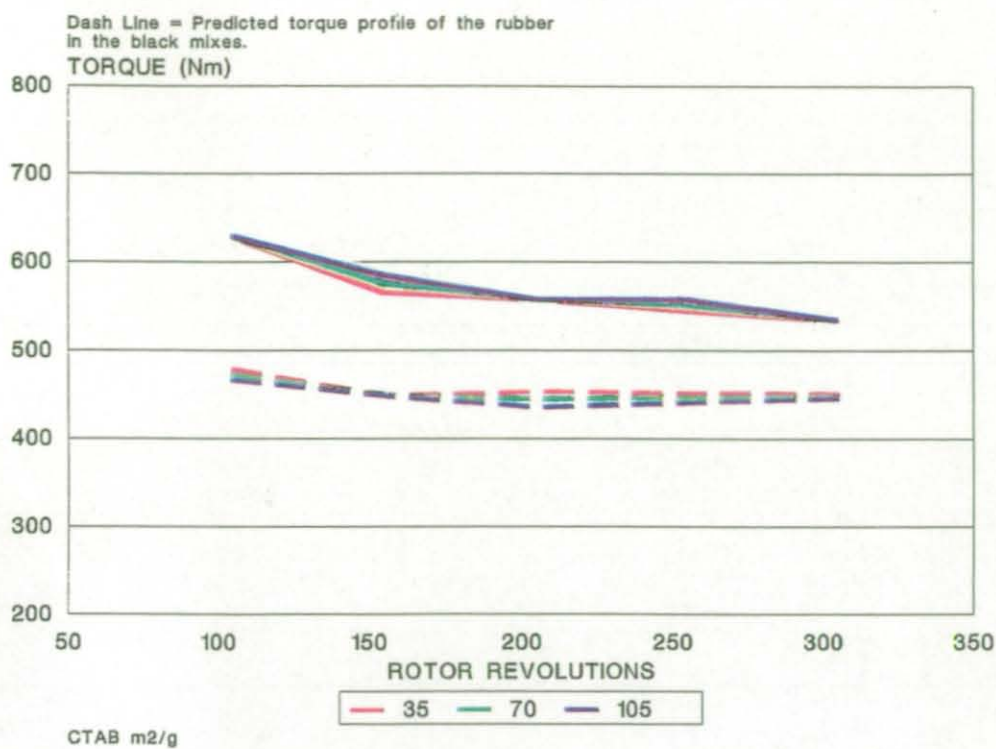


Figure 6.5 - The effect of the CTAB of the carbon black in the torque profile.

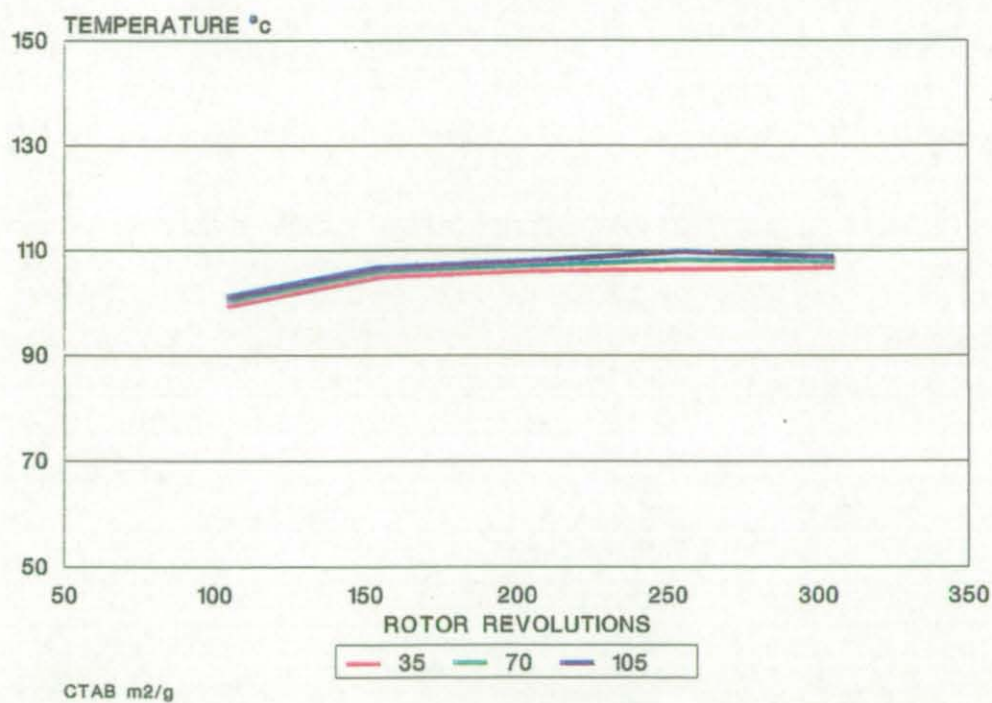


Figure 6.6 - The effect of the CTAB of the carbon black on the batch temperature profile.

Figure 6.1 shows that carbon black loading is the most significant parameter to effect the torque profile. An increase carbon black loading from 20 to 70 phr results in increase of approximately 300 Nm in torque. The simulated natural rubber torque profiles show a decrease in torque with increased carbon black loading. Looking at this figure in isolation the most obvious explanation for this observation is that as higher loadings of carbon black are used the shear stress obtained during each rotor revolution becomes progressively greater and hence the efficiency of mastication is improved. However when figure 6.2 is examined, showing a significant increase in batch temperature with increase in carbon black loading, the variation observed in the natural rubber torque profiles is more likely be due to the rise in batch temperature.

Figure 6.3 shows that as the structure (DBPA) of the carbon black increases the torque during dispersive mixing also increases but to a lesser degree. Also, again consistent with the effect of carbon black loading, a slight increase in the efficiency of mastication and batch temperature rise (figure 6.4) is observed with increase in DBPA. The reasons for these observations are likely to be the same as for the carbon black loading.

Figures 6.5 and 6.6 confirms that the specific surface area (CTAB) of the carbon black has no effect on torque or batch temperature.

6.5.4.2 Effect of mixing parameters.

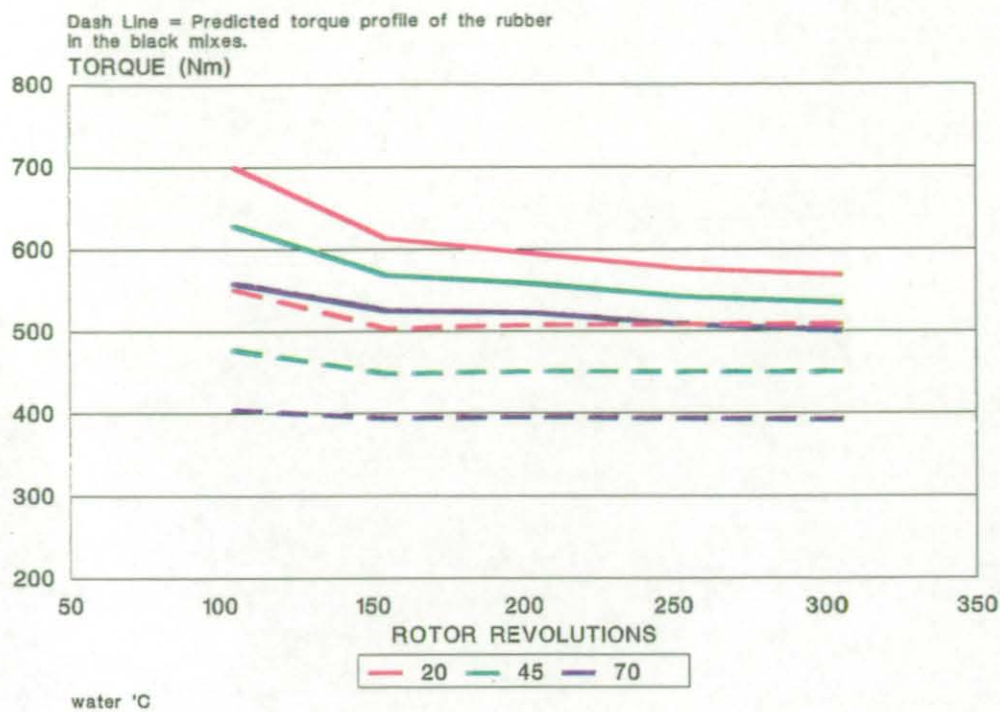


Figure 6.7 - The effect of the water temperature on the torque profile.

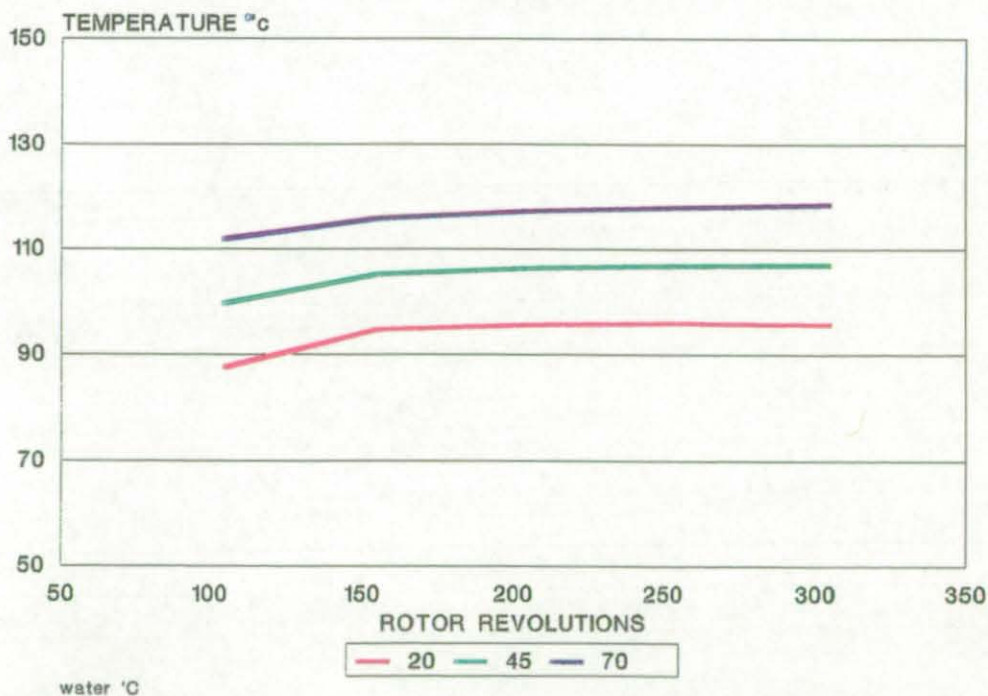


Figure 6.8 - The effect of the water temperature on the batch temperature profile.

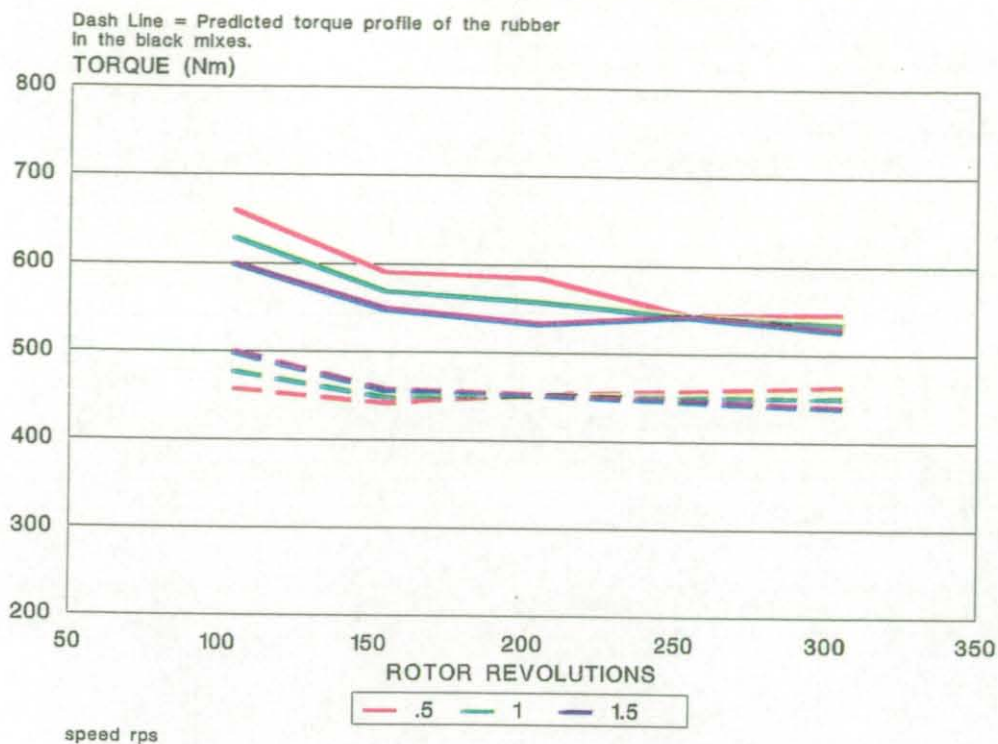


Figure 6.9 - The effect of the rotor speed on the torque profile.

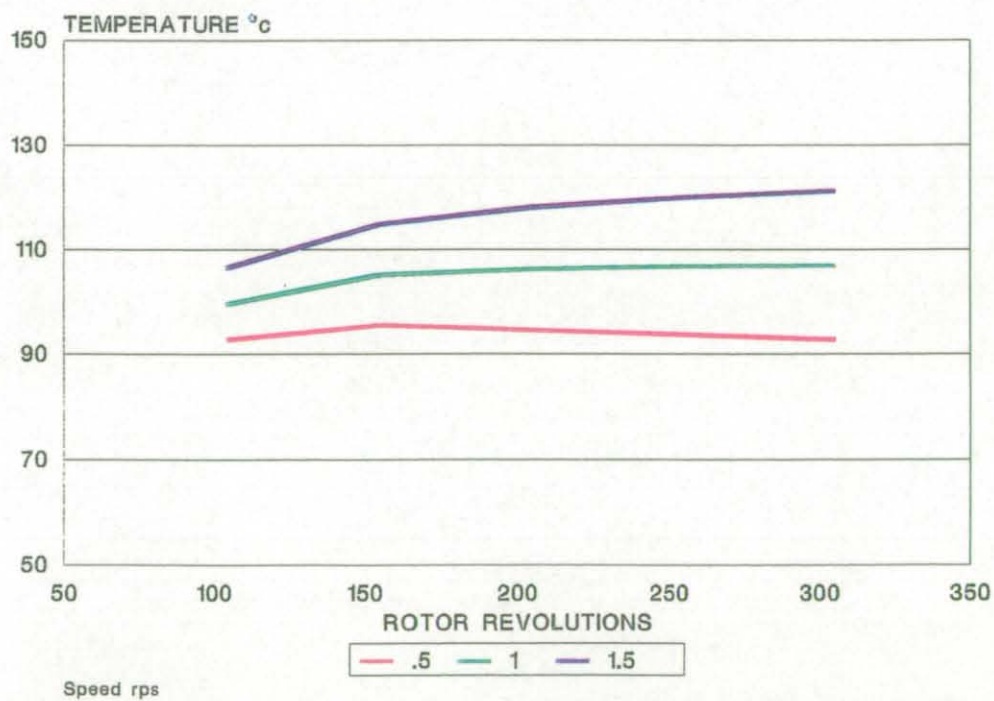


Figure 6.10 - The effect of the rotor speed on the batch temperature profile.

Figures 6.7 and 6.8 show that both torque and the temperature of the batch are significantly affected by changes to the circulating water temperature. The torque profiles of both the carbon black mixes and the simulated natural rubber mixes were reduced as the batch temperature increased as a consequence of the water temperature being increased.

Figure 6.9 shows that the torque profile for both the carbon black mixes and the predicted natural rubber mixes were not significantly influenced by changes in rotor speed. The reason for this is probably because, as figure 6.10 shows, batch temperature is strongly influenced by rotor speed. The batch temperature increases by approximately 30°C by moving from a rotor speed of 0.5 rps to 1.5 rps. Therefore it is likely that the increase in torque that occurs due to an increase in rotor speed is counteracted by the consequent increase in batch temperature.

6.6 The use of the batch thermocouple to predict rubber temperature in the Banbury mixer.

During the development of the initial predictive model (see section 5.4.1) a regression equation (equation 5.18) was developed for one carbon black compound (27 phr of N660) that incremented the batch thermocouple values to give improved monitoring of the batch profile during mixing in the Banbury mixer. At the time of development, the source of the error on the batch thermocouple was thought to be due to the poor thermal conductivity of the compound and because the thermocouple is influenced by the mixer temperature around it [35]. During the development of the material

database this regression equation was used to predict the dump temperature of the 45 carbon black mixes where the loading of carbon black varied from 20 --> 0 75 phr, as shown in figure 6.12. The regression equation gave a consistent improvement in predicting the dump temperatures over the whole range of loadings. This was particularly emphasised when the mixes were characterised in terms of carbon black loadings and there was no systematic error between the groups. This finding suggests that changes in the thermal conductivity of the compound has little effect on the amount of error of the thermocouple.

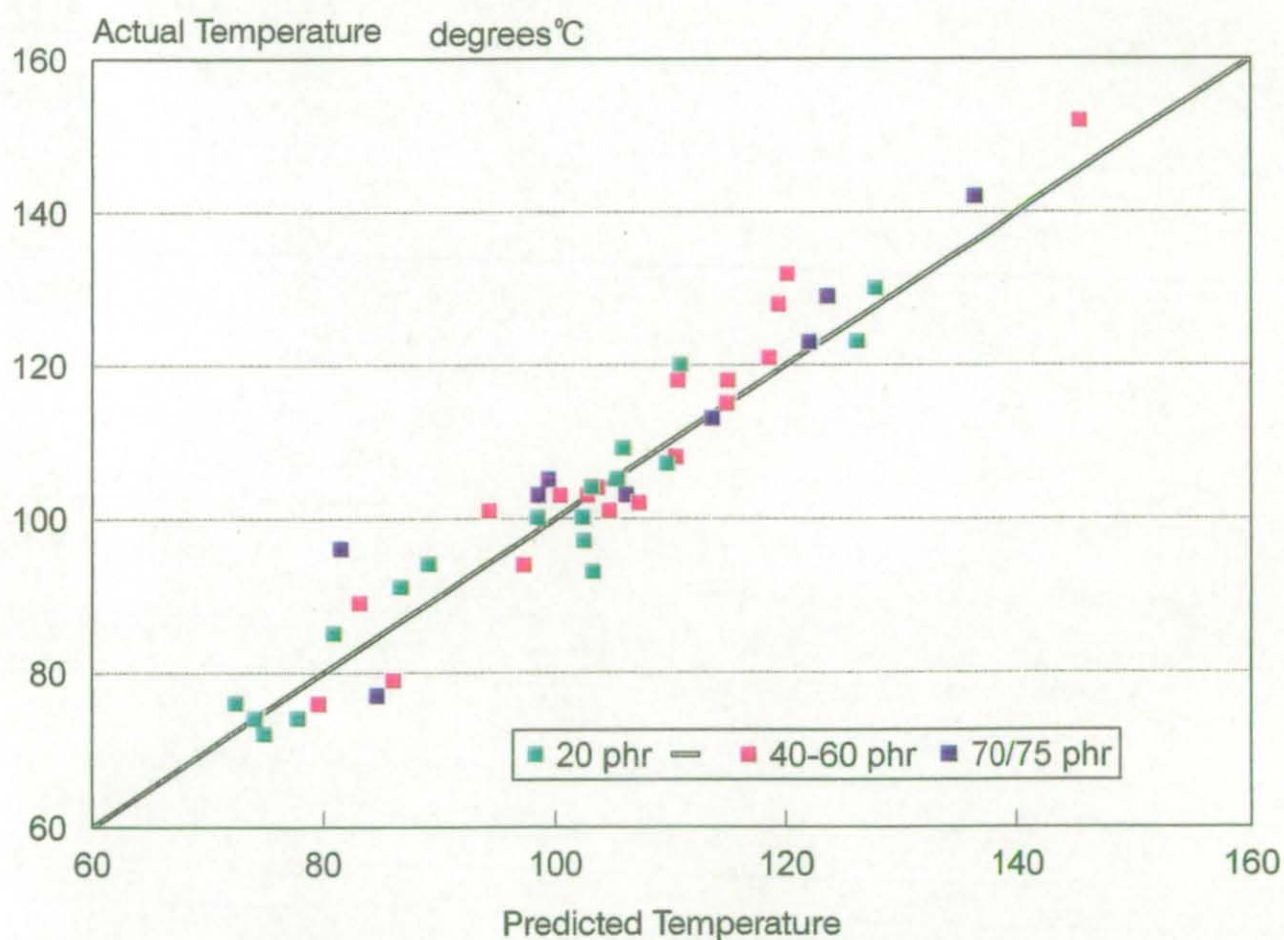


Figure 6.11 - Comparison of actual and predicted dump temperature of the 45 mixes.

CHAPTER SEVEN.

CONCLUSIONS AND POSSIBLE FUTURE WORK.

7.0 Chapter 4 - Evaluation of Mastication.

(i) The investigation confirmed that rotor speed, circulating water temperature, fill factor and mixing time all have an effect on the efficiency of mastication. It also illustrated that the effect is repeatable and that each individual parameter could be isolated. The results indicated that fill factor is the most significant mixing parameter for the efficiency of mastication.

(ii) If the same number of rotor revolutions are undertaken and the heat history received during mixing is approximately the same then a consistent reduction in viscosity is achieved independent of rotor speed.

7.1 Chapter 5 - Development of a predictive model for the rubber mixing process.

(iii) An initial predictive model has been developed for a premasticated SMR L natural rubber/27 phr N660 carbon black mix that can predict accurately both batch temperature rise and power consumption in the laboratory Farrel BR Banbury mixer over the following range of mixing conditions

| | |
|-------------------|---------------|
| Rotor speed | 43 - 107 rpm. |
| Water temperature | 27 - 63 °C |
| Mixing time | 26 - 180 secs |
| Fill factor | 35 - 75 % |

Of the mixing cycles studied 90% of the predictions were found to be within +/- 5°C of the actual final batch temperature and within 7% of the monitored power consumption.

(iv) Additions of aromatic process oil, up to 10 phr, were found not to have sufficient effect on mixer power consumption to justify alterations to the predictive model.

(v) During the development of the initial predictive model it was found that the J-type batch thermocouple attached to an end plate in the Farrel BR Banbury mixer measured consistently lower than the actual temperature of the batch and that the level of error was not consistent. Separate regression equations for the premasticated SMR L natural rubber/27 phr N660 carbon black mix were generated for mastication and dispersive mixing which incremented the values monitored by the batch thermocouple. The adjusted R-squared values for the two regression equations were 96.8% for mastication and 95.4% for dispersive mixing.

7.2 Chapter 6 - Development of a material database for the predictive model.

(vi) Modelling the power consumption during incorporation of the carbon black could not be achieved accurately since the process itself is not systematic. This was illustrated by the fact that a best-fit regression equation generated to predict the number of rotor revolutions before incorporation had an adjusted R-squared value of only 63.5% (for definition of R-squared see Appendix 1).

(vii) The viscosity information obtained from the experimental work was insufficient to discriminate between changes in the relationship between the relative stress of the compound and the number of rotor revolutions undertaken as a function of mixing conditions, type and loading of carbon black. Therefore the necessary coefficients required for the predictive model to function for a wide range of carbon black at different loadings could not be obtained. The most likely reason for this is that the number of experimental mixes undertaken were relatively small when considering the wide range of variables involved. An alternative approach was investigated which used the torque profiles to quantify the disagglomeration process. However, this method also did not generate the necessary coefficients since only a poor correlation between viscosity and torque (adjusted R-squared value of 49.5%) could be generated after taking into consideration batch temperature and rotor speed.

(viii) To utilise the data collected a series of regression equations were generated to study the effect material and mixing parameters have on the torque and temperature profiles during dispersive mixing. Also through manipulation of the data it was

possible to estimate the torque profiles of the natural rubber in the carbon black mixes. The equations generated from this analysis cannot be related to the predictive model and are specific to the Farrel BR Banbury mixer used. Fill factor was not studied in this analysis.

This analysis results in the following observations:

(a) The loading of carbon black has a greater affect on torque and batch temperature than the specific surface area (CTAB) and the structure (DBPA) of the carbon black. Also the predicted torque profile of the natural rubber, masticated under the same conditions as the carbon black mixes, showed a decrease in torque with an increase in loading. This suggests that as the loading of carbon black increases the rate of mastication improves. However as the loading of carbon black has such a strong effect on batch temperature it is more likely that these differences in the torque curves are due to changes in batch temperature.

(b) The structure (DBPA) of the carbon black has a similar effect on torque and batch temperature as carbon black loading but to a lesser extent. For example an increase in the DBPA value of 70 to 100 ml/100g results in an estimated 100 Nm increase in torque after 100 rotor revolutions whilst an increase in carbon black loading from 20 to 70 phr results in estimated 300 Nm increase in torque.

(c) The specific surface area (CTAB) of the carbon black has an insignificant influence on both batch temperature and torque.

(d) Circulating water temperature had a significant effect on both torque and batch temperature. As the circulating water temperature increases the efficiency of the heat transfer from the mixing batch to the cooling system is reduced which results in a decrease in torque.

(e) Rotor speed did not have a significant effect on torque but did have a strong influence on the batch temperatures. The most probable reason why the regression equation showed rotor speed not to have an effect on torque is because the increase in torque that occurs due to an increase in rotor speed was counteracted by the consequent increase in batch temperature.

(ix) As discussed in (v) a regression equation was generated during the development of the initial predictive model to improve the monitoring of the batch temperature during dispersive mixing of one carbon black at one specific loading by incrementing the value monitored by the batch thermocouple. It was found that the same regression equation improved the monitoring over the wide range of types and loadings of carbon blacks used in chapter 6. In a previous study [35] it was suggested that the source of error on a J-type thermocouple was due to the poor thermal conductivity of the compound and because the thermocouple is influenced by the mixer temperature. This finding suggests that the poor thermal conductivity of the compound must only be a minor contributor to the source of error on the batch thermocouple.

7.3 Future work.

(i) Extensive experimental work needs to be undertaken to develop a working material database for the predictive model. From observations made in chapter 6 either a much larger experimental program needs to be undertaken incorporating more data points or alternatively a smaller range of carbon blacks could be investigated.

(ii) Development of a single regression equation that increments the batch thermocouple value to improve batch monitoring across the compound range during dispersive mixing is something that could be quickly and practically generated for other mixers. Its introduction would improve temperature monitoring and would consequently result in better control.

APPENDIX ONE.

DEFINITION OF STATISTICAL TERMS.

1. Standard Deviation (StD).

The standard deviation of a set of n numbers $x_1, x_2, x_3, \dots, x_n$ with mean \bar{x} is:

$$\text{std} = \sqrt{\frac{\sum (x_i - \bar{x})^2}{n}} \quad \text{where } i = 1, 2, 3, \dots, n$$

The standard deviation is a measure of spread. For most deviations the bulk of the readings lie within ± 2 std of the mean.

2. Tukeys criteria - this is the procedure used by Minitab to determine the "best" regression equations.

This determines the "best" regression equation by taking the standard deviation (StD), the number of observations (n) and the number of fitted parameters in the equation (p) and minimises the equation for:

$$\text{StD}/(n-p).$$

3. Adjusted correlation coefficient (R-squared).

The term R-squared is the adjusted correlation coefficient and is a measurement of the variation in y that can be explained by the fitted equation.

It has been adjusted to take into consideration the degrees of freedom.

4. BREG - a Minitab function which produces a series of "best" regressions equations using increasing numbers of input variables.

This function enabled the computer to generate the best regression for

determining the variation in y using the other variables inputed. The software initially looks at all one variable regression equations and selects the equation giving the largest R-squared value. Information on this regression and the next best one variable regression is printed. Then the BREG looks at all two variable regression equations, finds the one with the largest R-squared value, prints information on this one and the next best. This process continues until all the variables have been used.

5. Standard error of estimate (s).

The value s can be thought of as a measure of how much the actual values differs from the predicted values (fitted) as given by the least square lines.

$$\text{i.e. } s = \frac{(\text{actual} - \text{fitted})^2}{n-2}$$

where n = the number of mixes

6. Correlation (r).

The closer the r is from -1 or +1 the easier it is to predict one variable from the other; in other words there is a high level of correlation. If there is almost no association between the variables then r will be near to zero.

7. Coefficients of variance (COV).

$$\text{COV} = \frac{\text{Standard deviation}}{\text{mean}}$$

COV enables the variation around means of different magnitude to be compared.

APPENDIX TWO.

CALCULATION OF CONSTANTS FOR THE INITIAL PREDICTIVE MODEL.

(1) Effect of rotor speed on torque.

(i) During mastication

$$n = .233$$

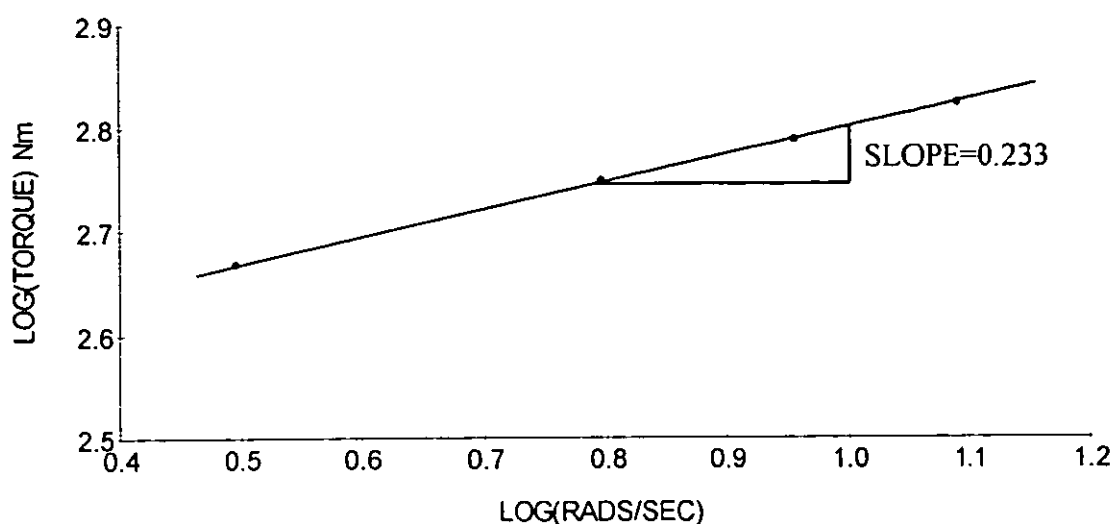
= slope of the plot Log(torque) vs Log(speed)

| Speed rpm | Speed rads/sec | Log (Speed) | Torque (Nm) | Log (torque) |
|--------------|-------------------|----------------|----------------|-----------------|
| 120 | 12.57 | 1.099 | 678.94 | 2.83 |
| 90 | 9.42 | 0.974 | 627.63 | 2.79 |
| 60 | 6.28 | 0.798 | 564.473 | 2.75 |
| 30 | 3.14 | 0.486 | 468.81 | 2.67 |

Torque values were taken 10 seconds after ram down.

For each mix the fill factor = 56%

water temperature = 45°C



Graph 1 - Plot of Log(torque) vs Log(speed) during mastication.

During dispersive mixing.

When 27 phr of N660 carbon black was added

$$n = .2$$

= slope of the plot Log(torque) vs Log(speed)

| Speed rpm | Speed rads/sec | Log (rads/sec) | Torque Nm | Log (Torque) |
|-----------|----------------|----------------|-----------|--------------|
| 100 | 10.46 | 1.02 | 682.33 | 2.834 |
| 80 | 8.37 | 0.923 | 653.13 | 2.815 |
| 60 | 6.28 | 0.798 | 618.02 | 2.791 |
| 40 | 4.19 | 0.622 | 576.77 | 2.761 |

Conditions for mastication

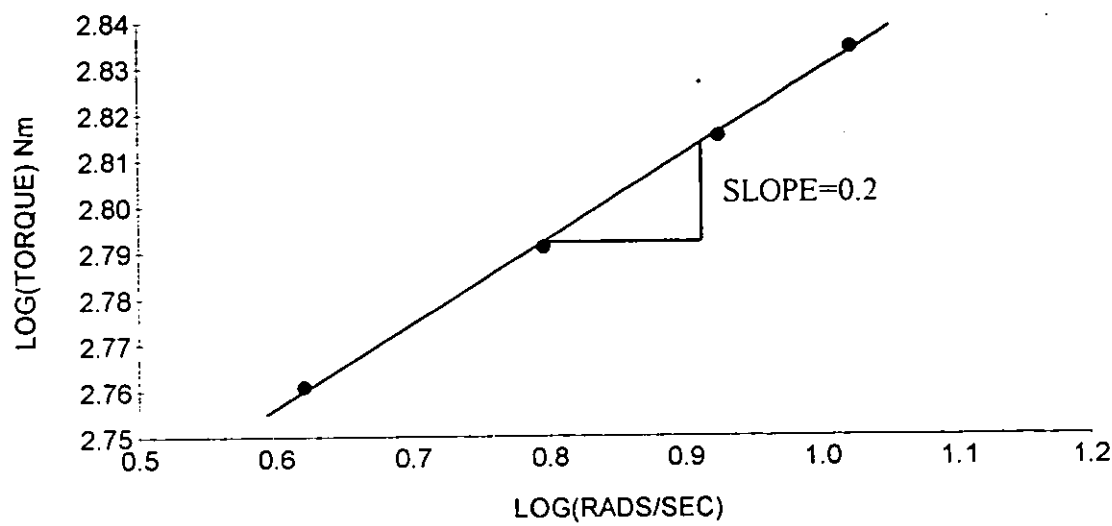
water temp 40°C

mixing time 70 secs

rotor speed 70 rpm

Fill factor 52%

The mixing speed was altered during carbon black addition to ensure that mastication stage of the mixing cycle was consistent from batch to batch. Torque values were taken 20 secs after ram down from carbon black addition. Water temperature remained constant at 45°C. Fill factor after carbon black addition was 58%.



Graph 2 - Plot of Log(torque) vs Log(speed) during dispersive mixing.

(2) Effect of batch temperature on torque.

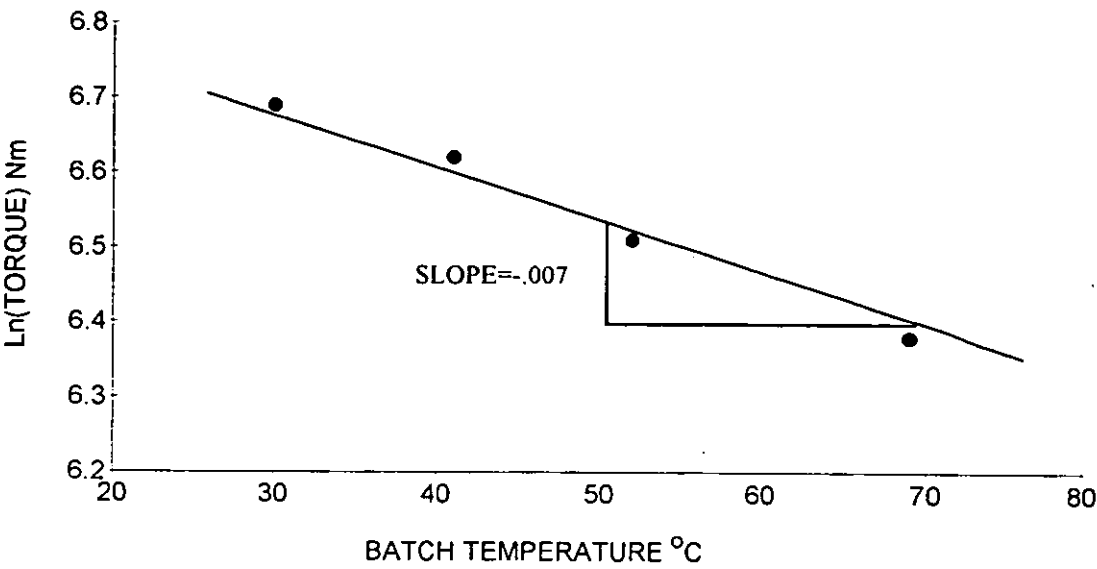
-b = - 0.007

= slope of the plot Ln(torque) vs batch temperature.

| Water temp. °C | Batch temp. °C | Torque Nm | Ln(Torque) |
|-------------------|-------------------|--------------|------------|
| 20 | 31 | 804.32 | 6.69 |
| 30 | 41.5 | 749.94 | 6.62 |
| 45 | 52 | 671.83 | 6.51 |
| 70 | 69 | 561.16 | 6.33 |

Torque values were taken 10 seconds after ram down.

For each mix the fill factor = 56% (only rubber) and the rotor speed = 75 rpm



Graph 3 - Plot of Ln(torque) vs batch temperature.

(3) Effect of mastication on torque.

$d = 0.0034$

= slope of the plot $1/(\eta/\eta_i)^2$ vs rotor revolutions.

$y_0 = 1.045$

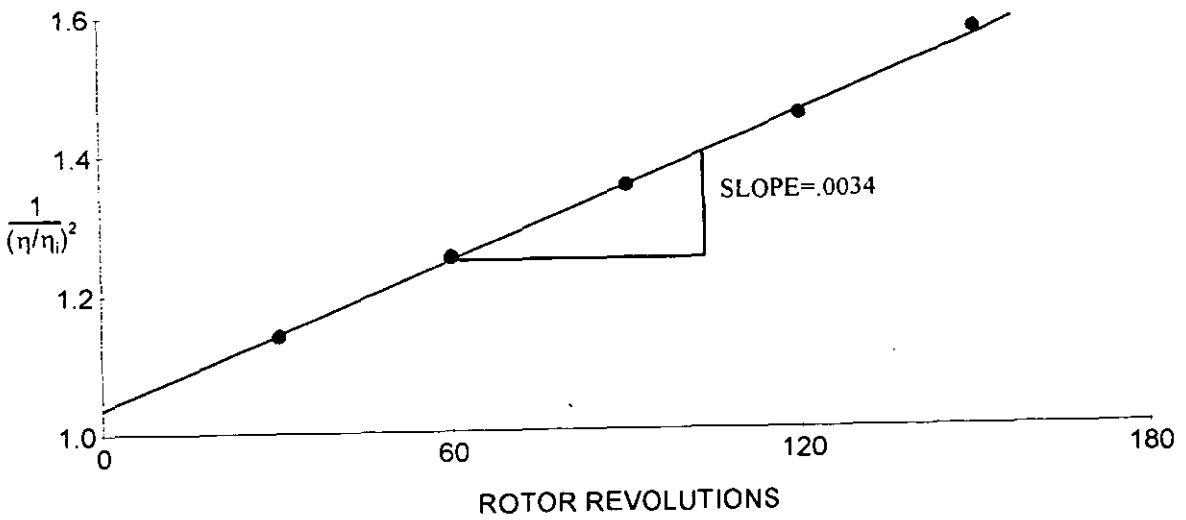
= the value of $1/(\eta/\eta_i)^2$ when rotor revolutions = 0 ie the value at the y intercept.

| Rotor Revs. | $1/(\eta/\eta_i)^2$ |
|-------------|---------------------|
| 30 | 1.139 |
| 60 | 1.246 |
| 90 | 1.349 |
| 120 | 1.462 |
| 150 | 1.568 |
| 180 | 1.610 |

η = apparent viscosity at shear rate 1 s^{-1}

η_i = initial apparent viscosity at shear rate 1 s^{-1} (ie zero mixing time).

The values for apparent viscosity were calculated using equation 4.3. Water temperature was kept constant in the equation at 50°C .



Graph 4 - Plot of $1/(\eta/\eta_i)^2$ vs rotor revolutions.

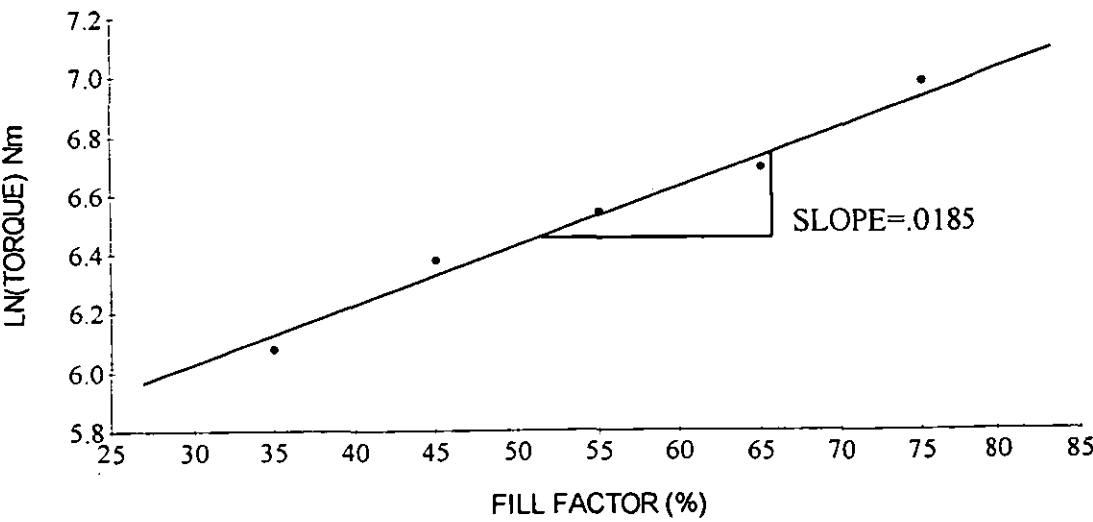
(4) Effect of fill factor on torque.

$x = .0185$

= slope of the plot Ln(torque) vs % fill factor.

| % Fill Factor | Torque | Ln(Torque) |
|---------------|---------|------------|
| 75 | 1074.91 | 6.98 |
| 65 | 804.32 | 6.69 |
| 55 | 692.28 | 6.54 |
| 45 | 589.93 | 6.38 |
| 35 | 437.02 | 6.08 |

Torque values were taken 10 seconds after ram down. For each batch the water temperature and rotor speed remained constant at 27 °C and 127 rpm respectively.



Graph 5 - Plot of Ln(torque) vs % fill factor.

(5) Generation of the regression equation to calculate the initial temperature of the batch when the ram comes down.

$$\text{Initial temp.} = 25.8 + 0.239(\text{speed rpm}) + 0.210(\text{water temp } ^\circ\text{C})$$

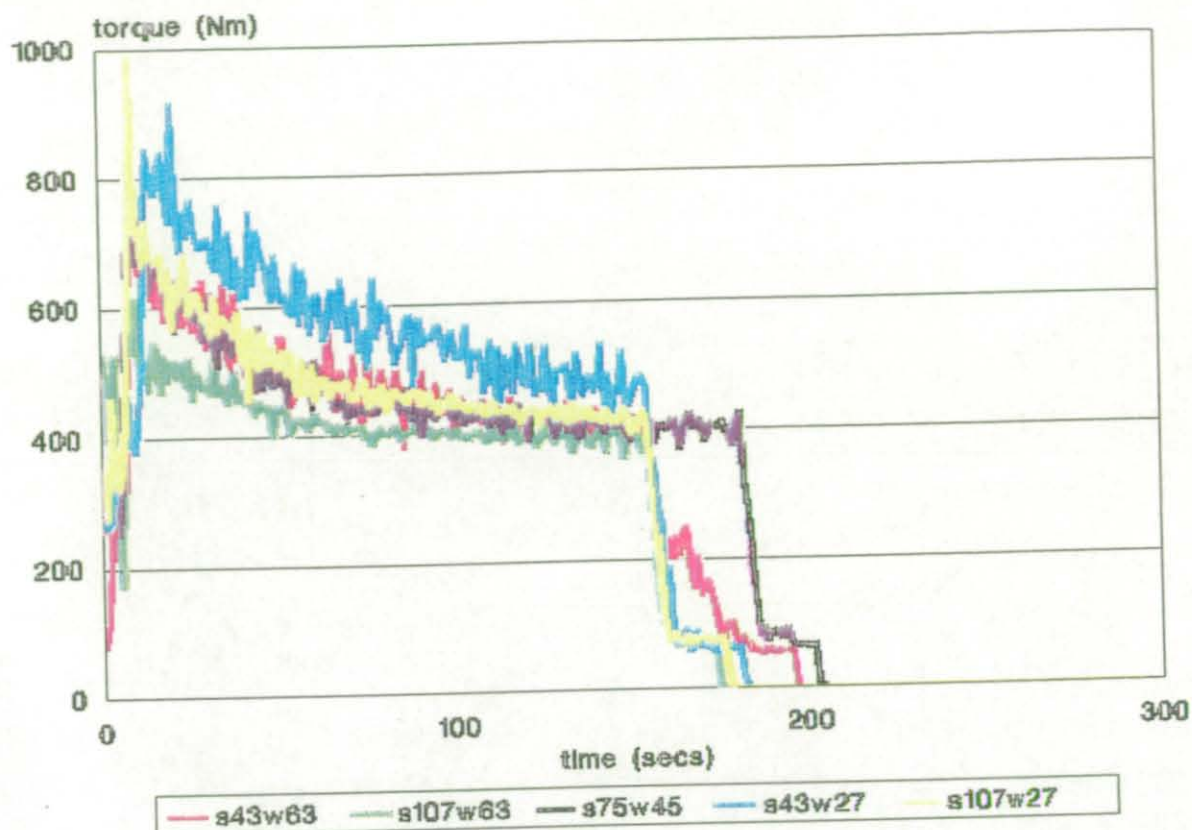
$$R\text{-sq} = 98.6\%$$

Results to generate this equation came from a separate experiment where the water temperature and rotor speed were varied during the loading of the raw rubber. The loading time remained constant from batch to batch (30 seconds) and once the ram was fully down the drop door was immediately opened releasing the batch. The temperature of the rubber was then measured using a hand held temperature probe. Fill factor at ram down for each batch was 56%.

| Batch | Water Temp. °C | Rotor Speed rpm | Batch Temp when dumped °C |
|-------|-------------------|--------------------|---------------------------------|
| 1 | 70 | 120 | 70 |
| 2 | 20 | 120 | 58 |
| 3 | 70 | 30 | 49 |
| 4 | 20 | 75 | 53 |
| 5 | 45 | 30 | 38 |

(6) To determine the minimum torque achievable in the mixer.

The minimum torque achievable in the mixer was determined by picking out a series of batches that all had a long mixing time but very different mixing conditions. By plotting these together on a graph it was found that they all veered towards the same minimum torque value.



s = rotor speed (rpm), w = water temperature ($^{\circ}\text{C}$).

Graph 6 - The series of mixes chosen to determine the minimum torque value during mastication.

(7) Details of procedure used to produce disagglomeration curve.

The rubber (800g) was masticated for 70 seconds before the carbon black N660 (213g) was added. Mixing was then continued for a further 60 seconds before the compound was discharged and a sample for testing was taken. After this the remainder was fed back into the mixer. This discharge and re-load procedure was repeated after 70, 100, 130, 170, 210, 270 rotor revolutions of dispersive mixing had been undertaken. The rotor speed was 40 rpm and the water temperature was 40°C . The same mixing cycle was then repeated but with no addition of carbon black so that the relative viscosity could be determined. The number of rotor revolutions quoted are the number of rotor revolutions undertaken with the ram down (ram up periods were not counted).

| Rotor revs | Shear stress at 1s^{-1} when rubber only | Shear stress at 1s^{-1} when rubber & black | Relative viscosity |
|------------|---|--|--------------------|
| 40 | 112 | 169 | 1.509 |
| 70 | 106 | 151 | 1.425 |
| 100 | 102 | 142 | 1.390 |
| 130 | 99 | 132 | 1.330 |
| 170 | 95 | 125 | 1.315 |
| 210 | 92 | 118 | 1.283 |
| 270 | 87 | 112 | 1.287 |

(8) Experimental work used to develop initial heat transfer model (the data from the mixes with carbon black in them was also used to develop the part of the model predicting the energy going in to the system during dispersive mixing).

| Mix No. | *Type | Mast. Time(s) | Disp. Time(s) | Rotor Speed(rpm) | Water Temp.(°C) | Fill Factor(%) |
|---------|-------|------------------|------------------|---------------------|--------------------|-------------------|
| 1 | 1 | 26 | - | 43 | 27 | 56 |
| 2 | 1 | 154 | - | 107 | 27 | 56 |
| 3 | 1 | 90 | - | 75 | 45 | 56 |
| 4 | 1 | 90 | - | 30 | 45 | 56 |
| 5 | 1 | 120 | - | 75 | 45 | 75 |
| 6 | 1 | 30 | - | 75 | 45 | 35 |
| 7 | 1 | 90 | - | 75 | 20 | 56 |
| 8 | 1 | 26 | - | 107 | 27 | 56 |
| 9 | 1 | 154 | - | 43 | 27 | 56 |
| 10 | 1 | 90 | - | 75 | 45 | 56 |
| 11 | 1 | 154 | - | 43 | 63 | 56 |
| 12 | 1 | 154 | - | 154 | 63 | 56 |
| 13 | 1 | 26 | - | 26 | 63 | 56 |
| 14 | 1 | 26 | - | 26 | 63 | 56 |
| 15 | 1 | 75 | - | 75 | 70 | 56 |
| 16 | 1 | 180 | - | 75 | 45 | 56 |
| 17 | 1 | 90 | - | 120 | 45 | 56 |
| 18 | 1 | 90 | - | 75 | 45 | 56 |
| 19 | 1 | 154 | - | 107 | 27 | 45 |
| 20 | 2 | 70 | 265 | 40 | 40 | 59 |
| 21 | 2 | 100 | 130 | 40 | 40 | 59 |
| 22 | 2 | 50 | 80 | 60 | 40 | 59 |
| 23 | 2 | 60 | 120 | 100 | 40 | 59 |
| 24 | 2 | 40 | 120 | 80 | 40 | 59 |
| 25 | 2 | 70 | 190 | 40 | 27 | 59 |
| 26 | 2 | 70 | 60 | 40 | 40 | 59 |
| 27 | 2 | 70 | 150 | 40 | 40 | 59 |
| 28 | 2 | 70 | 230 | **40/70 | 40 | 59 |

*Type 1 = mastication of natural rubber only.

2 = mastication of natural rubber + dispersive mixing with 27 phr of N660 carbon black.

** Rotor speed changes from 40 rpm to 70 rpm after 245 secs of mixing time.

(9) Predictions Made Using The Heat Transfer Model.

Mix number correspond with conditions in (8).

| Mix No. | Rubber temp (°C) at dump, using heat transfer model. | | Batch temp (°C) indicated by thermocouple, predicted using algorithm 5.19. | | Mixer temp (°C). indicated by thermocouple, predicted using algorithm 5.20. | |
|---------|---|-------|---|-------|--|-------|
| | Actual | Pred. | Actual | Pred. | Actual | Pred. |
| 1 | 49 | 54 | 39 | 37 | 30 | 30 |
| 2 | 103 | 111 | 97 | 99 | 45 | 49 |
| 3 | 97 | 95 | 81 | 83 | 56 | 57 |
| 4 | 75 | 74 | 61 | 61 | 53 | 50 |
| 5 | 120 | 121 | 103 | 102 | 56 | 63 |
| 6 | 71 | 67 | 54 | 56 | 50 | 49 |
| 7 | 84 | 83 | 64 | 68 | 31 | 34 |
| 8 | 76 | 70 | 58 | 58 | 34 | 35 |
| 9 | 80 | 74 | 63 | 63 | 39 | 37 |
| 10 | 97 | 95 | 79 | 81 | 55 | 56 |
| 11 | 100 | 99 | 84 | 86 | 70 | 71 |
| 12 | 130 | 135 | 120 | 121 | 77 | 81 |
| 13 | 94 | 94 | 74 | 75 | 68 | 68 |
| 14 | 73 | 76 | 62 | 61 | 65 | 64 |
| 15 | 115 | 110 | 97 | 99 | 78 | 79 |
| 16 | 109 | 107 | 95 | 94 | 59 | 60 |
| 17 | 118 | 115 | 104 | 102 | 59 | 62 |
| 18 | 97 | 95 | 79 | 82 | 55 | 56 |
| 19 | 99 | 92 | 78 | 83 | 41 | 44 |
| 20 | 94 | 96 | 81 | 81 | 52 | 51 |
| 21 | 94 | 94 | 81 | 79 | 52 | 50 |
| 22 | 98 | 91 | 91 | 86 | 53 | 53 |
| 23 | 114 | 118 | 109 | 108 | 59 | 61 |
| 24 | 105 | 108 | 99 | 97 | 55 | 57 |
| 25 | 87 | 86 | 79 | 73 | 42 | 38 |
| 26 | 81 | 88 | 65 | 70 | 47 | 48 |
| 27 | 92 | 96 | 82 | 79 | 51 | 50 |
| 28 | 95 | 92 | 81 | 82 | 49 | 52 |

APPENDIX THREE.

MIXING CONDITIONS AND RESULTS OF THE EXPERIMENTAL WORK UNDERTAKEN IN CHAPTER SIX, TO TRY AND DEVELOP A MATERIAL DATABASE FOR THE PREDICTIVE MODEL.

Table One - Mixing conditions of the 45 carbon black mixes.

Details of all carbon black mixes undertaken - refers to section 6.1.1

| Mix no. | DBPA ml/ 100g | CTAB m ² /g | CB phr | rotor revs | rotor speed rpm | water temp °C | rotor revs before sweep |
|---------|---------------------|---------------------------|--------|---------------|-----------------------|------------------|----------------------------------|
| 1 | 111 | 41 | 20 | 50 | 30 | 45 | 40 |
| 2 | 111 | 41 | 20 | 270 | 30 | 20 | 40 |
| 3 | 111 | 41 | 20 | 270 | 90 | 70 | 40 |
| 4 | 111 | 41 | 50 | 90 | 30 | 20 | 72 |
| 5 | 111 | 41 | 50 | 90 | 90 | 70 | 72 |
| 6 | 111 | 41 | 50 | 370 | 30 | 70 | 72 |
| 7 | 111 | 41 | 50 | 370 | 90 | 20 | 72 |
| 8 | 90 | 38 | 20 | 50 | 90 | 20 | 40 |
| 9 | 90 | 38 | 40 | 70 | 30 | 70 | 56 |
| 10 | 90 | 38 | 60 | 370 | 60 | 45 | 72 |
| 11 | 102 | 83 | 50 | 250 | 60 | 20 | 72 |
| 12 | 102 | 83 | 50 | 450 | 30 | 45 | 72 |
| 13 | 65 | 33 | 20 | 50 | 30 | 20 | 40 |
| 14 | 65 | 33 | 20 | 50 | 90 | 70 | 40 |
| 15 | 65 | 33 | 20 | 270 | 30 | 70 | 40 |
| 16 | 65 | 33 | 20 | 270 | 60 | 45 | 40 |
| 17 | 65 | 33 | 20 | 270 | 90 | 20 | 40 |
| 18 | 65 | 33 | 47.5 | 70 | 90 | 45 | 56 |
| 19 | 65 | 33 | 47.5 | 320 | 30 | 20 | 56 |
| 20 | 65 | 33 | 2075 | 90 | 30 | 70 | 72 |

| | | | | | | | |
|----|-----|-----|----|-----|----|----|----|
| 21 | 65 | 33 | 75 | 90 | 90 | 20 | 72 |
| 22 | 65 | 33 | 75 | 370 | 30 | 20 | 72 |
| 23 | 65 | 33 | 75 | 370 | 90 | 70 | 72 |
| 24 | 120 | 94 | 20 | 50 | 60 | 70 | 40 |
| 25 | 120 | 94 | 20 | 320 | 90 | 20 | 40 |
| 26 | 120 | 94 | 45 | 90 | 90 | 20 | 72 |
| 27 | 120 | 94 | 45 | 250 | 30 | 70 | 72 |
| 28 | 120 | 94 | 45 | 450 | 30 | 20 | 72 |
| 29 | 120 | 94 | 45 | 450 | 90 | 70 | 72 |
| 30 | 72 | 83 | 20 | 50 | 30 | 70 | 40 |
| 31 | 72 | 83 | 20 | 50 | 90 | 20 | 40 |
| 32 | 72 | 83 | 20 | 320 | 30 | 20 | 40 |
| 33 | 72 | 83 | 20 | 320 | 90 | 70 | 40 |
| 34 | 72 | 83 | 45 | 385 | 60 | 70 | 56 |
| 35 | 72 | 83 | 70 | 90 | 30 | 20 | 72 |
| 36 | 72 | 83 | 70 | 90 | 90 | 70 | 72 |
| 37 | 72 | 83 | 70 | 250 | 30 | 45 | 72 |
| 38 | 72 | 83 | 70 | 450 | 30 | 70 | 72 |
| 39 | 72 | 83 | 70 | 450 | 90 | 20 | 72 |
| 40 | 114 | 110 | 20 | 50 | 30 | 20 | 40 |
| 41 | 114 | 110 | 20 | 50 | 90 | 70 | 40 |
| 42 | 114 | 110 | 20 | 320 | 30 | 70 | 40 |
| 43 | 114 | 110 | 45 | 90 | 30 | 70 | 72 |
| 44 | 114 | 110 | 45 | 250 | 90 | 45 | 72 |
| 45 | 114 | 110 | 45 | 450 | 60 | 20 | 72 |

Table Two - Results of the 45 carbon black mixes.

Measured results from the carbon black mixes - refers to section 6.1.2

| Mix no. | Dump temp °C | Shear stress at 1 s ⁻¹ | *RS initial method | *RS - 2nd method |
|---------|-----------------|--------------------------------------|-----------------------|---------------------|
| 1 | 85 | 156.68 | 1.57 | 1.42 |
| 2 | 74 | 101.16 | 1.33 | 1.00 |
| 3 | 123 | 129.12 | 1.30 | 1.25 |
| 4 | 89 | 229.09 | 2.41 | 2.15 |
| 5 | 132 | 270.40 | 2.53 | 2.50 |
| 6 | 108 | 220.80 | 2.32 | 2.17 |
| 7 | 115 | 191.43 | 2.75 | 1.91 |
| 8 | 91 | 138.36 | 1.40 | 1.31 |
| 9 | 103 | 184.50 | 1.71 | 1.65 |
| 10 | 118 | 232.27 | 2.84 | 2.30 |
| 11 | 101 | 274.79 | 3.52 | 2.70 |
| 12 | 94 | 262.42 | 3.33 | 2.61 |
| 13 | 76 | 150.31 | 1.52 | 1.38 |
| 14 | 107 | 131.83 | 1.22 | 1.20 |
| 15 | 100 | 126.77 | 1.28 | 1.23 |
| 16 | 104 | 117.49 | 1.36 | 1.14 |
| 17 | 93 | 112.72 | 1.47 | 1.11 |
| 18 | 102 | 170.22 | 1.73 | 1.59 |
| 19 | 76 | 123.88 | 1.71 | 1.23 |
| 20 | 103 | 273.53 | 2.57 | 2.48 |
| 21 | 103 | 242.10 | 2.56 | 2.32 |
| 22 | 77 | 162.93 | 2.34 | 1.62 |
| 23 | 142 | 228.03 | 2.39 | 2.26 |
| 24 | 109 | 178.65 | 1.65 | 1.60 |
| 25 | 105 | 128.83 | 1.78 | 1.28 |
| 26 | 101 | 291.07 | 3.10 | 2.83 |
| 27 | 118 | 284.45 | 2.84 | 2.73 |
| 28 | 79 | 251.77 | 3.87 | 2.52 |

| | | | | |
|----|-----|--------|------|------|
| 29 | 152 | 276.69 | 2.98 | 2.84 |
| 30 | 100 | 167.88 | 1.55 | 1.47 |
| 31 | 97 | 146.56 | 1.48 | 1.37 |
| 32 | 72 | 111.17 | 1.53 | 1.10 |
| 33 | 130 | 139.00 | 1.43 | 1.36 |
| 34 | 111 | 207.97 | 2.19 | 2.05 |
| 35 | 96 | 301.30 | 3.21 | 2.84 |
| 36 | 129 | 348.34 | 3.27 | 3.21 |
| 37 | 105 | 127.68 | 1.27 | 2.05 |
| 38 | 113 | 312.61 | 3.36 | 3.12 |
| 39 | 123 | 293.09 | 4.50 | 2.93 |
| 40 | 74 | 166.73 | 1.68 | 1.53 |
| 41 | 120 | 165.58 | 1.53 | 1.50 |
| 42 | 97 | 156.68 | 1.61 | 1.53 |
| 43 | 103 | 305.49 | 2.87 | 2.76 |
| 44 | 128 | 274.16 | 3.13 | 2.68 |
| 45 | 101 | 268.85 | 4.03 | 2.65 |

* RS = Relative Stress

For explanation of: Original method - 6.3.2.1
2nd method - 6.3.2.2

Table Three - Additional mastication mixes undertaken.

Refers to section 6.3.2.2

| Mast no. | Mixing time sec | Water temp °C | Speed rpm | Dump temp °C | Shear stress at 1 s ⁻¹ |
|----------|--------------------|---------------|--------------|-----------------|--------------------------------------|
| 1 | 500 | 70 | 30 | 101 | 89.74 |
| 2 | 1000 | 70 | 30 | 100 | 87.09 |
| 3 | 500 | 70 | 60 | 116 | 83.56 |
| 4 | 200 | 90 | 30 | 100 | 95.94 |
| 5 | 280 | 90 | 30 | 104 | 92.04 |
| 6 | 280 | 90 | 30 | 105 | 95.94 |
| 7 | 500 | 90 | 30 | 113 | 93.32 |
| 8 | 740 | 90 | 30 | 115 | 85.11 |
| 9 | 1000 | 90 | 30 | 113 | 79.43 |
| 10 | 500 | 90 | 60 | 129 | 71.77 |
| 11 | 740 | 70 | 60 | 113 | 80.54 |
| 12 | 740 | 90 | 60 | 129 | 66.83 |

Fill factor was 56% for all these mastication mixes

Table four - Predictions of what the shear stress of the masticate would be mixed under the same conditions as the 45 carbon black mixes.

Results of analysis undertaken to predict the torque profile of the rubber in the carbon black mixes - refers to section 6.5.1.1

| Mix no. | X Σ (rps/tem) | Y $\Sigma(\text{tem}-80)^3$ | Shear stress of masticate at 1 s ⁻¹ |
|---------|-------------------------|--------------------------------|--|
| 1 | 1.88 | 0.01 | 110.22 |
| 2 | 4.96 | 0.00 | 101.17 |
| 3 | 3.69 | 10959.65 | 102.95 |
| 4 | 2.63 | 1.28 | 106.36 |
| 5 | 2.24 | 2563.527 | 108.15 |
| 6 | 4.32 | 16756.65 | 101.56 |
| 7 | 5.84 | 6089.41 | 100.40 |
| 8 | 2.76 | 3.84 | 105.85 |
| 9 | 1.66 | 583.08 | 111.72 |
| 10 | 4.93 | 9499.10 | 101.07 |
| 11 | 4.35 | 1782.32 | 101.93 |
| 12 | 5.96 | 4231.88 | 100.36 |
| 13 | 2.15 | 0.00 | 108.63 |
| 14 | 1.89 | 588.14 | 110.16 |
| 15 | 3.60 | 4406.22 | 103.31 |
| 16 | 3.55 | 1348.30 | 103.45 |
| 17 | 4.83 | 1116.57 | 101.31 |
| 18 | 2.47 | 524.09 | 107.05 |
| 19 | 5.70 | 15.44 | 100.55 |
| 20 | 1.84 | 1433.47 | 110.48 |
| 21 | 3.26 | 226.34 | 104.22 |
| 22 | 5.76 | 149.47 | 100.50 |
| 23 | 4.40 | 276.63 | 100.79 |
| 24 | 1.66 | 578.31 | 111.72 |
| 25 | 5.42 | 1824.46 | 100.74 |
| 26 | 3.08 | 131.91 | 102.90 |

| | | | |
|----|------|----------|--------|
| 27 | 3.24 | 11628.81 | 104.06 |
| 28 | 6.76 | 309.09 | 100.01 |
| 29 | 4.79 | 52112.76 | 97.31 |
| 30 | 1.38 | 324.69 | 113.92 |
| 31 | 2.53 | 12.21 | 106.78 |
| 32 | 5.41 | 0.00 | 100.77 |
| 33 | 4.00 | 15495.30 | 102.17 |
| 34 | 4.56 | 16316.37 | 101.25 |
| 35 | 2.67 | 0.19 | 106.20 |
| 36 | 2.19 | 3650.24 | 108.40 |
| 37 | 3.75 | 2699.67 | *** |
| 38 | 5.27 | 21908.35 | 100.16 |
| 39 | 6.24 | 13045.51 | 99.99 |
| 40 | 2.07 | 0.00 | 109.08 |
| 41 | 1.90 | 791.83 | 110.09 |
| 42 | 3.95 | 6893.41 | 102.53 |
| 43 | 1.83 | 1369.87 | 110.54 |
| 44 | 4.09 | 4730.87 | 102.32 |
| 45 | 6.47 | 5171.43 | 100.09 |

X = equation 6.8

Y = equation 6.9

REFERENCES

1. Rubber Technol. and Manufact., Newnes-Butterworths, edited by Blow CM, London, (1971).
2. Jerdonek J A, Rubber World, 191(5), 35(1985).
3. Chronos Richardson Appli. Report, Chronos Richardson, Nottingham (1994).
4. Banbury F H, US Patent 1,200,070, Oct. (1961).
5. Manas-Zloczower I, Nir A & Tadmor Z, Rubber Chem. Technol., 55, 1250(1982).
6. Parshall C M & Saulino A J, Rubber World 156(2),78(1967).
7. Peakman M G, Journal of the IRI, 4(2), 35(1970).
8. Freakley P K & Wan Idris W Y, Rubber Chem. Technol., 50, 163(1977).
9. Kim M H & White J L, Inter. Poly. Process., VII(1), (1992).
10. Killefer D J, Banbury the master mixer, Palmerston, New York, (1992).
11. Cheng J J & Manas-Zloczower I, Inter. Poly. Process., 5, 178(1990).
12. Kakouris A P, M-Phil thesis, Loughborough University, (1983).
13. Asai T, Fukui T, Inoue K & Kuriyama M, Int. Rubber Conference, Paris, III(9), (1982).
14. Wiedmann W M & Schmid H M, Rubber Chem. Technol.,55, 363(1982).
15. Melotto M A (Farrel Corp.), Rubbercon, Harrogate, (1987).
16. H L Jacob, A C S Rubber Division 95th meeting, LA, Calif, (1960).
17. Basir K B and Freakley P K, Kautsch. Gummi Kunstst., 35, 205(1982).
18. Griffin H D, Inter. Poly. Sci. Technol., 7, 11(1984).
19. Min K & White J L, Rubber Chem. Technol., 58, 1024(1986).
20. Wiedmann W M & Schmid H M, Rubber division meeting, ACS, Houston, Texas, paper no. 39, Oct 24, (1983).
21. Wiedmann W M & Schmid H M, Rubber Chem. Technol., 55, 363(1982).

22. Ellwood H, Europ. Rubber Journal, 159(1/2), 17(1977).
23. Melotto M A (Farrel corp.), Elastomerics, 118(8), 22(1986).
24. Freakley P K & Clarke J, Journal Applied Poly. Sci: Applied Poly. symposium, 53, 121(1994).
25. Freakley P K, Rubber Chem. Technol., 65, 706(1992).
26. Van Bushirk P R, Turetzky S B & Gunberg P K, Rubber Chem. Technol., 48, 577(1975).
27. Comes D A, Ind. Rubber World, 2, 180(1950).
28. Funt J M, Mixing of rubbers, RAPRA publications, Shawbury, England (1977).
29. Holfmann W, Rubber Tech. Handbook, Hanser, Munich, (1989).
30. Nekola K and Asada M, Rubber Chem. Technol., 65, 862,(1992).
31. Mutagahywa B M, Ph D thesis, Loughborough Uni., (1984).
32. Melotto M A (Farrel corp), Rubber World, 199(5), 34(1989).
33. Wiedmann W M ahd Schmid H M, Europ. Rubber Journal. 164, 33(1982).
34. Hess W M, Chirico V E & Vegvari P C , Elastomerics, 112(1), 24(1980).
35. Long H, Basic Compounding and Process. of Rubber, Rubber Division, American Chemical Society, (1985).
36. Feature: Material handling, The Plant Eng., 366, 10(1992).
37. Freakley P K, Rubber Process. and Production Organisation, Plenum Press London, (1985).
38. White L, Europ. Rubber Journal, 175(5), 16(1993).
39. Freakley P K & Murray G A W, Journal Applied Poly. Sci.: Applied Poly. Symposium, 50, 159(1992).
40. Freakley P K & Butler J, Plastics Rubber Comp Process Appli., 15, 249(1991).
41. Rawlings K, British Plastics Rubber, June, 14(1994).
42. Brett P N and Moore J M, IMechE, C419/047, (1990).
43. Bristow G M, Variability in laboratory, Raw Rubber and Process. group,

MRPRA., (1982).

44. Feature: The new SMR scheme, Rubber Develop., 44(4), (1991).
45. Patel A C & Jackson D C, Kautschuk Gummi, 45, 838(1992).
46. Medalia A I, Conference: Structure-property relations. of rubber, Ind. Institute Technol., W Bengal, India, Dec, (1980).
47. Manas-Zloczower I, Mixing and Compounding of Poly., chap 3, edited Manas -Zloczower I & Tadmor Z, Hanser, New York.
48. Herd R, McDonald G C, Smith R E & Herd W M, Conference: 142nd Meeting of the Rubber Devision, American Chem. Society, Nashville, Tennessee, paper no. 10, Nov, (1992).
49. Medalia A I & Heckman F A, Conference: First Australian rubber technol. Convention of the Instit. of the Rubber ind., Terrigal, NSW, Sept., (1968).
50. Hess W M, Ban L L & McDonald G C, Rubber Chem. Technol., 42, 1209(1969).
51. Hess W M, McDonald G C & Urban E M, Rubber Chem. Technol., 46, 204(1972).
52. McDonald G C & Hess W M, Rubber Chem. Technol., 50, 842(1977).
53. ASTM classification system D1765, American Society for Testing & Materials, Philadelphia.
54. Dalmgren H, Rubber Chem. Technol., 48, 462(1975).
55. Hancock T, Origin & Progress of India-Rubber Manufacture in England, Longman, Brown, Green, Longmans and Roberts, London, (1857).
56. Bristow G M, Nat. Rubber Technol., 10(3), 53(1979).
57. Fernando W S E & Perera M C S, Kautsch. Gummi Kunst., 40(12), 1149(1987).
58. Vargas H, Hule Mex. Plast., 45(521), 23(1989).
59. Fries H, Pandit R R & Voigtlander K, Iter. Poly. Sci. Technol., 11(6), (1985).
60. Studebaker M L & Bealty J R, Rubber Age, 108(5), 21(1976).
61. Bristow G M & Watson W F, MRPRA., The chemistry and physics of rubber like substances, Chap. 4, edited by Bateman C, (1963).

62. Corant A Y & Donnet J B, Rubber Chem. Technol., 65, 973(1992).
63. Medalia A, Measurement of Carbon black dispersion an educational symposium, Efficient rubber mixing technol., ACS, Rubber Division Meeting, Cleveland, Oct., paper 13, (1981).
64. Tokita N & Pliskin I, Rubber Chem. Technol., 46, 1166(1973).
65. Pliskin I, Rubber Chem. Technol., 46, 1218(1973).
66. Freakley P K & Clarke J, Reduction in viscosity of an SBR compound caused by mastication & disagglomeration during mixing, (submitted to Rubber Chem. Technol., 1994).
67. Bolen W R & Colwell R E, SPEJ, 14, 24(1958).
68. Shiga S & Furuta M, Rubber Chem. Technol., 58, 1(1985).
69. Kewi S P, Manas-Zloczower I & Feke D L, Poly. Eng. Sci., 31, 558(1991).
70. Cotten G R, Rubber Chem. Technol., 57, 118(1984).
71. Beach K C, Comper L F & Lowery V E, Rubber Age, 85, 253(1959).
72. Cotten G R, Rubber Chem. Technol., 58, 774(1985).
73. Gessler A M, Hess W M & Medalia A I, Plastic Rubber Process, 3(1), 109(1978).
74. Ebell P C, ph.D thesis, Loughborough University, (1984).
75. Boonstra B B & Medalia A I, Rubber Age, 87(3), 92(1963).
76. Hiemenz P C, Principles of colloid and surface chemistry, Marcel Dekker Inc, New York, Chap. 7, (1977).
77. Medalia A I, Colloid Interface Sci., 32, 115(1970).
78. Boonstra B B & Medalia A I, Rubber Age, 87(4), 82(1963).
79. Danneberg E M, Ind. Eng. Chem. 44(4), 813(1952).
80. BS. 903:Part A2, (1971).
81. Dizon E S & Papazian L A, Rubber Chem. Technol., 50, 765(1977).
82. Hillberry B M, SAE International Automotive Eng. Congress, Detroit, Michigan, edited symposium, Jan., (1973).

83. Lindley P B, Eng. Design with Natural Rubber, The Malaysian Rubber Producers Research Association, (1st edition 1964, reprinted 1978).
84. Funt J M, Rubber Chem. Technol. 61, 842(1988).
85. Lee B L & Nielen L E, Journal Poly. Sci., Poly. Phys Ed, 15, 683 (1977).
86. Payne A R, Reinforcement of Elastomer, Chap 3, Edited Kraus G, Wiley-Interscience, New York, (1965).
87. Payne A R, Rubber Plast. Age, Aug, 363(1961).
88. Payne A R, Journal Applied Poly. Sci, 9, 2273(1965).
89. Cembrola R, Poly, Eng. Sci, 22, 601(1982).
90. Eng-Long Orig, Rubber Division American Chemicals Society Conference, Cleveland, Ohio, 132nd meeting, Oct., (1987).
91. Brown R P & Scott J R, The Institution of the Rubber Ind., 36, (1972).
92. Boonstra B B, Rubber Chem. Technol., 50, 194(1979).69.
93. Sweitze C W, Hess W M & Callan J E, Rubber World, 38, 869(1958).68.
94. Stumpe Jr N A & Railsback H E, Rubber World, 152(12), 141(1964).
95. Hess W M, Rubber Chem. Technol, 64, 386(1991).
96. Lee B L, Mixing & Compounding of Poly., Chap 3, Edited Manas-Zloczower & Tamor Z, Hanser, New York, (1994).
97. Freakley P K & Patel S R, Rubber Chem. Technol., 58, 751(1985).
98. Ghafouri S N & Freakley P K, Poly. Testing, 13, 171(1994).
99. David B, Sapir T, Nir A & Tadmor Z, Inter. Poly. Process., VII(3),(1992).
100. Nasseki V & Freakley P K, Inter. Poly. Process., VI(2),(1991).
101. Basir K B and Freakley P K, Belgium Group Of Rheology and the British Rheological Society, University Of Liege, April,(1981).
102. Hu B & White J L, Rubber World, 208(4), 17(1993).
103. Freakley P K, Relations between process variables and mixed material properties, Rubbercon, (1981).

104. Hess W M, Swor R A & Miceh E J, Rubber Chem. Technol., 57, 959(1984).
105. Menges G & Grajewski F, Kautsch. Gummi Kunstst., 40, 706(1987).
106. Grajewski F and Sunder J, Kautsch. Gummi Kunstst., 42, 604(1989).
107. Michcieli W and Sunder J, Plastics Rubber Inter., 14, 17(1989).
108. Khunkamchoo P, ph.D thesis, Loughborough Uni., (1993).
109. Seza J A, Rubber World, 207(4), 12(1993).
110. MDR 2000, Moving Die Rheometer, Monstanto plc, (1988).
111. Kenny T, M-Phil thesis, Loughborough University, (1995).
112. Singh M, Batchelor J & Freakley P K, Plastics & Rubber Process. & Appli, 11, 175(1989).
113. Flagert W F, Rubber Division, American Chemical Society, (1988).
114. Communication with Mr D Turner, a consultant for Avon Rubber Plc.
115. EVK Compounder cuts cost and reduces plant inventory, Europ. Rubber Journal, 158(10), 27(1976).
116. Kraus G, Rubber Chem. Technol., 38, 1079(1965).
117. Labtech, Adept scientific micro systems ltd, 6 Business centre west, Avenue One, Letchworth, Herts, SG6 2HB.
118. Experimental design & optimising program., Avon Polymer Products Ltd, Bath Road, Melksham, Wilts.
119. CA-Supercalc, Silverado database Option, CA. Computer associates Ltd, 1 York Road, Uxbridge, Middlesex, UB8 1RN.
120. Minitab statistical software, version 10.1, 3 Mercia business village, Torwood Close. Westwood, Coventry, CV4 8HX.
121. Algorithm for construction of experimental designs, Loughborough ???

